CRYOGENICS

An International Journal of Low Temperature Engineering and Research

VOL. 1 NO. 4 JUNE 1961

Low Temperature Refrigeration

M. Ruhemann *Petrocarbon Developments Ltd, Manchester*

Received 12 January 1961

A refrigerating cycle is one in which the working substance absorbs heat at temperatures below ambient. Every such cycle must fulfil two conditions. It must involve, at some stage, a reduction in the enthalpy of the working substance, so that this substance may be in a position to absorb heat, and it must involve, at some stage, a drop in the temperature of the working substance as otherwise the system would never cool down.

There are, in the main, two types of refrigeration cycle: those in which the working substance is made to perform work, and those in which it is not. In the first type, the two conditions are fulfilled simultaneously. Expansion of a gas in a reciprocating machine or a turbine reduces enthalpy and temperature at the same time. On the other hand, in a refrigerating cycle which does not rely on the performance of work by the working substance, the two conditions are fulfilled separately. In a vapour compression cycle, the enthalpy reduction occurs mainly in the condenser by the liquefaction of the working substance at ambient temperature. Passage through the expansion valve lowers the temperature but not the enthalpy. In a gas cycle based on the Joule–Thomson effect, the enthalpy of the working substance is reduced by isothermal compression (in practice generally by adiabatic compression and aftercooling). Here again, passage through the expansion valve lowers the temperature but not the enthalpy.

Normal commercial refrigeration, in which heat has to be absorbed at temperatures not very far below ambient temperature, generally uses vapour compression cycles; firstly because the enthalpy reduction caused by the condensation of conventional refrigerants is large compared with that obtainable by the isothermal compression of 'permanent' gases, and secondly because the required temperature difference between condensing and evaporating sides is small enough to permit the use of practically acceptable compression ratios. In practice, with normal ambient temperatures, this limits the application of vapour compression cycles to evaporating temperatures in the region of $-50°$ C. Lower temperatures can, however, be obtained economically by 'cascading' several refrigerants of different boiling points. Two-stage cascades can operate satisfactorily down to temperatures around $-100°$ C.

To absorb heat at the temperatures around -180 to $-200°$ C, associated with the liquefaction and separation of air, engineering practice has frequently combined cycles based on Joule–Thomson expansion with cycles involving the performance of work by the working substance.

The use of Joule–Thomson expansion in air separation plants was found attractive for three reasons.

(1) As the plants were intended to produce oxygen at ambient temperature, the required cold production was relatively small and limited to overcoming heat losses and imperfect cold recuperation in the exchangers.
(2) The non-ideality of air at ambient temperature, and in particular at temperatures attainable with industrial vapour compression cycles, is adequate to ensure a cold production able to cope with the moderate requirements.
(3) Joule–Thomson expansion requires no machinery operating at low temperatures.

On the other hand, cycles based on Joule–Thomson expansion have several inherent disadvantages, among which the following appear most important.

(1) Joule–Thomson expansion is essentially irreversible.
(2) It requires the use of fairly high pressures.

Cycles based on the performance of external work were initially employed on relatively small plants and used reciprocating expanders, operating either at medium pressures (around 15–20 atm) for gas production or at higher

pressures (around 180 atm) for the production of liquid. As the production of liquid in the expander itself was not feasible, these cycles were always combined with isenthalpic expansion of a part of the air.

Increase in plant capacity with the resulting relative reduction in refrigeration requirements led to the development of low pressure cycles for the production of 'tonnage' oxygen, and consequently to the use of turbines for cold production. These are ideally suited for passing large volumes of gas with relatively small pressure differentials and a high expansion efficiency. A modern oxygen plant producing 250 tons a day features an expansion turbine passing about 3,000 ft^3(n.t.p.)/min with an expansion ratio of 4:1 at an efficiency of some 82 per cent of the isentropic. Recent advances in turbine design have made it possible to employ these machines to advantage on small scale plants also, and efficiencies between 75 and 80 per cent are obtained with turbines passing less than 200 ft^3/min. It is therefore no longer correct to associate expansion turbines exclusively with large gas flows.

The particular features of expansion turbines in connection with their use in low temperature refrigeration are the following:

(1) Their efficiency becomes greater the closer the working substance approaches a perfect gas. This is in direct contrast to isenthalpic expansion.
(2) Their efficiency is generally higher the smaller the pressure differential. It is thus often advantageous to use several turbines in series, separated by heat exchangers, to produce cold at a number of temperature levels.

Applications of refrigeration at liquid hydrogen and liquid helium temperatures

Refrigeration at hydrogen temperatures is today required in three distinct fields of application:
(1) Distillation of hydrogen/deuterium mixtures for heavy water production.
(2) Production of liquid hydrogen as a rocket fuel.
(3) Refrigeration of large bubble chambers for experiments in nuclear physics.

Quite irrespective of the different sizes of installations to serve these various purposes, the type of cold requirement is very different in the three cases.

In the separation of hydrogen and deuterium the final products are required at ambient temperature. The low temperatures are needed only to bring about a phase separation. Refrigeration is therefore required only to cool down the plant, to maintain it cold against heat ingress from the environment, and to maintain the necessary reflux conditions in the distillation columns.

The production of liquid hydrogen as a rocket fuel requires a much greater refrigerating performance in relation to the amounts of hydrogen treated, as the product has to be withdrawn as a cold liquid. However, refrigeration is needed over a large temperature interval. The latent heat of vaporization of hydrogen is small but its specific heat is that of a normal diatomic gas. Thus the refrigeration required at the lowest temperatures for liquefaction of the hydrogen is small compared with the cold needed to cool the hydrogen down to liquefaction temperature. The cold needed at the lowest temperature is only about 12 per cent of the total cold.

The cold used for maintaining stable conditions in a bubble chamber is all needed at the lowest temperatures. Thus, although these installations are small compared with those of the other two types, the low temperature refrigerating performance is relatively high.

Applications of refrigeration at the still lower temperatures associated with liquid helium are confined to groups (2) and (3) above. The purpose of the installation is either to produce liquid helium, which is to be tapped off and evaporated outside the plant, or to produce cold at very low temperatures in a closed cycle. In this respect, the same arguments hold as in the case of refrigeration at hydrogen temperatures. The special problems connected with refrigeration at helium temperatures, such as the low latent heat of vaporization of helium, the high thermal conductivity of pure metals, the importance of radiation shielding, etc., are not treated in this paper.

Low temperature refrigerating cycles to remove heat at the lowest temperatures only

The following considerations appear appropriate for the design of a plant according to group (3) in the previous section to produce cold at liquid hydrogen temperatures.

(1) Hydrogen shall be used as the only refrigerant.
(2) Expansion turbines shall be used for cold production.
(3) Low pressures only shall be used (e.g. around 10 atm).
(4) Hydrogen at ambient temperature up to 10 atm can be considered as a perfect gas.
(5) At temperatures close to the critical, hydrogen can no longer be considered a perfect gas at pressures around 10 atm. In particular, $(\partial H/\partial P)_t$ in this region is significantly negative.

With these premises a plant to produce refrigeration around 20° K can be developed as follows:

(1) As a first approximation assume that hydrogen can be considered as a perfect gas throughout. Neglect the difference between *ortho* and *para* states and assume that the specific heat is independent of pressure. Assume perfect cold recuperation in exchangers and isentropic expansion in turbines. Neglect cold losses to surroundings.

We thus arrive at the simplest form of refrigeration unit, shown in Figure 1(a), and the cycle is shown on a T–S diagram in Figure 1(b). The state of the working substance follows the lines 1–2–4–5–10. The 'available' cold $h_5 - h_4$ equals the cold produced $h_2 - h_4$. The temperature approach at both ends of the exchanger is zero. The temperature at which the expanded gas enters the heat exchanger is the same as that at which the compressed gas enters the turbine.

(2) Now assume, as the next approximation, that the

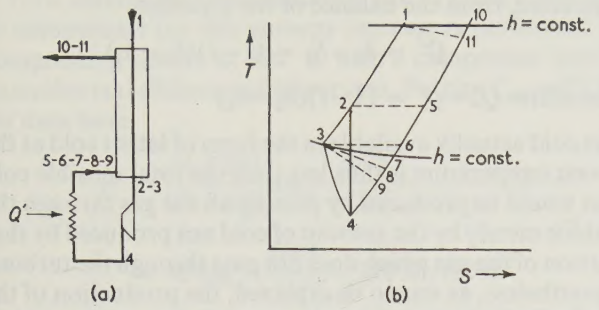

Figure 1. Simple low temperature refrigeration cycle

turbine efficiency is no longer equal to unity. If the same turbine outlet temperature is required, the turbine inlet temperature will have to be lower. The working substance will follow the line 1–3–4–6–10, as the gas will have to re-enter the exchanger at temperature 3. The available cold is still equal to the cold production, but it will now be

$$(h_6-h_4) < (h_5-h_4)$$

(3) If we now drop the assumption that hydrogen is a perfect gas throughout and assume that it is no longer perfect at the lowest temperatures, the line of constant h through point 3 will no longer intersect the low pressure constant pressure line at point 6 but at a lower temperature given by point 7. The gas will thus re-enter the exchanger at this lower temperature. The available cold still equals the cold production but it will be further reduced as (h_3-h_4) will now be smaller.

(4) We may now drop the assumption of perfect cold recuperation in the exchanger and assume that the return hydrogen leaves the exchanger at a point 11 colder than point 10. So that the exchanger may balance, it will have to re-enter the exchanger at a point 8 which is colder than point 7 by the same amount. The available cold (h_8-h_4) is now smaller than the cold production (h_3-h_4) and the temperature interval over which this cold is available has been still further reduced.

(5) Finally, we may assume that a certain amount of cold is lost as a result of heat ingress into the exchanger from the environment. In order to compensate for this, the returning hydrogen will have to absorb more heat than that which is contained in the incoming gas passing through the exchanger in countercurrent with it. It will therefore have to enter the exchanger at a still lower temperature, as shown by point 9.

The available cold is thus still further reduced and we now have available only

$$(h_9-h_4) < (h_8-h_4) < (h_3-h_4)$$

It is thus seen that the cold production is reduced by the inefficiency of the turbine and by the non-ideality of the gas. The available cold is reduced by these two factors, but also by the recuperation losses and the direct cold losses resulting from heat ingress from the surroundings.

To obtain a quantitative assessment of one of the above factors which diminish the available cold in a simple low temperature refrigerating plant, consider the cold losses caused by heat ingress from the surroundings. Assume a certain efficiency of the turbine and a certain warm end temperature approach ΔT°. Neglect the non-ideality of the gas, assuming that the specific heat is constant and independent of pressure. Let T_9 be the temperature at which the expanded gas re-enters the exchanger, so that the state of the gas is given by the lines 1–3–4–9–11. Let q be the cold lost through heat ingress from the surroundings, between T_1 and some lower temperature T. Then the balance of the exchanger down to point T reads

$$C_p(T_{11}-T') = C_p(T_1-T)+q$$

where T' is the temperature of the returning gas at that point in the exchanger where the temperature of the incoming gas is T. Therefore

$$T-T' = T_1-T_{11}+q/C_p = \Delta T^\circ+q/C_p$$

Now assume that the heat ingress from the environment is given by an equation of the type

$$\mathrm{d}q = -a(T_1-T)\,\mathrm{d}T$$

where a is a heat transfer coefficient. (If heat ingress is due to radiation, this equation will of course be different.) Therefore

$$q = \tfrac{1}{2}a(T_1-T)^2$$

and for the whole exchanger

$$T_3-T_9 = \Delta T^\circ+\frac{a}{2C_p}(T_1-T_3)^2$$

or

$$T_9 = T_3-\Delta T^\circ-\frac{a}{2C_p}(T_1-T_3)^2$$

Now the refrigeration efficiency ϵ of the plant can be defined as

$$\epsilon = \frac{\text{cold available}}{\text{cold produced}} = \frac{T_9-T_4}{T_3-T_4}$$

$$= \frac{T_3-T_4-\Delta T^\circ-(a/2C_p)(T_1-T_3)^2}{T_3-T_4}$$

and, finally,

$$\epsilon = 1-\frac{\Delta T^\circ+(a/2C_p)(T_1-T_3)^2}{T_3-T_4}$$

Now for a liquid hydrogen refrigeration plant, we may take as typical figures:

$$\begin{aligned}\Delta T^\circ &= 3^\circ\mathrm{C}\\ T_1 &= 290^\circ\mathrm{K}\\ T_3 &= 35^\circ\mathrm{K}\\ T_4 &= 23^\circ\mathrm{K}\\ C_p &= 0{\cdot}3\ \mathrm{kcal/m^3(n.t.p.).deg.C}\\ q &= 1{\cdot}0\ \mathrm{kcal/m^3(n.t.p.)}\end{aligned}$$

Then

$$a = \frac{2q}{(T_1 - T_3)^2} = \frac{2}{(255)^2} = \frac{2}{65000}$$

and

$$\epsilon = 1 - \frac{3 + 3{\cdot}33}{12} = 0{\cdot}47$$

Without direct cold losses, the refrigeration efficiency would be 0·75.

We see that under these conditions the direct cold losses are rather greater than the losses through incomplete recuperation in the exchanger.

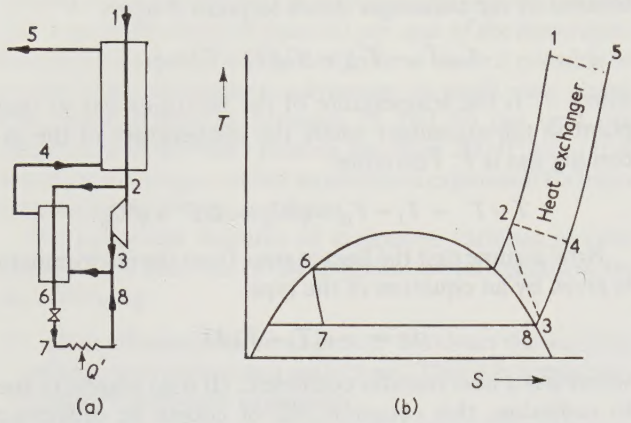

Figure 2. Low temperature cycle with isothermal cold

Isothermal cold production

The simple cycle described above supplies refrigeration within a temperature interval in the form of sensible cold in gas. In many cases this is not acceptable and the cold has to be delivered at a single (generally the lowest) temperature level in the form of latent cold of vaporization. In these cases the cycle has to be amended in such a way that a part of the circulating hydrogen is liquefied and subsequently re-evaporated at a constant temperature. This can be achieved, as shown in Figure 2, by using the sensible cold in the expanded hydrogen to condense a portion of the gas which is not passed through the turbine. The effect of this modification on the efficiency of the cycle can be shown as follows:

Let i be the portion of the circulating hydrogen passing through the turbine. Let Q be the cold produced and Q' the available cold.

Use the notation given in Figure 2 and assume for simplicity that state 8 is the same as state 3. Assume that all the hydrogen passing through the liquefier is in fact condensed. Then

$$Q = i(h_2 - h_3)$$
$$Q' = (1-i)(h_8 - h_7) = (1-i)(h_3 - h_6)$$

The total cold available from the turbine in the form of sensible cold in gas is

$$Q'' = h_4 - h_3$$

Therefore, from the balance of the liquefier,

$$Q'' = h_4 - h_3 = (1-i)(h_2 - h_6)$$

Therefore $Q'' - Q' = (1-i)(h_2 - h_3)$

The cold actually available in the form of latent cold at the lowest temperature is thus less than the total sensible cold that would be produced by passing all the gas through the turbine merely by the amount of cold not produced by that portion of the gas which does not pass through the turbine. Nevertheless, as was to be expected, the production of the whole cold as latent cold at the lowest temperature requires a greater gas circulation, and hence a greater power consumption, than is needed to produce the same amount of cold in a temperature interval bounded on the low side by this lowest temperature.

Additional turbines to compensate for non-ideality and cold losses

It has been shown that the efficiency of low temperature refrigeration plants based on the performance of work in expansion turbines is reduced by four factors.

(1) Inefficiency of turbines.
(2) Imperfect recuperation in exchangers.
(3) Non-ideality of working gas.
(4) Cold losses through heat ingress.

The first two factors allow of no compensation except by the production of the equivalent amount of additional cold at the lowest temperature. This involves the performance of additional work equal to $T_1 \Delta S/\eta$ where T_1 is ambient temperature, η is the efficiency of the gas compressor, and ΔS is the entropy increase caused by the widened temperature approach at the cold end of the exchanger.

To assess the significance of this additional work, consider a heat exchanger passing 100 m^3(n.t.p.)/hr of helium gas in either direction, operating from 20° K downwards with a constant temperature difference of 1° C between 'warm' and 'cold' streams. Assume for the sake of argument that helium may be considered as a perfect gas down to the lowest temperatures. Let 'w' and 'c' refer to the warm and cold stream respectively, and '1' and '2' to entry and outlet conditions.

Then, neglecting the effect of pressure drop in the exchanger passages, the entropy increase of the cold gas is

$$nC_p \cdot \ln(T_{c2}/T_{c1})$$

and the entropy decrease of the warm gas is

$$nC_p \cdot \ln(T_{w1}/T_{w2})$$

where n is the number of moles flowing and C_p is the molar specific heat assumed constant and equal for both streams. Putting $T_c = T_w - 1$, and inserting values for n and C_p, the overall entropy increase may be written

$$\Delta S = 24 \log \frac{1-(1/T_{w1})}{1-(1/T_{w2})} \text{ kcal per } 100 \text{ m}^3\text{(n.t.p.)} \cdot \text{deg.C}$$

Now assume that the additional work $(T\Delta S)/\eta$ required to compensate for this entropy increase is performed by compressing helium at 290° K with a compressor having an isothermal efficiency of 60 per cent. Putting $T_{w1} = 20°$ K, we then have

$$W = \frac{24 \times 290}{0{\cdot}6 \times 643} \log \frac{0{\cdot}95}{1-(1/T_{w2})}$$

$$= 18 \log \frac{0{\cdot}95}{1-(1/T_{w2})} \text{ HP.hr/100 m}^3$$

which is represented by the lower curve in Figure 3. In fact this additional work is greater because it will be necessary to pass through the heat exchanger the additional quantity of gas which has had to be compressed, and this will increase ΔS and hence W. In the upper curve in Figure 3, this additional item has been taken into account. Comparing the ordinates of this curve with the 10 HP required to compress 100 m³/hr of helium from 1 to 5 atm (the normal operating pressure of this type of plant), we see that a temperature difference of 1° C across one low temperature heat exchanger may entail considerable additional power consumption over that needed in the ideal case of perfect heat exchange.

The non-ideality of the gas at low temperatures and the cold losses due to heat ingress from the surroundings can be partially compensated with a smaller increase in power consumption, as these losses are not all incurred at the lowest temperatures. If the increased cold production needed is obtained by raising the inlet pressure and thus increasing the pressure differential across the turbine, it will be advantageous to introduce a second turbine in series with the first and separated from it by a heat exchanger. The arrangement is shown schematically in Figure 4(a) and explained in Figure 4(b). The latter shows the heat absorbed from the warm gas and taken up by the cold gas as a function of temperature. Assume that T_1 and T_2 are fixed. In the case of a uniformly perfect gas, a perfect

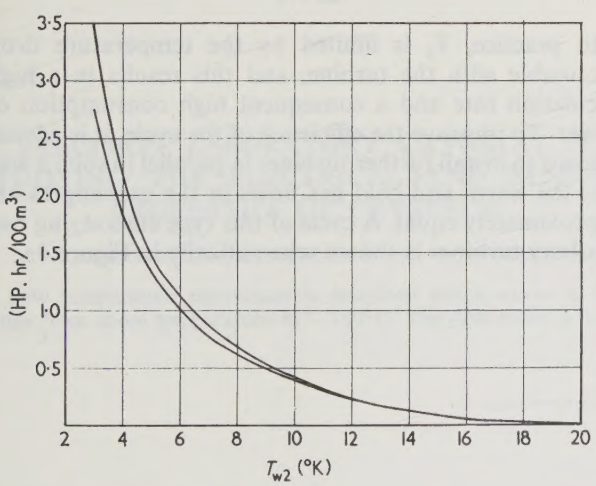

Figure 3. Additional power requirement for 1° temperature approach in low temperature exchanger

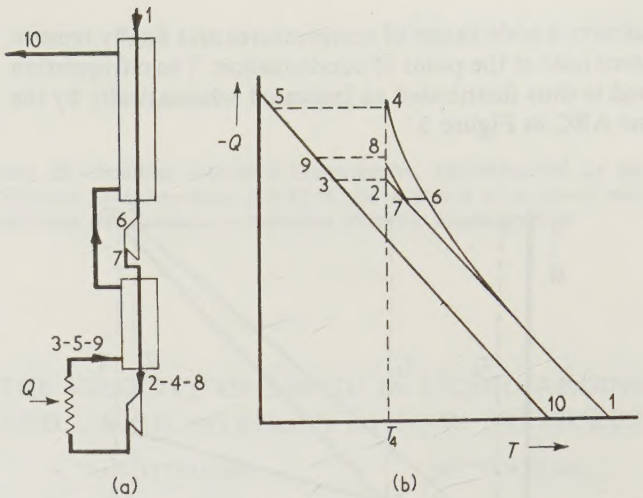

Figure 4. Low temperature cycle with two turbines in series

heat exchanger and a perfect turbine, the warm gas will be represented by the line 1–2 and the cold gas by the parallel line 3–10. As a result of gas non-ideality and cold losses through heat ingress from the surroundings, the amount of heat that has to be withdrawn from the warm gas is increased, especially in the low temperature region. To reach the temperature T_2 the warm gas therefore has to follow the line 1–4. As the cold gas, being at low pressure, remains virtually a perfect gas throughout, it has to re-enter the heat exchanger at a substantially lower temperature T_5 in order to withdraw the larger amount of heat from the warm gas. By introducing a second turbine with its inlet at point 6 and its outlet at point 7, the heat absorbed by this machine no longer has to be taken up by the cold gas. The warm gas then reaches the temperature T_2 at point 8 and the cold gas has to re-enter the exchanger at point 9, which is colder than point 3 but warmer than point 5. As the cold production per unit flow and pressure differential is greater at the higher temperatures 6–7 than at the lower temperatures 8–9, the overall compression costs are smaller for the two turbines than they would be if all the lost cold had to be made up by expansion at the lowest temperatures.

To avoid misunderstanding, it should be pointed out that Figure 4(b) is not an H–T diagram. Thus the line 1–6–4 does not represent the enthalpy of unit mass of hydrogen at a certain pressure as a function of temperature, but the amount of heat that has to be withdrawn from the initially warm gas by initially cold gas. The horizontal line 6–7 does not mean that expansion in a turbine occurs at constant enthalpy, but that in the temperature interval between T_6 and T_7 no heat has to be transferred from the warm gas to the cold gas. The heat that has to be removed from the warm gas to cool it from T_6 to T_7 is removed by the turbine (in the form of work) and not by the cold gas.

Low temperature cycles to remove heat over a wide temperature interval

As explained earlier, a refrigeration plant to be used for liquefying a low-boiling gas has to withdraw heat from the

gas over a wide range of temperatures and finally remove latent heat at the point of condensation. The refrigeration load is thus distributed as indicated schematically by the line ABC in Figure 5.

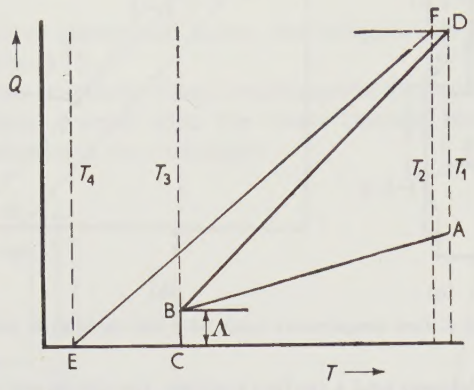

Figure 5. Liquefaction cycle with one turbine

To carry this load, a certain portion of the gas—or of another refrigerant gas—has to be circulated and passed through one or more turbines, thereupon returning to the compressor.

In many cases the working substance of the refrigerating cycle may be the same as the gas to be liquefied, but for practical reasons it is generally advantageous to keep the two streams separate and to employ a closed refrigerating cycle. Then only the process stream requires careful purification and the pressures of the two streams at various points in the plant can be chosen independently in such a way as to reduce the overall power consumption to a minimum.

If only one turbine is used at the lowest temperature, the flow of warm gas to be cooled is greater than the flow of cold gas by the amount being liquefied and withdrawn from the system. Thus the cold end temperature approach of the exchanger is bound to be wider than the warm end approach. If the total load (liquefied gas plus circulating refrigerant) is given by the line DBC in Figure 5, the heat content of the returning refrigerant may be represented by the line EF, which is less steep than BD. In this Figure: T_1 is the temperature at which process and refrigerant gas enter the exchanger; T_2 is the outlet temperature of the refrigerant at the warm end; T_3 is the liquefaction temperature of the process gas, assumed for the sake of simplicity to be the same as the turbine inlet temperature; T_4 is the turbine outlet temperature; Λ is the latent heat of condensation of the process gas.

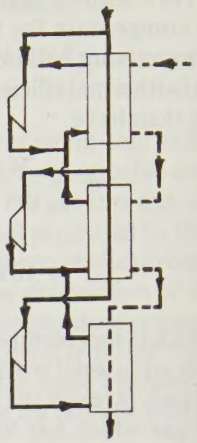

Figure 6. Liquefaction cycle with turbines in parallel

If M is the ratio of refrigerant to process gas flow, it can be shown that, with fair approximation

$$M = \frac{(\Lambda/C_p)+(T_1-T_3)}{(T_3-T_4)-(T_1-T_2)}$$

where C_p is the specific heat, assumed to be the same, for process and refrigerant gases.

Thus the 'circulation rate' M increases with increasing Λ and decreases with falling T_4. As an example, let

$\Lambda = 46$ kcal/kg
$C_p = 0{\cdot}24$
$T_1 = 280°$ K
$T_2 = 276°$ K
$T_3 = 115°$ K
$T_4 = 90°$ K

Then

$$M = \frac{191+175}{25-4} = 17$$

In practice, T_4 is limited by the temperature drop obtainable with the turbine, and this results in a high circulation rate and a consequent high consumption of power. To improve the efficiency of the cycle, it is advantageous to install further turbines in parallel in such a way that the warm and cold gas flows in the exchangers are approximately equal. A cycle of this type embodying two auxiliary turbines is shown schematically in Figure 6.

Abstracts

THE MAGNETIC FORCES ON SUPERCONDUCTORS AND THEIR APPLICATIONS FOR MAGNETIC BEARINGS

T. A. BUCHHOLD

THE electromagnetic forces acting in a thin layer at the surface of a superconductor are treated as the interaction of the magnetic flux with the surface currents. The calculated forces agree well with experiments. In using the surface forces, which are repellent, stable superconductive bearings can be built with proper coil arrangements. Several schemes are discussed and a theory of the bearing stiffness is developed which is supported by experiments as long as the material is entirely superconductive. In order to obtain stiff bearings the leakage flux must be kept small.

THE SPECIFIC HEAT AT CONSTANT VOLUME, THE ENTROPY, THE INTERNAL ENERGY, AND THE FREE ENERGY OF LIQUID HELIUM-4 BETWEEN 1·2 AND 2·9° K

O. V. LOUNASMAA

TABLES of the specific heat at constant volume (from 1·2 to 2·9° K), the entropy, and the internal energy (both from 1·5 to 2·9° K) of liquid helium-4 between the solidification and vaporization curves are published, together with diagrams of these functions and of the free energy. The results are based on new measurements of the equation of state (p and $(\partial p/\partial T)_V$) near 1·75° K, on specific heat data by Lounasmaa and Kojo (*Ann. Acad. Sci. fenn.* **AVI,** No. 36 (1959)) between 1·5 and 2·9° K, and, from 1·2 to 1·5° K, on specific heats by Hercus and Wilks (*Phil. Mag.* **45,** 1163 (1954)), after a correction was applied to them. The accuracy of the results is estimated as 2 per cent between 1·5° K and the λ curve, and 1 per cent in the helium-I region.

A PRECISION LABORATORY CRYOSTAT FOR STUDYING THE ELECTRICAL AND ELASTIC PROPERTIES OF CRYSTALS

V. A. KOPTSIK B. A. STRUKOV L. A. ERMAKOVA

A LOW temperature thermostat is described which works in the range from room temperature to −140° C. The possibility is foreseen of obtaining stabilized temperatures, thermostatted to an accuracy no worse than ±0·005° C for a period of an hour and sufficient for carrying out precision dielectric measurements.

THE VELOCITY OF SOUND IN LIQUID ARGON AND LIQUID NITROGEN AT HIGH PRESSURES

A. VAN ITTERBEEK W. VAN DAEL

THE velocity of propagation of ultrasonic pulses in liquid argon and liquid nitrogen has been measured at pressures up to 200 kg/cm² and at temperatures between 77° K and 90° K.

A DIRECT READING CONSTANT VOLUME GAS THERMOMETER

J. K. HULM R. D. BLAUGHER

A CONSTANT volume helium gas thermometer was made direct reading by utilizing a low dead space aneroid manometer for pressure determination. This arrangement eliminates the time-consuming adjustments which are characteristic of the constant volume gas thermometer when a mercury-in-glass manometer is used. The new system is easy to calibrate, rapid reading, and permits temperatures between 4·2 and 20° K to be determined with an accuracy of 0·02° K.

THE CLARENDON LABORATORY HELIUM LIQUEFIER

A. J. CROFT B. R. BLIGH

THIS paper describes the Linde helium liquefier which was designed and built at the Clarendon Laboratory. It is supplied with liquid hydrogen from an existing plant and makes 10 l./hr. The belief that such a plant would prove more reliable and would require less maintenance than an expansion engine liquefier has been borne out by experience over the four years since it was in operation. Details are given of the associated machinery, the purification arrangements, the design of the heat-exchangers, the safety precautions, the operating procedure, and the performance.

Résumés

LES FORCES MAGNETIQUES SUR LES SUPRACONDUCTEURS ET LEURS APPLICATIONS POUR LES PALIERS MAGNETIQUES

T. A. BUCHHOLD

Les forces électromagnétiques qui agissent dans une fine pellicule à la surface d'un supraconducteur sont considérées, par l'auteur, comme résultant de l'interaction du flux magnétique et des courants superficiels. Les forces calculées théoriquement correspondent bien à celles qu'on trouve dans les expériences. En se servant des forces superficielles qui sont répulsives, on peut fabriquer des paliers supraconducteurs stables avec des dispositifs de bobines appropriés. L'auteur examine plusieurs schémas et formule une théorie de la rigidité des paliers qui s'accorde avec l'expérience aussi longtemps que le matériau utilisé est entièrement supraconducteur. Pour obtenir des paliers rigides, il faut que le flux de fuite soit aussi faible que possible.

LA CHALEUR SPECIFIQUE A VOLUME CONSTANT, L'ENTROPIE, L'ENERGIE INTERNE ET L'ENERGIE LIBRE DE L'HELIUM-4 LIQUIDE ENTRE 1,2 ET 2,9° K

O. V. LOUNASMAA

L'auteur publie des tableaux de la chaleur spécifique à volume constant (de 1,2 à 2,9° K), de l'entropie et de l'énergie interne (toutes deux entre 1,5 et 2,9° K) de l'hélium-4 liquide entre les courbes de solidification et de vaporisation; il donne également des diagrammes de ces fonctions et de l'énergie libre. Les résultats sont fondés sur de nouvelles mesures de l'équation de l'état près de 1,75° K (p et $(\partial p/\partial T)_V$), sur des données de chaleur specifique établies par Lounasmaa et Kojo (*Ann. Acad. Sci. fenn.* **AVI**, No. 36 (1959)) entre 1,5 et 2,9° K et, entre 1,2 et 1,5° K, sur des chaleurs spécifiques de Hercus et Wilks (*Phil. Mag.* **45**, 1163 (1954)) après correction. On estime que la précision des résultats est de l'ordre de 2 pour cent entre 1,5° K et la courbe λ, et de 1 pour cent dans la région de l'hélium-I.

UN CRYOSTAT DE LABORATOIRE DE PRECISION POUR L'ETUDE DES PROPRIETES ELECTRIQUES ET ELASTIQUES DES CRISTAUX

V. A. KOPTSIK B. A. STRUKOV L. A. ERMAKOVA

Les auteurs décrivent un thermostat basses températures qui fonctionne dans une gamme comprise entre la température de la chambre et −140° C. Ils envisagent la possibilité d'obtenir au thermostat, avec une précision qui serait inférieure à ±0,005° C, des températures suffisamment stabilisées, pendant une heure, pour des mesures diélectriques précises.

LA VITESSE DU SON DANS L'ARGON LIQUIDE ET L'AZOTE LIQUIDE AUX PRESSIONS ELEVEES

A. VAN ITTERBEEK W. VAN DAEL

La vitesse de propagation des impulsions ultrasoniques dans l'argon liquide et l'azote liquide a été mesurée à des pressions allant jusqu' à 200 kg/cm² et à des températures de 77 à 90° K.

THERMOMETRE A GAZ A VOLUME CONSTANT ET LECTURE DIRECTE

J. K. HULM R. D. BLAUGHER

On a réalisé un thermomètre à hélium à volume constant pouvant être lu directement en utilisant un manomètre anéroïde à faible espace mort pour déterminer la pression. On élimine ainsi les réglages qui font perdre tellement de temps et qui caractérisent les thermomètres à gaz à volume constant utilisant un manomètre à mercure dans du verre. Le nouveau système est facile à calibrer, rapide à lire et permet de mesurer des températures de 4,2 à 20° K avec une précision de 0,02° K.

LE LIQUEFACTEUR D'HELIUM DU LABORATOIRE CLARENDON

A. J. CROFT B. R. BLIGH

L'article décrit le liquéfacteur d'hélium Linde qui a été étudié et construit dans le Laboratoire Clarendon. Il est alimenté en hydrogène liquide à partir d'une installation existante et produit 10 litres par heure. On croyait que cette installation serait plus sûre et demanderait moins d'entretien que les liquéfacteurs à moteur à détente; quatre ans d'expérience pratique ont démontré que cette prévision était bien fondée. L'article donne des détails sur les machines connexes, les dispositions prises pour la purification, le dessin des échangeurs de chaleur, les précautions de sécurité, le mode d'opération et la performance.

Auszüge

DIE MAGNETISCHEN KRÄFTE IN SUPRALEITERN UND IHRE BEDEUTUNG FÜR MAGNETISCHE LAGER

T. A. BUCHHOLD

Die in einer dünnen Schicht auf der Oberfläche von Supraleitern wirkenden elektromagnetischen Kräfte werden als Wechselwirkung zwischen dem magnetischen Fluss und den Oberflächenströmen behandelt. Die berechneten Kräfte stimmen gut mit den Versuchsergebnissen überein. Unter Benützung der abstossenden Oberflächenkräfte lassen sich mittels geeigneter Spulenanordnung stabile supraleitende Lager aufbauen. Der Artikel bespricht einige Lösungen und entwickelt eine Theorie über steife Lager, die durch Versuche gestützt wird, vorausgesetzt dass das Material vollkommen supraleitend ist. Um steife Lager zu erhalten, muss der Streufluss klein gehalten werden.

DIE SPEZIFISCHE WÄRME BEI GLEICHBLEIBENDEM VOLUMEN, DIE ENTROPIE, DIE INNERE ENERGIE UND DIE FREIE ENERGIE VON FLÜSSIGEM HELIUM-4 ZWISCHEN 1,2 UND 2,9°K

O. V. LOUNASMAA

Eine Veröffentlichung von Tabellen der spezifischen Wärme bei gleichbleibendem Volumen (von 1,2 bis zu 2,9°K), der Entropie und der inneren Energie (beide von 1,5 bis zu 2,9°K) von flüssigem Helium zwischen den Erstarrungs- und Verdampfungskurven, mit Diagrammen dieser Funktionen und der freien Energie. Die Resultate beruhen auf neuen Messungen der Zustandsgleichung (p und $\partial p/\partial T)_V$) bei ca. 1,75°C, auf spezifischen Wärmedaten von Lounasmaa und Kojo (*Ann. Acad. Sci. fenn.* **AVI**, Nr. 36 (1959)) zwischen 1,5 und 2,9°K und von 1,2 bis zu 1,5°K, auf spezifischen Wärmen von Hercus und Wilks (*Phil. Mag.* **45**, 1163 (1953)), nach durchgeführter Korrektur. Die Genauigkeit der Resultate wird zwischen 1,5°K und der λ-Kurve auf 2% und in der Helium-I Zone auf 1% geschätzt.

EIN PRÄZISIONSKRYOSTAT ZUR UNTERSUCHUNG ELEKTRISCHER UND ELASTISCHER EIGENSCHAFTEN VON KRISTALLEN

V. A. KOPTSIK B. A. STRUKOV L. A. ERMAKOVA

Ein Tieftemperaturkryostat wird beschrieben, der im Gebiet zwischen Zimmertemperatur und −140°C arbeitet. Die Möglichkeit ist vorgesehen, Temperaturen bis zu ±0,005° oder besser auf die Zeitdauer einer Stunde konstant zu halten, um sehr genaue dielektrische Messungen auszuführen.

DIE SCHALLGESCHWINDIGKEIT IN FLÜSSIGEM ARGON UND FLÜSSIGEM STICKSTOFF BEI HOHEN DRÜCKEN

A. VAN ITTERBEEK W. VAN DAEL

Die Fortpflanzungsgeschwindigkeit von Überschallimpulsen in flüssigem Argon und flüssigem Stickstoff wurde bei Drücken von bis zu 200 kg/cm² und bei Temperaturen zwischen 77°K und 90°K gemessen.

GLEICHRAUMGASTHERMOMETER MIT DIREKTER ANZEIGE

J. K. HULM R. D. BLAUGHER

Ein Gleichraumheliumthermometer mit direkter Anzeige benützt ein Aneroidmanometer mit niedrigem Totraum zur Druckbestimmung. Diese Anordnung beseitigt die zeitraubenden Einstellungen, welche für Gleichraumgasthermometer charakteristisch sind, wenn ein Quecksilber-Glas-Manometer benützt wird. Dieses neue System lässt sich leicht kalibrieren, leicht ablesen und gestattet es, Temperaturen zwischen 4,2°K und 20°K mit einer Genauigkeit von 0,02°K zu bestimmen.

HELIUMVERFLÜSSIGER IN CLARENDON LABORATORIUM

A. J. CROFT B. R. BLIGH

Der Artikel beschreibt den Linde-Heliumverflüssiger, der im Clarendon-Laboratorium konstruiert und gebaut wurde. Er wird aus einer bestehenden Anlage mit flüssigem Wasserstoff beliefert und erzeugt 10 l./h. Die Annahme, dass eine solche Anlage verlässlicher und im Betrieb billiger sei als eine Expansionsmaschine, wird durch die vierjährige Praxis bestätigt. Der Artikel gibt Einzelheiten über die maschinelle Einrichtung, die Reinigungsanlagen, die Konstruktion der Wärmeaustauscher, die Sicherheitmassnahmen, den Betrieb und die Leistung.

Резюме

МАГНИТНЫЕ СИЛЫ НА СВЕРХПРОВОДНИКАХ И ИХ ПРИМЕНЕНИЯ ДЛЯ МАГНИТНЫХ ОПОР

T. A. BUCHHOLD

Электромагнитные силы действующие в тонком слое у поверхности сверхпроводника рассматриваются как взаимодействие магнитного потока с поверхностными токами. Вычисленные силы хорошо соглашаются с опытами. Применяя поверхностные силы, которые являются отталкивающими, возможно построить устойчивые сверхпроводящие опоры с подходящими системами катушек. Обсуждается несколько схем и излагается теория жесткости опоры, которая подтверждается опытами пока материал является совсем сверхпроводящим. Необходимо поддерживать поток рассеяния маленьким чтобы достать жесткие опоры.

УДЕЛЬНАЯ ТЕПЛОТА ПРИ ПОСТОЯННОМ ОБЪЕМЕ, ЭНТРОПИЯ, ВНУТРЕННЯЯ ЭНЕРГИЯ И СВОБОДНАЯ ЭНЕРГИИ ЖИДКОГО ГЕЛИЯ-4 МЕЖДУ 1,2 И 2,9° К

O. V. LOUNASMAA

Подаются таблицы удельной теплоты при постоянном объеме (от 1,2 до 2,9° К), энтропии, и внутренней энергии (оба от 1,5 до 2,9° К) жидкого гелия-4 между кривыми отвердевания и исцарения вместе с диаграммами этих функциями и свободной энергии. Результаты основаны на новые измерения уравнения состояния (p и $(\partial p/\partial T)_v$) близ 1,75° К, на данные удельной теплоты Лоунасмаа и Коджо (*Ann. Acad. Sci. fenn. AVI*, № 36 (1959)) между 1,5 и 2,9° К и, от 1,2 до 1,5° К, на удельные теплоты Геркус и Вилкс (*Phil. Mag.* 45, 1163 (1954)), после того, как поправка приложена к ним. Вычислена точность результатов — 2% между 1,5° К и λ кривой и 1% в области гелия-I.

ПРЕЦИЗИОННЫЙ ЛАБОРАТОРНЫЙ КРИОСТАТ ДЛЯ ИССЛЕДОВАНИЯ ЭЛЕКТРИЧЕСКИХ И УПРУГИХ СВОЙСТВ КРИСТАЛЛОВ

V. A. KOPTSIK B. A. STRUKOV L. A. ERMAKOVA

Описан низкотемпературный термостат, работающий в интервале температур от комнатной до —140° С. Предусмотрена возможность получения стабилизированных температурных точек, точность термостатирования не хуже ± 0,005° С в течение 1 hr и достаточна для проведения прецизионных диэлектрических измерений.

СКОРОСТЬ ЗВУКА В ЖИДКОМ АРГОНЕ И ЖИДКОМ АЗОТЕ ПРИ ВЫСОКИХ ДАВЛЕНИЯХ

A. VAN ITTERBEEK W. VAN DAEL

Скорость распространения ультразвуковых импульсов в жидком аргоне и жидком азоте измерилась при давлениях до 200 кг/см² и при температурах между 77° К и 90° К.

ПРЯМООТСЧЕТНЫЙ ТЕРМОМЕТР С ГАЗОМ ПОСТОЯННОГО ОБЪЕМА

J. K. HULM R. D. BLAUGHER

Термометр газообразного гелия постоянного объема был сделан прямоотсчетным путем применения анероидного манометра с низким мертвым пространством для определения давлений. Это устройство исключает долговременные установки характерирующие термометр с газом постоянного объема когда применяется манометр типа „ртуть-в-стекле". Новый систем легко калибрируется, измерения быстро отсчитаны и систем позволяет определять температуры между 4,2° К и 20° К с точностью 0,02° К.

РАЗЖИЖИТЕЛЬ ГЕЛИЯ У ЛАБОРАТОРИИ КЛАРЕНДОН

A. J. CROFT B. R. BLIGH

В этой статье описывается разжижитель гелия типа Линдэ который был разработан и построен у Лаборатории Кларендон. Он питается жидким водородом из существующей установки и производит 10 л/ч. Предположение что такая установка является более надежной и требует меньшего обслуживания чем разжижитель с детандера пара подтвердилось опытом за четыре года от его приведения в действие. Даются подробности связанного оборудования, очистительных устройств, конструкции теплообменников, предосторожностей для обеспечения безопасности, рабочего процесса и производительности.

The Magnetic Forces on Superconductors and Their Applications for Magnetic Bearings

T. A. Buchhold *General Electric Company, Schenectady, N.Y.*

Received 27 July 1960
In revised form 6 December 1960

ABOUT twenty metals and many alloys and compounds are known which lose their electrical resistivity entirely and become superconductive if cooled to a temperature of a few degrees Kelvin. Good conductors at normal temperature, such as copper and silver, and ferromagnetic metals such as iron generally do not become superconductive. If a superconductor is exposed to a magnetic field which exceeds the critical field strength H_c of the material, the superconductivity is destroyed and the material becomes resistive. Figure 1 shows this behaviour for a few metals. The abscissa is the absolute temperature T and the ordinate is the critical field strength H_c where the material loses superconductivity. The critical field depends on the measuring method and the geometry of the specimen. The author used the method of sending a d.c. current through a 1 mm wire and determined the field strength at the surface before breakdown of superconductivity. The metal niobium becomes superconductive at about 8°K. At 4·2°K, the boiling point of liquid helium, niobium shows zero resistance in fields up to about 3,000 oersteds. The critical field for niobium and also for other metals can, however, vary considerably depending on impurities and on stresses in the material. Alloys and compounds are known which have a higher transition temperature (e.g. 18°K for Nb_3Sn). Not much is known about their critical fields.

In our study we are interested in materials, such as niobium, with a high critical field strength so that the material is always superconductive.

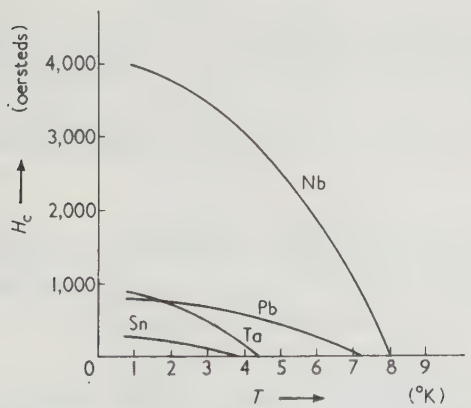

Figure 1. Critical field strength as a function of absolute temperature

Under ideal conditions magnetic flux cannot penetrate into a superconductor. Since this feature is of fundamental importance in connection with electromagnetic surface forces on superconductors and in the design of superconductive bearings, it will be discussed in more detail.

Surface forces

Figure 2(a) shows the cross-section (i) of a wire and adjacent to it a plate (ii) of a non-superconductive metal.

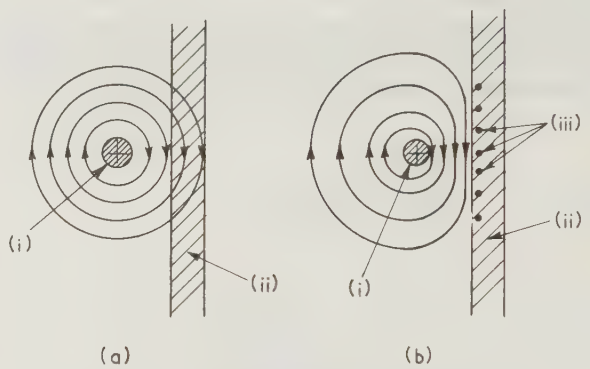

Figure 2. Magnetic field of a current: (a) Penetrates a non-superconductor; (b) Does not penetrate a superconductor

If a current flows through the wire and builds up quickly from zero to full value, the increasing magnetic flux penetrates the plate and produces countercurrents in it which oppose the flux. These currents decay and the flux lines in Figure 2(a) are no longer influenced by the metal plate. However, it is known that a high frequency current produces continuously opposing eddy current in a thin surface layer of the metal plate, and the flux can penetrate only into this layer which becomes thinner with higher frequency and higher conductivity of the metal.

The conditions in a superconductor are somewhat similar. Let us assume that in Figure 2(b) the d.c. current in the wire increases from zero to its full value. Surface countercurrents (iii) which exactly cancel the flux are produced in the plate. Since the resistance is zero, such currents do not decay. They are proportional to the current in the wire. Since the magnetic flux is thus prevented from entering the metal, the superconductor appears perfectly diamagnetic. The theory, which takes into

account the mass of the electrons, shows that the penetration depth for the currents and the flux is finite but small (of the order of 10^{-4} mm), and for our applications can be neglected. Complete diamagnetism is only achieved if the material is made superconductive prior to the application of the magnetic field. If the field is first applied and then superconductivity achieved by cooling down, frequently less than the entire flux is expelled from the material (Meissner effect) and a part stays frozen in.

Figure 3(a) and (b) shows how the flux density B_x, which is parallel to the surface, and the current density j_x decrease with increasing distance x from the surface (x is exaggerated in the drawing). Figure 3(a) indicates how the so-called penetration depth λ is normally defined. In the electromagnetic system of units the field strength H_x is equal to B_x if the permeability is $\mu = 1$ as is true in this case. Figure 3(c) shows the surface current which is defined as

$$i_x = \int_0^x j_x \mathrm{d}x$$

This term becomes the specific surface current i if x is large compared with λ.

It will be derived that the specific surface current i and the flux density B_0 (or the field strength H_0) at the surface are proportional to each other. The line integral $\int H \mathrm{d}l$ for

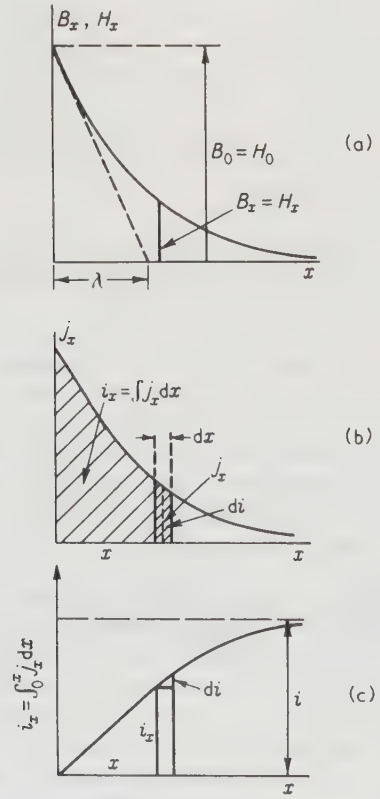

Figure 3. (a) Flux density B_x; (b) Current density j_x; (c) Surface current i_x as a function of penetration x

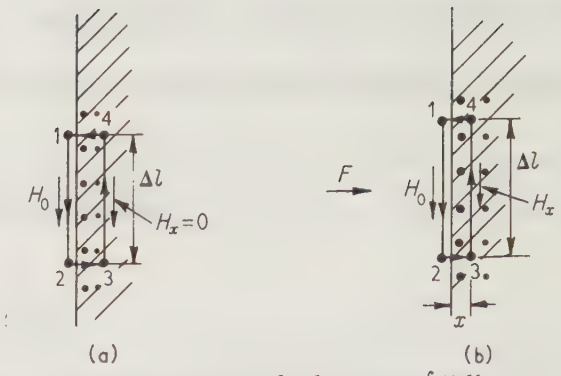

Figure 4. Diagram for determining $\int H \mathrm{d}l$

the magnetic field strength H may be formed along the path 1–2–3–4–1 in Figure 4(a). The line element Δl at 3–4 is at such a distance that B_x and H_x and j_x are practically zero. The line integral becomes $H_0 \Delta l$ (H_0 = field strength on surface) and encloses the surface current $i\Delta l$. The line integral according to Maxwell's law is

$$H_0 \Delta l = 4\pi i \Delta l$$

or, since $H_0 = B_0$,

$$B_0 = H_0 = 4\pi i \qquad \ldots (1)$$

If B is measured in gauss and the specific surface current not in electromagnetic units but in amperes per centimetre, one obtains

$$B_0 = \frac{4\pi}{10} i \qquad \ldots (2)$$

This equation is not only valid for the induced currents in the plate of Figure 2(b) but for any superconducting surface, and therefore for the wire (i) in which the current flows in a thin layer of the surface.

According to Figure 3, at the distance x from the surface, the flux density is B_x and a current $j_x \mathrm{d}x = \mathrm{d}i$ flows in the interval $\mathrm{d}x$. Therefore a force $\mathrm{d}F$ is produced which in e.m.u. is

$$\mathrm{d}F = B_x \mathrm{d}i \Delta l \Delta a \qquad \ldots (3)$$

Δl is the length of the surface element and Δa its width (perpendicular to plane of paper in Figure 4(b)). The integral

$$F = \Delta l \Delta a \int_{x=0}^{x=\infty} B_x \mathrm{d}x$$

can be rewritten according to the integral calculus

$$F = \Delta l \Delta a \left[B_x i_x - \int i_x \mathrm{d}B_x \right]_{x=0}^{x=\infty}$$

The first term in the bracket disappears since $i_x = 0$ for $x = 0$ and $B_x = 0$ for $x = \infty$; therefore

$$F = -\Delta l \Delta a \int_{x=0}^{x=\infty} i_x \, dB_x \qquad \ldots(4)$$

To express i_x by B_x the line integral for H along the path 1–2–3–4–1 in Figure 4(b) is formed. The element 3–4 is at a distance x from the surface, the field strength is H_x and the current within 0–x is i_x. The field strength at the surface will be H_0. The line integral yields

$$H_0 \Delta l - H_x \Delta l = 4\pi i_x \Delta l$$

or
$$i_x = \frac{H_0 - H_x}{4\pi}$$

or
$$i_x = \frac{B_0 - B_x}{4\pi} \qquad \ldots(5)$$

Inserting equation (5) in equation (4)

$$F = -\frac{\Delta l \Delta a}{4\pi} \int_{x=0}^{x=\infty} (B_0 - B_x) dB_x$$

or
$$F = -\frac{\Delta l \Delta a}{4\pi} \left[B_0 B_x - \frac{B_x^2}{2} \right]_{x=0}^{x=\infty}$$

Since $B_x = B_0$ for $x = 0$, $B_x = 0$ for $x = \infty$

$$F = \frac{B_0^2}{8\pi} (\Delta l \Delta a) \qquad \ldots(6)$$

Since $\Delta l \Delta a$ is the surface area, the specific force per unit surface is

$$f = \frac{B_0^2}{8\pi} \qquad \ldots(7a)$$

The direction of the force is always perpendicular to the surface. Figure 2(b) gives the impression that the magnetic lines are compressed and press against the surface of the superconductor. This impression is justified by equation (7*a*) because, according to the Maxwell theory, parallel magnetic lines repel each other and their repulsive force per unit area is also $B_0^2/8\pi$. One obtains, therefore, correct results in assuming that the magnetic lines press against the surface of the superconductor with the surface force of equation (7*a*). However, one has to be aware that in reality the forces are produced by the interaction of the magnetic field and the currents in the surface layer. In equation (7*a*) the specific force f is obtained in dyn/cm² if B_0 is measured in gauss. If f is measured in kg/cm², the following simplified equation can be obtained (error only 1·5 per cent)

$$f = \left(\frac{B_0}{5000} \right)^2 \quad \text{(in kg/cm}^2\text{)} \qquad \ldots(7b)$$

For example, with a flux density of $B_0 = 2{,}500$ gauss, a force

$$f = \left(\frac{2500}{5000} \right)^2 = 0{\cdot}25 \text{(kg/cm}^2\text{)}$$

can be obtained.

For niobium the critical field may be 3,000 or sometimes even 4,000 oersteds at 4·2° K. Improvements in the critical field yield considerable improvements in the force because it grows with the second power of the flux density.

Superconductive bearings

Figure 5(a) shows the cross-section of a flat cylinder 'a' of iron in which a coil 'b' of superconductive material (e.g. niobium) is embedded. Above the coil, separated by a gap of length x, is a superconductive disk 'c' with a shaft which can move up and down and which is guided by mechanical bearings 'd'.

If the coil with N turns is excited by a current I (in amperes), a flux density B in gauss

$$B = \frac{4\pi}{10} \frac{IN}{l_0 + \Delta l} = \frac{4\pi}{10} \frac{IN}{l}$$

$$l = l_0 + \Delta l \qquad \ldots(8)$$

is obtained where l_0 is the width of the coil. Δl is a correction that takes into account that the magnetic path in the gap is a little longer than l_0 and also that the iron has some reluctance. For small gaps and good iron Δl can often be neglected or at least taken as constant.

The magnetic force F pushes the disk upwards with (equation (7*b*))

$$F = 2\pi r l_0 \left(\frac{B}{5000} \right)^2 \text{(in kg)} \qquad \ldots(9)$$

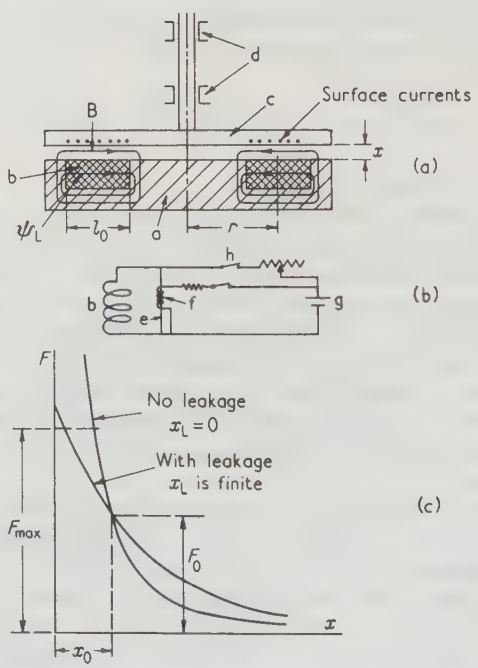

Figure 5. (a) Bearing test model; (b) Circuitry to trap a flux; (c) Bearing force as a function of gap

r is the average radius of the coil and $(2\pi r l_0)$ is the effective surface for the force. B is the average flux density in the gap. If $l = l_0 + \Delta l$ is constant, B and F are also constant and independent of the gap x for a given current. Tests show sometimes that with increasing gap the force decreases slightly because Δl increases somewhat with the gap. In the following discussion we will neglect a change of Δl with x and assume that l is constant.

After a current is established and a flux is linked with the superconductive coil 'b' the coil is short-circuited. For a coil circuit with a resistance R the flux ψ decays according to

$$-\frac{d\psi}{dt} = IR \qquad \ldots(10a)$$

ψ is the linked flux. For a superconductive coil $R = 0$, so equation (10a) becomes

$$-\frac{d\psi}{dt} = 0$$

$$\psi = \psi_0 = \text{constant} \qquad \ldots(10b)$$

This law of the constancy of the linked flux is important and means for Figure 5(a) that moving the disk 'c' does not change the flux. If we neglect any leakage flux through the coil the flux going through the gap x is

$$\psi = k_1 Bx \qquad \ldots(11)$$

where k_1 is a constant or

$$B = \frac{\psi}{k_1 x} \qquad \ldots(12)$$

Since the force (equation (9)) is proportional to B^2 and since ψ is constant the force becomes

$$F = \frac{k}{x^2} \qquad \ldots(13)$$

where k is another constant.

This repelling force increases rapidly if x is decreased. It has to be emphasized that with decreasing gap x only the flux ψ stays constant, while the flux density B increases. Therefore, according to equation (8), the coil current increases too. To push down the disk requires mechanical work which is stored as magnetic energy in the gap. The force is a repelling force and not an attractive force as obtained in normal magnetic or electrostatic devices. This is the reason for being able to build stable superconductive bearings.

Figure 5(b) shows schematically how the coil 'b' in Figure 5(a) can be short-circuited. In Figure 5(b) the coil 'b' is shunted by a superconductive wire 'e' which is surrounded by a heater coil 'f' made of resistive wire. If the coil 'f' is energized, heat is produced and the temperature of the shunt 'e' increases a few degrees and the shunt loses superconductivity and becomes resistive. A current from the supply 'g' flows only through the coil 'b' which has no resistance. The heating of the shunt wire 'c' is interrupted and 'e' becomes superconductive again. The switch 'h' can be opened and the current in the coil flows over the superconductive shunt 'e' and the coil flux is trapped.

The influence of the leakage flux ψ_L going through the coil 'b' in Figure 5(a) shall be studied. This flux cannot go through the superconductive wires because they act as magnetic insulators. However, it can penetrate their electrical insulation. This leakage has a considerable influence if comparable with the flux going through a small gap. The entire flux linked with the coil 'b' of Figure 5(a) can be written

$$\psi = k_1 Bx + LI \qquad \ldots(14)$$

The first term is the flux in the gap (equation (11)) and the second term is the leakage flux, independent of x. Since B is proportional to the current I the leakage flux may be expressed in terms of a fictitious constant gap x_L which has the same flux density B

$$\psi_L = LI = k_1 Bx_L \qquad \ldots(15)$$

Equation (14) and equation (15) yield

$$\psi = k_1 B(x + x_L) \qquad \ldots(16)$$

or

$$B = \frac{\psi}{k_1}\frac{1}{x + x_L} \qquad \ldots(17)$$

Since the force is proportional to B^2, the force F becomes:

$$F = \frac{k_0}{(x + x_L)^2} \qquad \ldots(18)$$

where k_0 is a constant.

Let us assume that the gap is x_0 when the coil 'b' is energized. The obtained force (equation (18)) is

$$F_0 = \frac{k_0}{(x_0 + x_L)^2} \qquad \ldots(19)$$

Equations (18) and (19) yield

$$F = F_0\left(\frac{x_0 + x_L}{x + x_L}\right)^2 \qquad \ldots(20)$$

The maximum force F_{max} is obtained if the critical field H_c is reached either at the coil or the disk surface. The force F is plotted in Figure 5(c) for $x_L = 0$ (no leakage) and for a finite x_L (leakage). The restoring force improves with decreasing gap and is much stronger for $x_L = 0$. Therefore, the leakage flux must be kept small.

In Figure 6(a) the disk 'a' is located between two coils 'b_1' and 'b_2' and both coils are energized (by flux trapping) with the disk in the middle $x_1 = x_2 = x_0$. If the disk is moved downward Δx the gap x_1 is reduced and the upper gap x_2 is increased

$$x_1 = x_0 - \Delta x$$

$$x_2 = x_0 + \Delta x \qquad \ldots(21)$$

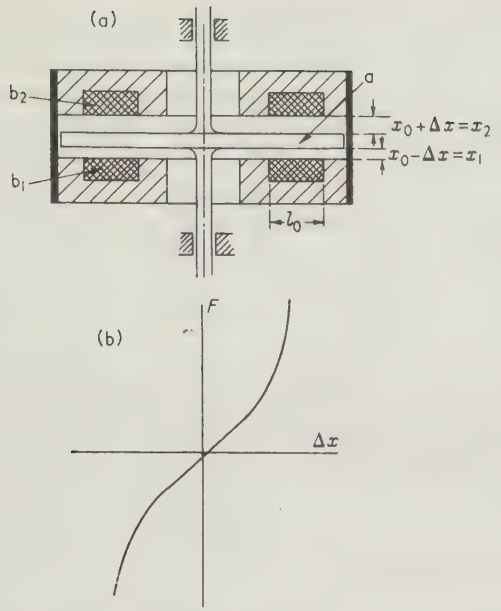

Figure 6. (a) Bearing with two coils; (b) Force as a function of gap

The force from the lower coil is

$$F_1 = F_0\left(\frac{x_0+x_L}{x_0+x_L-\Delta x}\right)^2$$

$$= F_0\Big/\left(1-\frac{\Delta x}{x_0+x_L}\right)^2 \qquad \ldots(22)$$

and the upper coil force is

$$F_2 = F_0\Big/\left(1+\frac{\Delta x}{x_0+x_L}\right)^2$$

The resultant force on the disk is

$$F = F_1-F_2$$

or

$$F = \frac{4F_0[\Delta x/(x_0+x_L)]}{\{1-[\Delta x/(x_0+x_L)]^2\}^2} \qquad \ldots(23)$$

Figure 6(b) shows this force as a function of Δx. The stiffness of the magnetic bearing or the spring constant is $c = \mathrm{d}F/\mathrm{d}(\Delta x)$ and is not constant. However, restricted to small Δx one obtains

$$c = \frac{4F_0}{x_0+x_L} \qquad \ldots(24)$$

If the leakage is assumed to be zero or $x_L = 0$, equation (24) becomes

$$c = \frac{4F_0}{x_0} \qquad \ldots(25)$$

The stiffness becomes better for smaller gaps x_0. A magnetic flux cushion of small thickness should be selected. However, equation (24) shows that a small x_0 is of little help if the leakage x_L is too large. It will be shown later how x_L can be made small.

A magnetic bearing (Figure 7) for a sphere will be studied which is stable in all directions. The sphere 'a' is floating in a vertical direction between the two coils 'b_1' and 'b_2' which may be embedded in an iron housing. The coils 'c_1', 'c_2' and 'd_1', 'd_2' (only 'd_1' is not shown) are needed for horizontal forces on the sphere.

The stiffness of the bearing in the vertical direction will now be determined. The surfaces of the two coils 'b_1' and 'b_2' and also the adjacent surfaces of the sphere are approximated by cones (shown for coil 'b_1') which form an angle α with the horizontal. If the sphere is in the middle, each coil produces a vertical force opposite in direction which, from equation (9), is modified to

$$F_0 = (2\pi l_0 r)\cos\alpha\left(\frac{B}{5000}\right)^2 \quad \text{(in kg)} \qquad \ldots(26)$$

where

$$B = \frac{4\pi}{10}\frac{IN}{l}$$

If the sphere is moved vertically at Δx the gap under the coils changes by $\Delta x\cos\alpha$. In equation (23) Δx has therefore to be replaced by $\Delta x\cos\alpha$. One obtains

$$F = 4F_0\frac{(\Delta x\cos\alpha)/(x_0+x_L)}{\{1-[(\Delta x\cos\alpha)/(x_0+x_L)]^2\}^2} \qquad \ldots(27)$$

The stiffness or the spring constant then becomes for small values of Δx

$$c = 4F_0\frac{\cos\alpha}{x_0+x_L}$$

or from equation (26)

$$c = (8\pi r l_0)\frac{\cos^2\alpha}{x_0+x_L}\left(\frac{B}{5000}\right)^2 \quad \text{(in kg/cm}^2\text{)} \qquad \ldots(28)$$

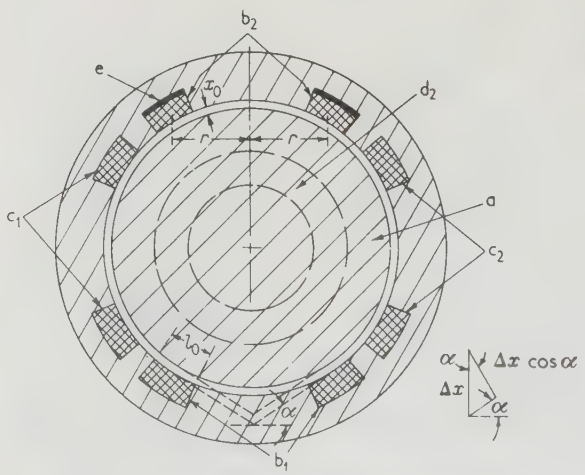

Figure 7. Spherical bearing

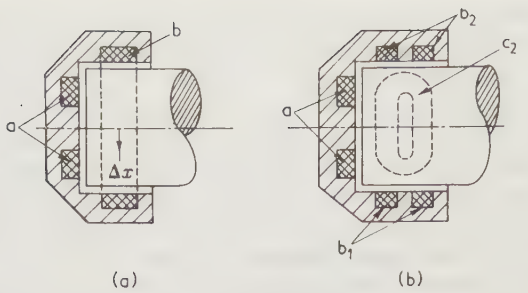

Figure 8. Cylindrical bearing: (a) With insufficient restoring force; (b) With good restoring force

Since the sphere has mass it can oscillate between the coils 'b_1' and 'b_2'. Damping is needed which can be provided by the eddy currents in the iron (not superconductive) caused by flux variations if the sphere oscillates. A thin copper ring 'e' (not superconductive) placed on the bottom of the coils (shown at coil 'b_2') also produces damping.

Figure 8(a) shows one end of a cylindrical shaft and its bearing. The coil 'a' in which a flux is trapped takes care of forces in the direction of the axis. One might think that a coil 'b' surrounding the shaft could produce the vertical restoring force. However, with a given current the flux density in the gap around the shaft is constant and does not vary if the shaft is vertically displaced. The flux distribution around the circumference does change but the total flux stays constant. The constant flux density produces a constant magnetic pressure on all sides of the shaft and no restoring force is obtained. Four coils are needed (Figure 8(b)) to obtain a good restoring force. The two coils 'b_1' and 'b_2' have a trapped flux and take care of vertical movements (similar to the spherical bearing). For displacement perpendicular to the plane of paper the coils 'c_1' and 'c_2' are needed (only coil 'c_2' is shown).

In Figure 9(a) it is shown that by connecting coils in parallel similar effects can be achieved as with flux trapping. For simplicity the arrangement of Figure 6(a)

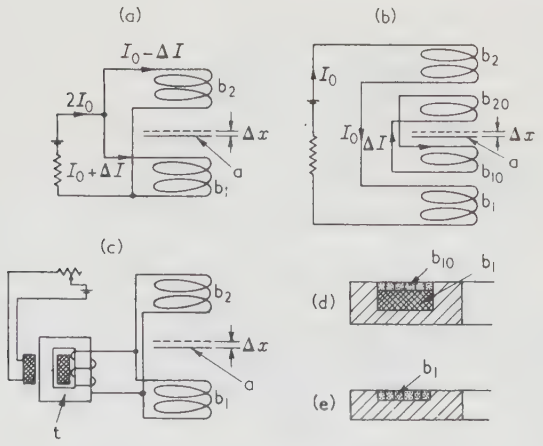

Figure 9. Different schemes for bearing coils

is studied and both coils 'b_1' and 'b_2' are connected in parallel as shown schematically in Figure 9(a). They are fed by a current $2I_0$ from a power source. If the current is increased from zero to its final value an equal voltage u is applied to both coils. This voltage gradually decays to zero. If the flux in the two coils is ψ_1 and ψ_2 the voltage is

$$u = \frac{d\psi_1}{dt} = \frac{d\psi_2}{dt}$$

or

$$\psi_1 = \psi_2 = \int_0^t u\,dt \qquad \ldots(29)$$

Both coils have the same flux ψ which, however, need not be constant. In the middle position ($\Delta x = 0$) of the disk, the current in each coil is I_0 and the flux density B_0. If the disk is moved by Δx the coil 'b_1' carries the current

$$I_1 = I_0 + \Delta I$$

and the flux density is

$$B_1 = B_0 + \Delta B$$

Similarly

$$I_2 = I_0 - \Delta I$$
$$B_2 = B_0 - \Delta B$$

These equations fulfil the condition that $I_1 + I_2 = 2I_0$ is constant.

Since the flux must be the same for both coils it follows

$$(B_0+\Delta B)(x_0+x_L-\Delta x) = (B_0-\Delta B)(x_0+x_L+\Delta x)$$

or

$$\frac{\Delta x}{x_0+x_L} = \frac{\Delta B}{B_0} \qquad \ldots(30)$$

The resultant force on the disk is

$$F = 2\pi rl\left[\left(\frac{B_0+\Delta B}{5000}\right)^2 - \left(\frac{B_0-\Delta B}{5000}\right)^2\right]$$

or

$$F = 4\left(\frac{B_0}{5000}\right)^2 \frac{\Delta B}{B_0}(2\pi rl)$$

Using equation (30) yields

$$F = (2\pi rl)\left(\frac{B_0}{5000}\right)^2 \frac{4\Delta x}{x_0+x_L}$$

and from equation (9)

$$F = 4F_0 \frac{\Delta x}{x_0+x_L} \qquad \ldots(31)$$

With this parallel connection the force F is a linear function of Δx and the spring constant

$$c = \frac{dF}{d(\Delta x)} = \frac{4F_0}{x_0+x_L}$$

and is independent of Δx.

For a spherical bearing, Δx in equation (31) has to be replaced by $\Delta x \cos\alpha$. One obtains

$$F = 4F_0 \frac{\Delta x \cos \alpha}{x_0 + x_L} \qquad \ldots (32a)$$

and

$$c = \frac{4F_0}{x_0 + x_L} \cos \alpha \qquad \ldots (32b)$$

By changing F_0 (by changing the current going to the coils), the stiffness of a bearing can be varied within a wide range.

A connection scheme which in its effect is identical to that of Figure 9(a) is given in Figure 9(b). Each coil is subdivided into two windings, 'b_1' and 'b_{10}' and 'b_2' and 'b_{20}'. Through the series connections of 'b_1' and 'b_2' a constant current I_0 flows. In the superconductive coils, 'b_{10}' and 'b_{20}', which are connected in parallel, the current ΔI is induced if the disk 'a' is moved at Δx. Because of the parallel connection, the flux linked with the coils 'b_{10}' must be equal to the flux linked with 'b_{20}' and ΔI provides the needed additional ampere-turns. In the preceding paragraphs it was mentioned that in order to obtain stiff bearings the leakage flux of the coils has to be kept small. Figure 9(d), which shows only the lower left portion of Figure 6(a), presents a solution. The coil is subdivided as in Figure 9(b) in two coils 'b_1' and 'b_{10}'. The coil 'b_1' consists of thin wire and has a leakage flux. The coil 'b_{10}' consists of one layer of heavy square wire and has no leakage flux since no flux can penetrate the wire. The coils 'b_2' and 'b_{20}' are similarly built (not shown) and connected with 'b_1' and 'b_{10}' as in Figure 9(b). Because in this scheme only the leakage flux linked with the coils 'b_{10}' and 'b_{20}' influences the stiffness, using heavy square wire provides good stiffness. One has to be careful that the two wires which connect 'b_{10}' and 'b_{20}' are kept close to each other in order to keep their leakage flux low because large currents of many hundreds of amperes are involved.

In Figure 9(e) only one coil 'b_1' with one layer of heavy square wire is used. This coil is connected in parallel to coil 'b_2' (see Figure 9(a)) and both are fed by a current $2I_0$. Since this current may be several hundreds of amperes it is not practical to bring this current from an outside power source which is at normal temperature to the low temperature environment. Because of the big wire cross-section which is needed, and because the wire is superconductive only at the low temperature, the heat influx to the helium bath is high and too much helium will evaporate. Therefore (see Figure 9(c)) a superconductive d.c.→d.c. transformer 't' in the helium bath is used which changes a small current (coming from the outside) in the primary winding into a large current in the secondary winding which feeds the bearing coils ('b_1' and 'b_2'). Such a d.c.→d.c. transformer is possible if the secondary winding and the load circuit are superconductive and no continuous power is taken out.

Figure 10 shows another method for reducing the leakage flux. Above the coil 'b_1', consisting of thin wire, is a flat superconductive ring 'c'. If the coil 'b_1' is excited, permanent countercurrents are introduced in the ring 'c' which prevent the flux from penetrating the ring and the bearing gap. Now, the superconductivity of the ring 'c'

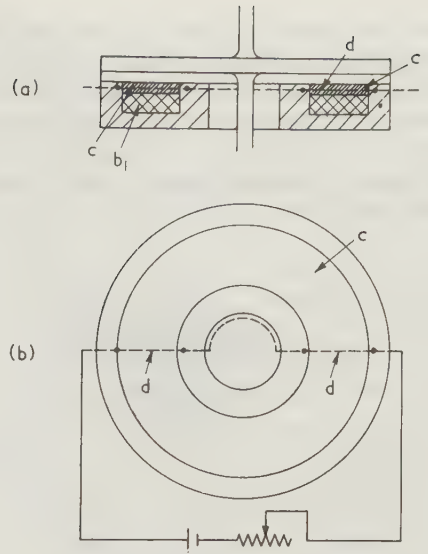

Figure 10. Test bearing with heating wire

(see Figure 10(b), top view) is temporarily destroyed in the vicinity of two resistance wires 'd' if these are energized and cause a temperature rise of a few degrees. The current in coil 'b_1' can now produce a flux which passes through the ring and through the bearing gap because the countercurrent in the ring decays away. The heating is then stopped and the ring becomes superconductive again and the flux which is linked with the ring remains even if the current in the coil 'b_1' is interrupted. The entire current to produce the flux is now flowing in the ring 'c' which does not have a leakage flux and good stiffness of the bearing is obtained. The procedure for trapping a flux into the ring 'c' is delicate because if the heating current and the heating time are not accurately chosen, other parts in the neighbourhood (which should stay superconductive) may become resistive. Instead of destroying the superconductivity by heat the same can be achieved in exposing the disk to a strong enough magnetic field. If the two heating wires 'd' could be replaced by superconductive wires which have a higher critical field than the disk, a strong current in the wires (which stay superconductive) could destroy the superconductivity of the disk.

The preceding mathematical derivations are based on the basic equations (7), (8), and (9). In order to check them experimentally the test arrangement of Figure 11(a) was used which is similar to that of Figure 5(a). The coil consisted of $N = 515$ turns of 0·25 mm niobium wire and was at the top covered by a niobium ring which had a slit in order to avoid a short circuit. On both sides of the ring, surface currents must flow with a density which is proportional to the adjacent flux density. In Figure 11(b) (front view of the ring) these currents are indicated by arrows. This ring, together with the upper niobium disk, provides a well-defined gap which was kept constant at $x = 0{\cdot}25$ mm. The upper disk was loaded with different weights and the current required to carry the load was

determined. The dots in Figure 11(c) are the measured values. Since the flux density B (equation (8)) is proportional to the current I and the force F (equation (9)) proportional to B^2, the force F must also be proportional to I^2 and may be represented by a parabola. The measured values in Figure 11(c) fit well with a parabola represented by the solid line.

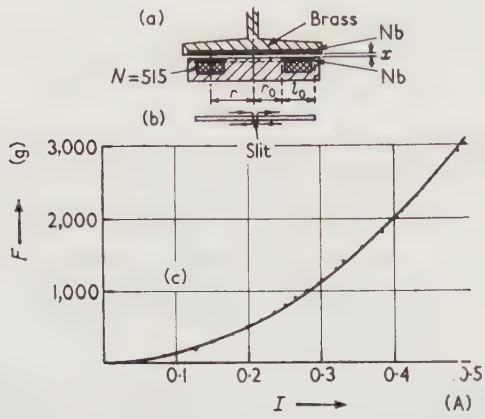

$r = 1{\cdot}5$ cm; $r_0 = 0{\cdot}937$ cm; $l_0 = 1{\cdot}125$ cm; $N = 515$

Figure 11. (a) Test set-up; (b) Front view of niobium ring with slit; (c) Measured force F as a function of current I

The absolute value of the force F will now be checked, e.g. for a current $I = 0{\cdot}4$ A corresponding to a measured force $F = 2$ kg (see Figure 11(c)). Equation (8) with $I = 0{\cdot}4$ A, $N = 515$ turns, and $l = l_0 = 1{\cdot}125$ cm ($\Delta l = 0$ assumed) yields $B = 2{,}300$ gauss. With this value and $r = 1{\cdot}5$ cm, equation (9) results in $F = 2{\cdot}22$ kg. This value is about 10 per cent higher than the measured value $F = 2{\cdot}0$ kg. A more correct calculation (not presented here) which does not use an average flux density but takes into account the variable flux density in the gap and uses the more accurate formula (7*a*) instead of (7*b*) yields a value 3 per cent lower so that $F = 2{\cdot}16$ kg.

If one considers that l is not equal to l_0 but $l = l_0 + \Delta l$, (equation (8)) the observed value $F = 2{\cdot}0$ kg can be obtained in assuming $\Delta l = 3{\cdot}5$ per cent of l_0 which looks very reasonable. If the approximate value $F = 2{\cdot}2$ kg is used the correction Δl becomes 5 per cent to yield $F = 2{\cdot}0$ kg.

If the current was increased beyond 0·5 A (corresponding to an average flux density in the gap of $B = 2{,}900$ gauss) the superconductivity of the coil was destroyed.

In order to check the basic equation (18) for flux trapping, a test set-up similar to Figure 11(a) was used which had the dimensions: $r = 1{\cdot}5$ cm, $r_0 = 1{\cdot}02$ cm, $l_0 = 0{\cdot}95$ cm. However, the ring did not have a slit but contained a heating wire similar to Figure 10 whereby a flux can be trapped as previously explained. Figure 12 shows the measured force F as a function of the gap x which should follow equation (18)

$$F = \frac{k_0}{(x + x_L)^2}$$

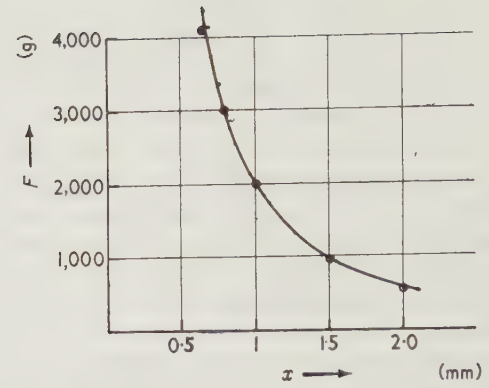

$r = 1{\cdot}5$ cm; $r_0 = 1{\cdot}02$ cm; $l_0 = 0{\cdot}95$ cm; $N = 321$

Figure 12. Measured force F as a function of displacement x

If $x_L = 0{\cdot}1$ mm is assumed, the circled points are obtained which fit well with the measured values. Theoretically x_L should be zero. The nature of the imperfections that caused $x_L = 0{\cdot}1$ mm was not determined.

In the measuring device of Figure 13(d), for the coil 'b', rectangular 1 mm niobium wire is used. In order to trap a flux the shunt wire 'e' is made resistive by energizing the heating coil 'f' as already explained with Figure 5(b). With the d.c. transformer 't' a current is supplied to the coil 'b'. The heating coil 'f' is then interrupted and the shunt 'e' becomes superconductive. The coil 'b' is now short-circuited and a flux is trapped. The solid curve in Figure 13 is measured. The theoretical curve

$$F = \frac{k}{(x + x_L)^2}$$

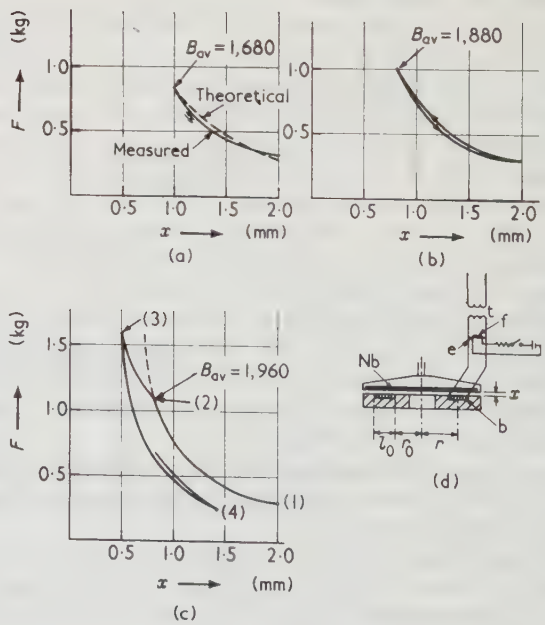

Figure 13. Force measurements as a function of displacement: (a) No hysteresis observed; (b) With hysteresis; (c) With partial breakdown of superconductivity; (d) Test set-up ($r_0 = 1$ cm, $r = 1{\cdot}42$ cm, $l_0 = 0{\cdot}83$ cm, $N = 7$)

which best fits the measured values is dashed and corresponds to $x_L = 0{\cdot}5$ mm. It is caused by a leakage flux, e.g. that of the leads going to the shunt 'e'. Within the measuring accuracy, the curve in Figure 13(a) shows no hysteresis as long as the maximum force does not exceed $F = 0{\cdot}85$ kg. This value of F corresponds to an average $B = 1{,}680$ gauss. In Figure 13(b) the force was increased to 1 kg ($B_{av} = 1{,}880$ gauss) and in reducing the force a slight hysteresis was obtained. It is believed that with increasing force the critical field is exceeded at the coil surface, especially at the sharp corner of the rectangular wire, and a resistive flux penetration starts which in turn causes losses and hysteresis when the disk is moved. Nevertheless, the bearing action is not yet impaired. However, in a rotating part (e.g. a sphere) of a bearing, especially if working in vacuum, such a resistive penetration must be avoided because losses increase the temperature and the superconductivity may be destroyed.

In Figure 13(c) from point (2) on, the increasing force deviates considerably from the theoretical shape. If at point (3) the force is reduced, the force is much smaller for a given gap. The shape of the curve between the points (2) and (3) can probably be explained by partial breakdown of superconductivity. Between (3) and (4) the current does not increase as much as it would have had the wire remained superconductive. In a bearing, the condition of Figure 13(c) must be avoided. The critical field is a strong function of the 'quality' of the material; that means of impurities, stresses, etc.

To determine the stiffness of complete bearings with small gaps it is often convenient to measure the frequency f of mechanical oscillation. The oscillations are induced by a sharp blow to the supported part of mass m. A small measuring coil is magnetically coupled with the current in the bearing coil and the induced current is used to obtain the frequency f needed to solve for the spring constant c

$$f = \frac{1}{2\pi}\sqrt{\left(\frac{c}{m}\right)}$$

Conclusions

The electromagnetic forces acting in a thin layer at the surface of a superconductor can be replaced in concept by the surface pressure of the magnetic lines.

Several schemes of superconductive bearings were theoretically investigated and their stiffness calculated. A number of experiments were performed to check the basic foundations of the theory. One uncertainty in the calculations is the flux leakage proportional to x_L. In order to have stiff bearings x_L should be kept small. The calculations which are restricted to axially symmetric coils are sufficient to explain the phenomena. If in practical bearings other coil shapes, e.g. oval ones, are used the calculations must be modified.

In arriving at the results of this paper, note that it has been assumed that the total magnetic resistance of the flux path is mainly in the gap—that is, approximated by an iron return path. If iron is not used, the magnetic resistance of the return path is increased and requires an assignment of a larger value Δl in equation (8) obtainable only by rough approximations.

GENERAL REFERENCES

Shoenberg, D. *Superconductivity* (Cambridge University Press, London, 1952)

Mendelssohn, K. *Cryophysics* (Interscience, New York, 1960)

Handbuch der Physik, Vol. 14. 'Low Temperature Physics I' (Ed. S. Flugge) (Springer, Berlin)

Handbuch der Physik, Vol. 15. 'Low Temperature Physics II' (Ed. S. Flugge) (Springer, Berlin)

Scott, R. B. *Cryogenic Engineering* (Van Nostrand, Princeton, N.J., 1959.)

Simon, I. 'Forces Acting on Superconductors in Magnetic Fields.' *J. appl. Phys.* **24**, 19 (1953)

Buck, D. A. 'The Cryotron.' Proc. Inst. Radio Engrs, N.Y. **44**, (1956)

Matthias, B. T. 'Superconductivity.' *Scientific American* (November, 1957)

Bardeen, J., Cooper, L. W., and Schrieffer, J. R. 'Theory of Superconductivity.' *Phys. Rev.* **108**, 1175 (1957)

The Specific Heat at Constant Volume, the Entropy, the Internal Energy, and the Free Energy of Liquid Helium-4 between 1·2 and 2·9°K

O. V. Lounasmaa

Argonne National Laboratory, Argonne, Illinois

and Wihuri Physical Laboratory, University of Turku, Turku, Finland

Received 3 January 1961

THE thermodynamic behaviour of liquid helium-4 in the temperature region near the λ curve is anomalous and in many respects quite interesting. However, until recently, there has been very little experimental data for calculating the thermal properties accurately. The early entropy diagram of helium by Keesom and Keesom[1] was computed on the basis of the rather extensive p–V–T measurements by the same authors.[2] As such calculations involve derivatives of the experimental quantities, the resulting accuracy was necessarily limited. The entropy table by Hercus and Wilks[3] between 1·2 and 1·9°K is not very reliable owing to the somewhat doubtful specific heat measurements used in their calculations.

Lounasmaa and Kojo[4] have recently published an entropy diagram of liquid helium-4 between 1·5 and 2·9°K. The diagram is based on their measurements of C_V, the specific heat at constant volume. The constants of integration were read from the entropy diagram of fluid helium by Hill and Lounasmaa[5] at 2·50°K, this being the low temperature limit of their measurements. Starting from here, the entropy towards lower temperatures was calculated by subtraction according to the relation

$$\Delta S_{V=\text{const}} = \int (C_V/T).\mathrm{d}T \qquad \ldots(1)$$

where S is the entropy. The relative accuracy thus becomes gradually poorer. Owing to this, the entropy diagram[4] was regarded as provisional and the results were presented at the experimentally measured densities only. However, this diagram showed, in contrast with earlier measurements,[1] that the entropy is decreasing with increasing volume not only in the helium-II region but also in the helium-I region near the λ curve.

For computing a more satisfactory entropy diagram by using specific heats, the constants of integration should be determined at the low temperature end of the diagram. Measurements of the absolute pressure p and of the pressure coefficient at constant volume, $(\partial p/\partial T)_V$, as a function of density were, therefore, undertaken in the temperature region around 1·75°K. For higher experimental accuracy, $(\partial p/\partial T)_V$ was determined directly with a differential mercury manometer. By employing the thermodynamic relation

$$\Delta S_{T=\text{const}} = \int (\partial p/\partial T)_V.\mathrm{d}V \qquad \ldots(2)$$

the constants of integration at 1·75°K for various densities can be determined by starting from the entropy of liquid helium under the saturation vapour pressure.

The internal energy U can be computed in a similar way as the entropy from measurements of C_V, p, and $(\partial p/\partial T)_V$ by using the equations

$$\Delta U_{V=\text{const}} = \int C_V.\mathrm{d}T \qquad \ldots(3)$$

and

$$\Delta U_{T=\text{const}} = \int [T(\partial p/\partial T)_V - p].\mathrm{d}V \qquad \ldots(4)$$

The thermodynamic functions tabulated for liquid helium-4 in this paper are the specific heat at constant volume C_V, the entropy S, and the internal energy $U-U_0$ (U_0 is the zero point energy of the liquid under zero pressure), all as functions of temperature (C_V between 1·2 and 2·9°K, S and $U-U_0$ between 1·5 and 2·9°K) and density (from $\rho = 0{\cdot}150$ g/cm^3 to $\rho = 0{\cdot}185$ g/cm^3). These quantities, together with the free energy $F-U_0 = U-U_0-TS$, are also presented in graphical form; some of the graphs include curves corresponding to liquid helium along the liquid–vapour and liquid–solid equilibrium lines. A Table giving the values of these thermodynamic functions along the λ curve is also included. The C_V measurements by Lounasmaa and Kojo[4] were used in the calculations between 1·5 and 2·9°K; between 1·2 and 1·5°K the C_V data are based on the results by Hercus and Wilks[3] after a correction was applied to them.

If the present work is combined with that of Hill and Lounasmaa[5] between 3 and 20°K and with the entropy

diagram by Keesom, Bijl, and Monté[6] above 20° K, the most important thermodynamic properties of liquid and fluid helium are known to an accuracy of 1–2 per cent in the temperature range from 1·5 to 300° K and up to pressures of at least 100 atm.

The following units are used in this paper:

pressure (p): the absolute atmosphere = $1{\cdot}01325 \times 10^6$ dyn/cm^2;
temperature (T): degree Kelvin (temperature scale[7] T_{58});
energy: the absolute joule. The relation 1 joule = 9·8693 atm.cm^3 has been used.
quantity: all extensive quantities are molar. The molecular weight of helium-4 = 4·0028.

Measurements of p and $(\partial p/\partial T)_V$

Experimental. The cryostat used in the experiments has been described in detail elsewhere.[4] The procedure adopted for measuring p and $(\partial p/\partial T)_V$ was essentially the same as that employed earlier,[5] and is only briefly explained here. Figure 1 shows schematically the pressure measuring apparatus. V_1 and V_2 are two ballast volumes, about 700 cm^3 each, made of heavy steel tube and immersed in a water bath. M_1 and M_2 are two mercury-in-glass manometers 180 and 40 cm long, respectively, and constructed of thick-walled capillary tubing to withstand pressures up to 30 atm. A_1, ..., A_6 are various needle valves, and B_1 and B_2 are special valves having negligible dead volume on the side of the sample container C. TG is a 25 cm dial standard test gauge and DWT is a dead weight tester. The tubing between C, the sample inlet valve B_1, the manometer M_2, and the valve A_5 was made of german-silver capillary of 0·3 mm inside diameter.

The calorimeter (Figure 2) employed earlier for C_V measurements[4] was used as the sample container. It had two compartments, the sample space and the pot, the latter acting as a container for liquid helium used for cooling purposes and for thermometer calibrations. The calorimeter was made of copper and the sample space packed with thin copper wire, which occupied about 30 per cent of the space available. Similarly, a number of copper rods were soldered to the bottom of the pot. These precautions ensured almost instant equilibrium during measurements even above the λ point. The volume left for helium in the sample space was 19·53 cm^3. To determine this the sample space was filled at 4·00° K with liquid helium to a known pressure (10–30 atm) and its density was calculated from the equation of state.[5] The amount of helium in the sample space was then determined by admitting the gas to an accurately known volume at room temperature and by measuring its pressure. The volume of the sample space could thus be computed; several determinations at different pressures agreed within 0·1 per cent.

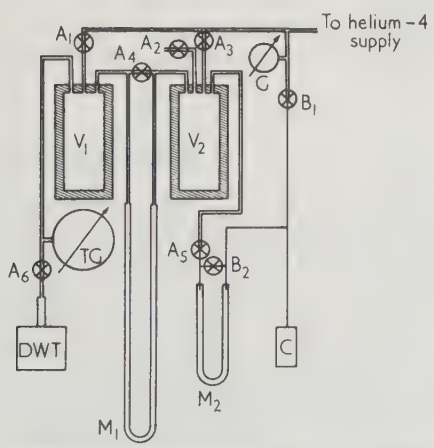

Figure 1. Schematic diagram of the pressure measuring equipment

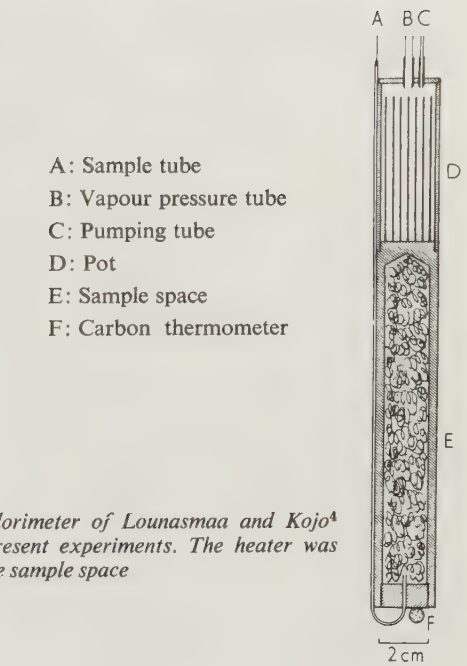

Figure 2. The calorimeter of Lounasmaa and Kojo[4] used in the present experiments. The heater was wound round the sample space

For measurements of $(\partial p/\partial T)_V$ the pressure change produced in the sample space by a small known temperature change was determined with the differential manometers. During these measurements, the smaller manometer M_2 was used as a null indicator so that the volume on the sample side remained constant. Pressure changes in the sample space were compensated by letting more gas into V_2 and measured by the resulting deflection of M_1. The absolute pressure in V_1, and hence in V_2 and C, was determined by the dead weight tester. Temperatures were measured with a carbon resistance thermometer, calibrated against the vapour pressure of liquid helium before every experiment. The very high sensitivity of carbon thermometers is of great importance in differential measurements. For more details the reader is referred to earlier papers.[4, 5, 8]

Results. The experimental results of the measurements of the pressure coefficient are given in Table 1 and they

Table 1. Experimental Measurements of $(\partial p/\partial T)_V$

ρ (g/cm^3)	T (°K)	$(\partial p/\partial T)_V$ ($atm/deg.K$)
0·14708	1·705	−0·48
	1·749	−0·56
	1·792	−0·62
0·15364	1·707	−1·19
	1·750	−1·31
	1·792	−1·50
0·15724	1·717	−1·75
	1·762	−2·01
	1·805	−2·25
0·15935	1·705	−2·10
	1·750	−2·48
	1·791	−2·74
0·16376	1·704	−3·16
	1·747	−3·45
	1·787	−3·95
0·16442	1·718	−3·51
	1·763	−4·03
	1·807	−4·36
0·16576	1·706	−3·58
	1·748	−4·09
	1·792	−4·67
0·16866	1·708	−4·77
	1·746	−5·49
	1·788	−5·68
0·17184	1·705	−6·45
	1·747	−7·28
	1·792	−8·33
0·17188	1·721	−6·74
	1·763	−7·86
	1·807	−8·73
0·17443	1·703	−8·35
	1·746	−9·50
	1·787	−10·58
0·17558	1·707	−9·60
	1·750	−11·04
	1·793	−12·72
0·17672	1·718	−11·31
	1·762	−13·28
	1·807	−15·49

are also plotted in Figure 3. For computing the entropy and internal energy diagrams, smooth values of $(\partial p/\partial T)_V$ are needed along the isotherm at 1·75° K. For determining these, experimental points belonging to each run were first joined by a curve as in Figure 3. Smooth values were then obtained by reading $(\partial p/\partial T)_V$ from these curves at 1·75° K. Next, to connect the different experiments with each other, these values were plotted against density and the points joined by a smooth curve. This is shown in Figure 4. The final values of the pressure coefficient were then read from this curve.

In computing the pressure coefficient, various corrections were applied. These include corrections for the dead volume outside the sample container (effectively 0·2 per cent of the volume of C) and for the compression of

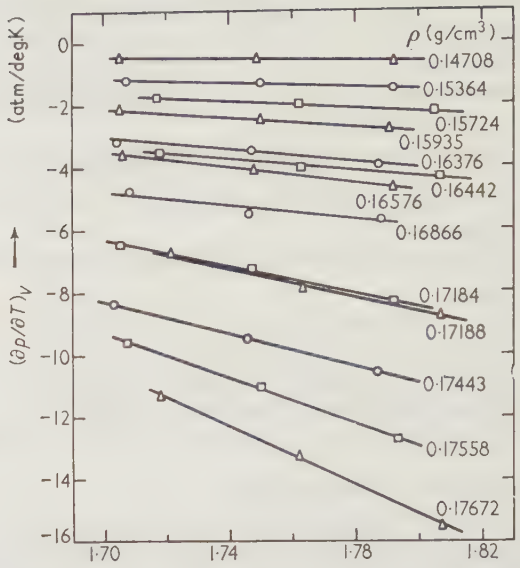

Figure 3. The experimental measurements of the pressure coefficient

the gas in V_1 due to movements of mercury in M_1. The latter correction was determined experimentally by connecting a third differential manometer between V_1 and a large gas tank. The pressure coefficient is rather sensitive to errors in the density; for instance, at $\rho = 0{\cdot}165$ g/cm³ an error of 0·1 per cent in the density (see below) results in an uncertainty of 1·5 per cent in $(\partial p/\partial T)_V$. Errors in the absolute temperature have a much smaller effect. After these considerations, the accuracy of the measurements of $(\partial p/\partial T)_V$ may be estimated as 2 per cent.

The absolute pressure at the experimental densities and at 1·75° K is given in Table 2. The dead weight tester used for determining p was a calibrated precision instrument

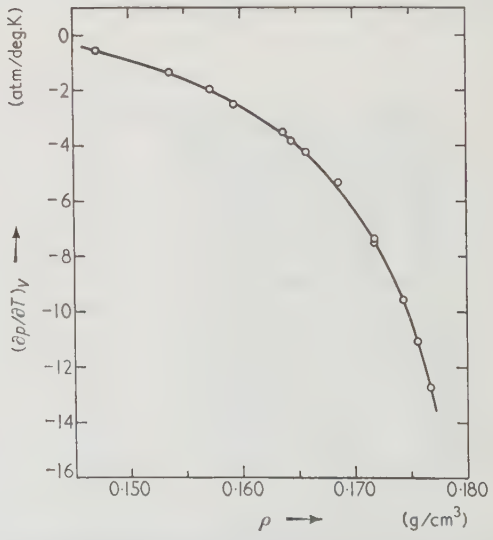

Figure 4. $(\partial p/\partial T)_V$ along the isotherm at 0·75° K

Table 2. The Pressure p along the Isotherm at 1·75° K

ρ (g/cm³)	p (atm)
0·14708	0·89
0·15364	5·00
0·15724	7·61
0·15935	9·42
0·16376	13·11
0·16442	13·78
0·16576	15·05
0·16866	17·90
0·17184	21·30
0·17188	21·41
0·17443	24·01
0·17558	25·17
0·17672	26·53

and should give values accurate to 0·1 per cent or better. However, the pressure is sensitive to small changes in the density. For example, at 1·75° K and at $\rho = 0{\cdot}165$ g/cm³ a change of 0·1 per cent in density affects the pressure by 1·0 per cent. As mentioned earlier (page 213), the volume of the sample container was determined by using the p–V–T data of Hill and Lounasmaa,[5] who give 0·3 per cent as the maximum error of their densities. The present values of ρ along the isotherm at 1·75° K are 0·6 per cent higher than those reported by Keesom and Keesom.[2] Our results are thus in good agreement with the data of Edeskuty and Sherman,[9] who made some p–V–T measurements of helium-4 in connection with their studies of the equation of state of helium-3. Their densities were at first reported to be 0·3 per cent higher than those of Keesom and Keesom,[2] but later (private communication) a further correction of +0·30 per cent was given. Edeskuty and Sherman claim an accuracy better than 0·1 per cent for their results. Therefore, one may perhaps estimate that the densities in the present paper are correct to 0·1 per cent. Experimental values of $(\partial p/\partial T)_V$ indicate that the pressure is insensitive to errors in temperature measurements. The systematic errors in p may thus be about 1 per cent, the random errors being considerably smaller. For more details concerning corrections, etc., earlier papers[5,8] should be consulted.

Thermodynamic functions

The specific heat C_V. Most of the experimental C_V points by Lounasmaa and Kojo[4] are shown in Figure 5. The gradual shift of the λ peak to lower temperatures when the density is increased is very evident. At the same time the peak diminishes, although it is still pronounced at the liquid–solid equilibrium line. Below the λ temperature high density corresponds to high specific heat; above the λ temperature the situation is reversed. The curve marked C_{sat}, representing the specific heat under the saturation vapour pressure, deviates markedly from the general trend of the C_V curves in the helium-I region. This is to be expected as C_{sat} is nearly equal to C_p and the difference $C_p - C_V$ is large above the λ transition temperature. All of the 274 experimental C_V points are tabulated elsewhere.[4]

To prepare a table of C_V for convenient intervals of density and temperature, smooth values have to be used. Such a table has been published earlier;[4] the specific heats were obtained by a careful graphical treatment of the experimental data. However, great difficulties are obviously encountered in the smoothing process near the λ region. For the C_V table published in the present paper the specific heats[4] were re-smoothed and particular attention was paid to the transition region. Experimental points belonging to a common density were first joined by a curve as in Figure 5. Smooth values were then obtained from these curves. The different experiments were connected with each other by plotting these values as graphs of C_V against the density at constant temperature (helium-I region), or by plotting the density against temperature at constant C_V (helium-II region). Specific heats at fixed temperatures and densities were then determined from these curves. Finally, a new plot of C_V against temperature was made. Only very small deviations from smoothness, except near the transition region, were observed at this stage and the values were listed as a table. Differences were calculated and small rounding-off errors still present in the last decimal were corrected.

In the λ transition region, the smoothing process just described was also used but it was supplemented by the following considerations:

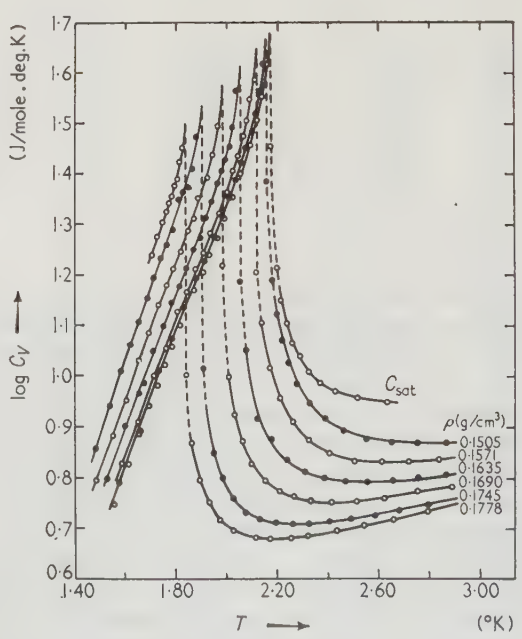

Figure 5. Experimental specific heat measurements by Lounasmaa and Kojo.[4] The curve marked C_{sat} *represents liquid under its saturation vapour pressure*

(1) When specific heat measurements are made, the primary observation is the temperature increase ΔT due to a known heat input ΔQ. Since at constant volume $\Delta U = \Delta Q$, the increase in the internal energy can be readily obtained. By using the relation $\Delta U = \int C_V . dT$ and the trapezoidal rule for integration one gets

$$C_{V,2} = 2(\Delta U/\Delta T) - C_{V,1} \qquad \ldots(5)$$

where $C_{V,1}$ and $C_{V,2}$ are the specific heats at the beginning and end of the heating interval, respectively. Thus, by computing a smooth table of ΔU in the λ region, which is easier than smoothing the specific heats, and by starting from a specific heat sufficiently far from the transition temperature, so that a reliable value may be obtained by the smoothing process described above, C_V can be computed towards the λ temperature. This was done both in the helium-I and helium-II regions and the specific heats thus obtained were used to assist in drawing the smooth C_V curves in the transition region.

(2) The apparent height of the λ peak as a function of density was determined by examining the original C_V curves (Figure 5), and the transition temperature corresponding to the experimental densities was computed by using the data of Lounasmaa and Kaunisto.[8] The height and position of the λ peaks could thus be determined for the tabulated C_V curves.

Table 3. Thermodynamic Properties of Helium-4 along the λ Curve

ρ (g/cm^3)	T† (°K)	p† (atm)	C_V ($J/mole.deg.K$)	S	$U-U_0$ ($J/mole$)
1·50	2·1510	2·07	(46·7)	6·01	11·10
1·55	2·1185	5·04	(43·8)	5·77	10·89
1·60	2·0785	8·48	(40·8)	5·60	11·06
1·65	2·0265	12·62	(37·5)	5·39	11·44
1·70	1·9600	17·44	(33·8)	5·14	12·02
1·75	1·8760	22·95	(29·8)	4·87	12·87
1·80	1·7695	29·30	(25·1)	4·53	13·93

† Computed from the data of Lounasmaa and Kaunisto.[8]

Specific heats along the λ curve are given in Table 3. They are enclosed in brackets since quite probably, due to the very rapid change of C_V with temperature near the λ curve, the values are very inaccurate. Continuous specific heat curves were drawn over the λ peak, although there might be a discontinuity at the transition point. It is also possible that C_V goes to infinity at the λ temperature (see Fairbank, Buckingham, and Kellers[10]). The measurements[4] were not done with sufficiently small temperature increments to decide these questions (see reference 8). The method described in the preceding paragraph for computing C_V in the transition region and the narrowness of the λ peak ensures, however, that this uncertainty contributes little to the possible errors in the entropy and internal energy diagrams.

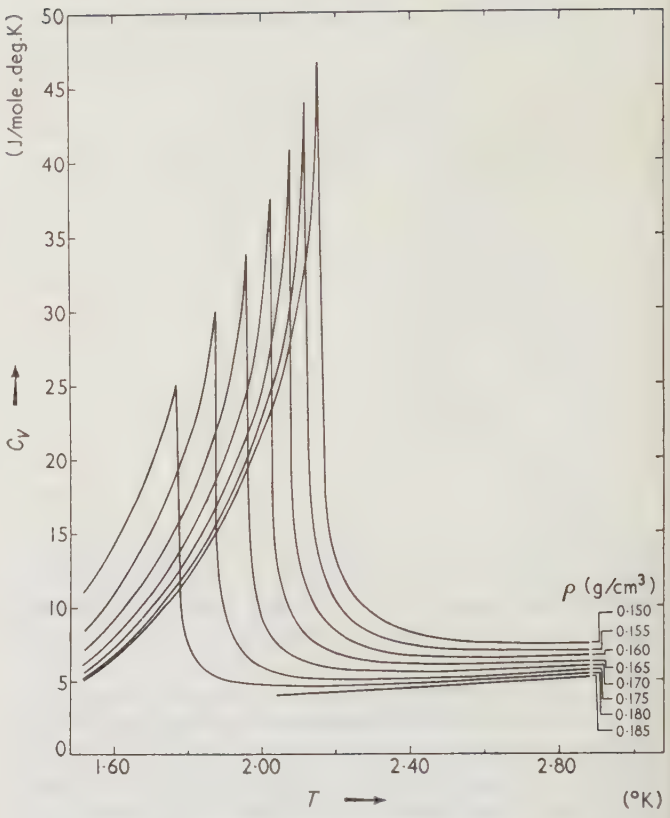

Figure 6. Smoothed values of C_V

In the temperature region between 1·2 and 1·5°K the specific heat measurements by Hercus and Wilks[3] were employed for computing the smooth C_V values. However, their results under the saturation vapour pressure are approximately 10 per cent higher than those of Kramers, Wasscher, and Gorter,[11] and at constant volume between 1·5 and 1·7°K about 7 per cent higher than the C_V data by Lounasmaa and Kojo.[4] The source of the discrepancy is not known, but since the results from papers[4,11] under the saturation vapour pressure agree within the experimental error, it seemed reasonable, before using the measurements of Hercus and Wilks,[3] to decrease their specific heats at all temperatures by 7 per cent. By doing this, their C_V data could be joined to those by Lounasmaa and Kojo[4] without difficulties. Admittedly this method is not too satisfactory, but in the absence of any other experimental results, it is the best possible.

The final smooth specific heats are given in Table 4. The results are also shown in Figure 6. In the helium-I region C_V is nearly a linear function of density; in the helium-II region C_V is almost independent of density near the liquid–vapour equilibrium line but strongly dependent on density near the liquid–solid equilibrium line.

The accuracy of the C_V measurements[4] was estimated by Lounasmaa and Kojo as 2 per cent below and 1 per cent above the λ curve. If their smooth specific heats are compared with Table 4, only small discrepancies, well

below 1 per cent, are usually found. In the λ region the differences are sometimes a little bigger. Since both C_V tables were computed by smoothing the experimental results independently, and partly by different people, this indicates that the smoothing can be done unambiguously and that the errors resulting from it are below the experimental accuracy. The specific heats from Table 4 can be compared at 2·50 and 2·75° K with earlier data;[5] the agreement is within 1 per cent. It may thus be claimed that, excluding the immediate vicinity of the λ peaks, the accuracy of Table 4 is 2 per cent between 1·5° K and the transition curve, and 1 per cent in the helium-I region. No estimate can be given for the temperature interval 1·2–1·5° K.

Table 4. The Specific Heat C_V (J/mole.deg.K) of Liquid Helium-4

T (° K)	ρ (g/cm^3)							
	0·150	0·155	0·160	0·165	0·170	0·175	0·180	0·185
1·20	1·36	1·38	1·48	1·70	2·11			
1·24	1·66	1·70	1·82	2·07	2·53			
1·28	1·98	2·04	2·19	2·48	2·99			
1·32	2·36	2·43	2·60	2·94	3·50			
1·36	2·78	2·87	3·07	3·46	4·09			
1·40	3·27	3·37	3·61	4·04	4·73			
1·44	3·81	3·92	4·20	4·70	5·44			
1·48	4·42	4·55	4·87	5·41	6·22			
1·52	5·11	5·25	5·61	6·20	7·10			
1·56	5·84	6·02	6·42	7·08	8·08			
1·60	6·64	6·86	7·32	8·05	9·18	10·98†		
1·64	7·52	7·80	8·30	9·11	10·40	12·50†	16·13†	
1·68	8·48	8·81	9·38	10·29	11·75	14·21†	18·29†	
1·72	9·56	9·94	10·58	11·60	13·26	16·14†	20·81†	
1·76	10·77	11·20	11·92	13·07	14·97	18·32	24·03†	
1·80	12·10	12·58	13·40	14·73	16·95	20·82	7·64	
1·84	13·57	14·10	15·07	16·63	19·28	24·31	5·89	
1·88	15·21	15·78	16·95	18·82	22·05	14·25	5·21	
1·92	17·03	17·69	19·08	21·38	25·62	8·05	4·93	
1·96	19·08	19·87	21·56	24·57	33·75	6·55	4·80	
2·00	21·48	22·51	24·66	29·54	9·23	5·91	4·71	
2·04	24·36	25·80	29·36	13·15	7·49	5·54	4·65	4·08
2·08	28·07	30·52	27·25	9·50	6·72	5·33	4·61	4·11
2·12	33·35	30·75	11·33	8·05	6·28	5·21	4·59	4·15
2·16	26·25	12·88	9·35	7·28	6·01	5·15	4·59	4·19
2·20	13·23	10·38	8·32	6·86	5·83	5·12	4·61	4·23
2·24	11·01	9·14	7·70	6·56	5·71	5·10	4·63	4·27
2·28	9·83	8·44	7·28	6·36	5·64	5·09	4·65	4·32
2·32	9·12	7·98	7·01	6·22	5·59	5·09	4·69	4·37
2·36	8·62	7·67	6·83	6·15	5·57	5·11	4·73	4·43
2·40	8·27	7·45	6·72	6·10	5·57	5·13	4·77	4·49
2·44	8·01	7·28	6·64	6·07	5·58	5·16	4·81	4·54
2·48	7·82	7·17	6·59	6·06	5·60	5·20	4·86	4·59
2·52	7·69	7·10	6·56	6·06	5·62	5·24	4·92	4·65
2·56	7·60	7·06	6·55	6·07	5·65	5·28	4·98	4·71
2·60	7·54	7·03	6·55	6·09	5·68	5·33	5·03	4·78
2·64	7·50	7·01	6·55	6·11	5·71	5·37	5·08	4·85
2·68	7·47	7·00	6·56	6·13	5·75	5·42	5·14	4·92
2·72	7·45	7·01	6·58	6·17	5·79	5·46	5·20	4·99
2·76	7·45	7·02	6·60	6·20	5·83	5·51	5·27	5·06
2·80	7·46	7·03	6·62	6·23	5·87	5·57	5·33	5·14
2·84	7·47	7·04	6·64	6·26	5·91	5·63	5·40	5·22
2·88	7·48	7·06	6·66	6·30	5·96	5·69	5·46	5·30

Transition from helium-II to helium-I is marked by a horizontal line.
† These values correspond to supercooled liquid and are included for interpolation purposes.

The entropy S. As explained at the beginning of the paper the entropy diagram of liquid helium can be calculated by combining the specific heats from Table 4 and the measurements of the pressure coefficient at 1·75° K. As a starting point, the entropy of the liquid in equilibrium with its vapour at 1·75° K was taken to be 1·853 J/mole.deg.K; this value has been given by Clement[12] after the C_{sat} measurements by Kramers, Wasscher, and Gorter[11] were corrected to the T_{55E} temperature scale. Further corrections to the T_{58} temperature scale are not necessary. Relation (2) was then employed to compute the entropy at various densities at 1·75° K. Simpson's 1/3 rule was used in the numerical integration; the length of step was 0·001 g/cm³. Relation (1) and the smooth specific heats were then used to compute the entropy diagram. Simpson's rule was again employed in the integration. The length of step was 0·02° K in the helium-I region, 0·01° K in the helium-II region, and 0·005° K in the vicinity of the λ curve. No further smoothing has been applied to the entropies obtained in this way and the final results are given in Table 5 and Figure 7. In this Figure, lines corresponding to the liquid along the vaporization and solidification curves are included; the former was drawn according to the measurements of Hill and Lounasmaa[13] and the latter by extrapolating the present entropy diagram to liquid

Table 5. The Entropy S (J/mole.deg.K) of Liquid Helium-4

T (°K)	ρ (g/cm³)							
	0·150	0·155	0·160	0·165	0·170	0·175	0·180	0·185
1·52	0·846	0·912	1·008	1·138	1·312			
1·56	0·988	1·058	1·164	1·310	1·509			
1·60	1·146	1·221	1·338	1·501	1·727	2·055†		
1·64	1·321	1·402	1·530	1·713	1·969	2·344†	3·007†	
1·68	1·513	1·602	1·743	1·946	2·235	2·666†	3·421†	
1·72	1·725	1·822	1·978	2·203	2·529	3·022†	3·880†	
1·76	1·958	2·065	2·236	2·486	2·853	3·418	4·393†	
1·80	2·215	2·332	2·520	2·798	3·211	3·857	4·704	
1·84	2·497	2·625	2·833	3·142	3·609	4·350	4·849	
1·88	2·806	2·945	3·176	3·523	4·052	4·914	4·967	
1·92	3·145	3·297	3·555	3·945	4·552	5·124	5·074	
1·96	3·517	3·684	3·973	4·417	5·141	5·272	5·174	
2·00	3·926	4·111	4·439	4·958	5·412	5·397	5·270	
2·04	4·378	4·588	4·969	5·508	5·575	5·510	5·362	5·200
2·08	4·886	5·131	5·619	5·720	5·712	5·616	5·452	5·280
2·12	5·467	5·796	5·893	5·886	5·835	5·716	5·540	5·358
2·16	6·160	6·110	6·084	6·028	5·950	5·813	5·626	5·436
2·20	6·462	6·321	6·245	6·158	6·059	5·907	5·710	5·513
2·24	6·677	6·495	6·389	6·279	6·162	5·999	5·793	5·590
2·28	6·861	6·651	6·521	6·393	6·263	6·089	5·876	5·666
2·32	7·025	6·793	6·645	6·502	6·360	6·178	5·957	5·742
2·36	7·177	6·927	6·763	6·608	6·456	6·265	6·037	5·817
2·40	7·318	7·054	6·877	6·711	6·549	6·351	6·117	5·892
2·44	7·453	7·175	6·988	6·811	6·641	6·436	6·196	5·966
2·48	7·582	7·293	7·095	6·910	6·732	6·520	6·275	6·041
2·52	7·706	7·407	7·200	7·007	6·822	6·604	6·353	6·114
2·56	7·826	7·518	7·303	7·102	6·911	6·686	6·431	6·188
2·60	7·943	7·628	7·405	7·197	6·999	6·769	6·509	6·262
2·64	8·058	7·735	7·505	7·290	7·086	6·850	6·586	6·335
2·68	8·171	7·840	7·603	7·382	7·172	6·932	6·663	6·409
2·72	8·281	7·944	7·701	7·473	7·257	7·012	6·739	6·482
2·76	8·390	8·046	7·797	7·563	7·342	7·092	6·816	6·555
2·80	8·497	8·147	7·892	7·652	7·426	7·172	6·892	6·629
2·84	8·603	8·247	7·986	7·741	7·510	7·251	6·968	6·702
2·88	8·707	8·345	8·079	7·829	7·593	7·331	7·044	6·776

Transition from helium-II to helium-I is marked by a horizontal line.
† These values correspond to supercooled liquid and are included for interpolation purposes.

densities at the solidification curve. The entropy along the λ curve is given in Table 3 and the entropy surface is shown in Figure 8.

The accuracy of the entropy diagram is determined by the accuracy of the C_V and $(\partial p/\partial T)_V$ measurements. It can be estimated as 2 per cent between 1·5° K and the λ curve, and 1 per cent in the helium-I region. At 2·50 and 2·75° K the entropies by Lounasmaa and Kojo[4] are 1·5–2 per cent lower than the present ones. This discrepancy is within the experimental accuracy of both diagrams. At 1·75° K the absolute difference between these diagrams is approximately the same as at 2·50° K, but due to the smaller value of the entropy it represents a discrepancy of 7–9 per cent. This indicates clearly the importance of determining the constants of integration at the low

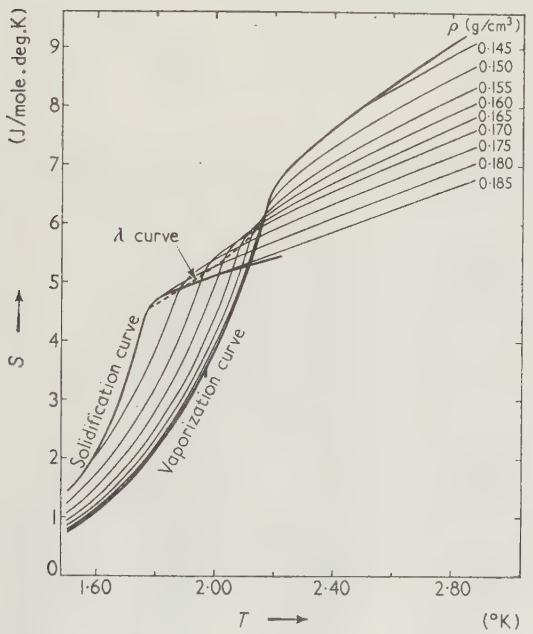

Figure 7. The entropy diagram of liquid helium-4

temperature end of the entropy diagram. Since these were computed at 1·75° K and since the specific heats of Hercus and Wilks[3] are somewhat uncertain, the present entropy diagram was not extended below 1·5° K. The entropy differences along constant density lines may be computed easily between 1·2 and 1·5° K by using the specific heats from Table 4. Since Keesom and Keesom[1] have published their entropy diagram of liquid helium as a very small graph only, comparisons with it are rather useless. In Table 5 entropies are given to three decimals; this permits an accurate calculation of ΔS along constant density lines between two temperatures close to each other. Owing to the method used in computing the entropy diagram the differences are not equally accurate along isotherms except near 1·75° K.

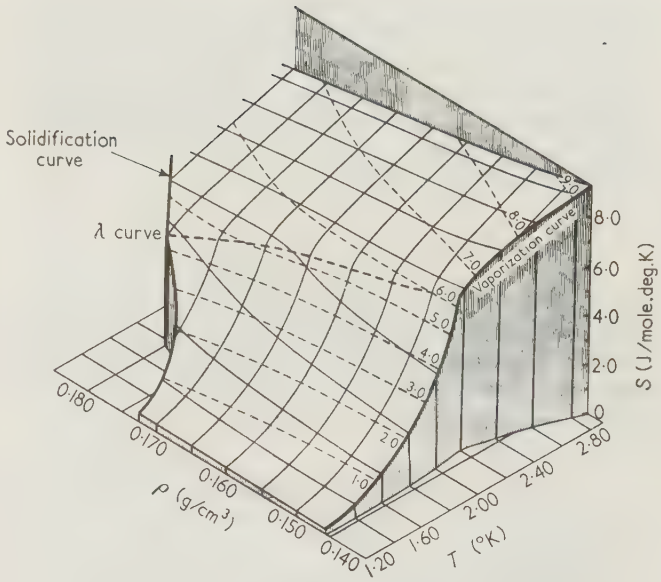

Figure 8. The entropy surface. Curves of constant density, constant temperature, and constant entropy (broken lines) are shown

It is observed from Figure 7 that the entropy is decreasing with increasing volume at constant temperature not only in the helium-II region but also in the helium-I region near the transition curve.[4] Since, according to thermodynamics,

$$(\partial p/\partial T)_V = (\partial S/\partial V)_T \qquad \ldots(6)$$

the pressure coefficient is negative in the same region. This is in agreement with the results of measurements of $(\partial p/\partial T)_V$ by Lounasmaa and Kaunisto[8] near the λ curve, which are reproduced in Figure 9. It shows that the pressure coefficient becomes positive in the helium-I region 0·04–0·07° K above the transition temperature.

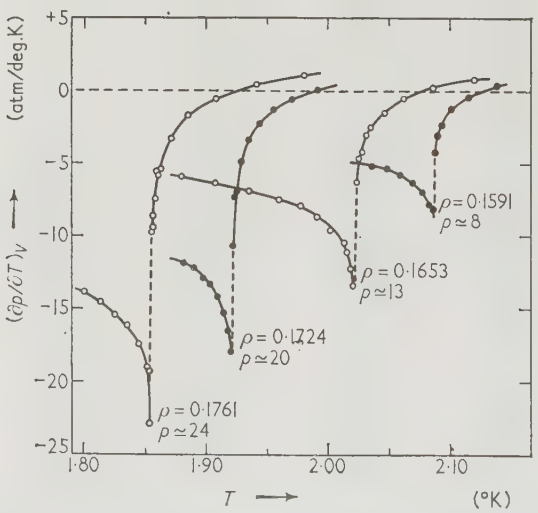

Figure 9. The pressure coefficient near the λ curve (Lounasmaa and Kaunisto[8])

Near the liquid–vapour equilibrium curve this temperature difference seems to become smaller than 0·01° K.[14]

Other thermodynamic functions. The internal energy diagram was computed very much in the same way as the entropy diagram. The starting value for liquid in equilibrium with its vapour at 1·75° K was first calculated according to the thermodynamic relation

$$\Delta U = \int C_{sat}.dT - \int p.dV \qquad \ldots(7)$$

The second term on the right can be ignored below 1·75° K. Measurements by Kramers, Wasscher, and Gorter,[11] corrected to the T_{55E} temperature scale,[12] were again used for C_{sat} and the result was $U - U_0 = 2{\cdot}752$ J/mole. Relations (4) and (3) were then employed for computing the internal energy diagram. The final results along the λ curve are given in Table 3 and the internal energy diagram is published in Table 6 and Figure 10. In the latter, curves corresponding to the liquid–vapour and liquid–solid equilibrium lines are again included. Since the specific heat below 1·5° K is relatively small at all densities the internal energy curves will become almost horizontal at lower temperatures. If the internal energy is plotted as a function of density at constant temperatures, the curves exhibit minima in the helium-I region. These minima satisfy the relation $(\partial U/\partial V)_T = T(\partial p/\partial T)_V - p = 0$, i.e. $p/T = (\partial p/\partial T)_V$. They can thus only be found in regions where the pressure coefficient is positive. The curve through the minima seems to terminate near the lower λ point. The accuracy of the internal energy

Table 6. The Internal Energy $U - U_0$ (J/mole) of Liquid Helium-4

T (°K)	ρ (g/cm³)							
	0·150	0·155	0·160	0·165	0·170	0·175	0·180	0·185
1·52	1·205	1·693	2·506	3·665	5·200			
1·56	1·424	1·918	2·746	3·930	5·503			
1·60	1·673	2·176	3·021	4·232	5·848	7·932†		
1·64	1·956	2·469	3·333	4·575	6·239	8·401†	11·333†	
1·68	2·276	2·801	3·686	4·963	6·682	8·935†	12·020†	
1·72	2·636	3·175	4·085	5·400	7·181	9·541†	12·801†	
1·76	3·042	3·597	4·534	5·893	7·746	10·229	13·694†	
1·80	3·499	4·072	5·040	6·448	8·383	11·011	14·244	
1·84	4·012	4·606	5·609	7·074	9·106	11·908	14·509	
1·88	4·587	5·203	6·249	7·782	9·932	12·958	14·729	
1·92	5·231	5·871	6·969	8·585	10·881	13·356	14·931	
1·96	5·953	6·621	7·780	9·500	12·024	13·644	15·125	
2·00	6·762	7·467	8·701	10·572	12·559	13·892	15·315	
2·04	7·677	8·431	9·774	11·681	12·889	14·120	15·502	17·186
2·08	8·722	9·550	11·113	12·118	13·171	14·337	15·688	17·350
2·12	9·942	10·947	11·687	12·466	13·431	14·548	15·872	17·515
2·16	11·427	11·619	12·095	12·771	13·676	14·755	16·055	17·682
2·20	12·083	12·078	12·447	13·054	13·913	14·960	16·239	17·850
2·24	12·562	12·465	12·766	13·322	14·143	15·164	16·424	18·020
2·28	12·977	12·816	13·065	13·580	14·370	15·368	16·610	18·192
2·32	13·355	13·143	13·350	13·831	14·594	15·572	16·796	18·366
2·36	13·709	13·456	13·627	14·078	14·818	15·776	16·985	18·542
2·40	14·047	13·758	13·898	14·323	15·040	15·980	17·175	18·720
2·44	14·372	14·052	14·165	14·567	15·263	16·186	17·366	18·901
2·48	14·688	14·341	14·429	14·809	15·487	16·393	17·560	19·083
2·52	14·998	14·627	14·692	15·051	15·711	16·602	17·755	19·268
2·56	15·304	14·910	14·954	15·294	15·937	16·812	17·953	19·455
2·60	15·607	15·191	15·216	15·537	16·163	17·025	18·153	19·645
2·64	15·908	15·472	15·478	15·781	16·391	17·239	18·356	19·838
2·68	16·207	15·752	15·740	16·026	16·620	17·455	18·560	20·033
2·72	16·505	16·032	16·003	16·272	16·851	17·672	18·767	20·231
2·76	16·803	16·313	16·267	16·519	17·083	17·892	18·976	20·432
2·80	17·101	16·594	16·531	16·768	17·317	18·113	19·188	20·636
2·84	17·400	16·875	16·796	17·017	17·553	18·337	19·403	20·843
2·88	17·699	17·157	17·062	17·268	17·790	18·564	19·620	21·054

Transition from helium-II to helium-I is marked by a horizontal line.
† These values correspond to supercooled liquid and are included for interpolation purposes.

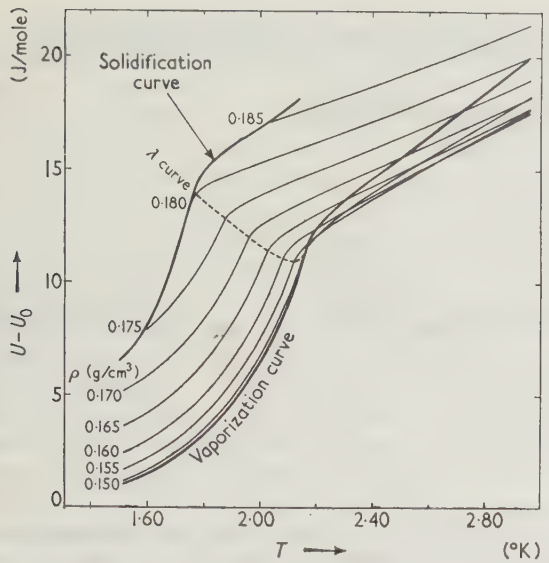

Figure 10. The internal energy diagram of liquid helium-4

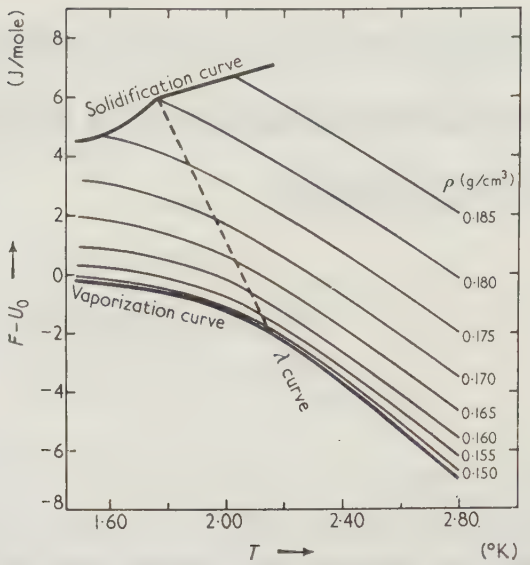

Figure 11. The free energy diagram of liquid helium-4

diagram is approximately the same as that of the entropy diagram. It depends not only on C_V and $(\partial p/\partial T)_V$, but also on p along the isotherm at 1·75° K.

The free energy $F-U_0=U-U_0-TS$ can now be computed from Tables 5 and 6. The slope of the free energy curves is equal to the negative of the entropy; this explains why nothing drastic happens to them at the λ transition point (Figure 11).

Other thermodynamic functions, like the enthalpy and the Gibbs free energy, can be calculated from the present results without differentiation if the equation of state is known. The only extensive p–V–T data available are the rather old measurements by Keesom and Keesom;[2] experiments by Edeskuty and Sherman[9] cover only the helium-I region. In the absence of more complete recent data such diagrams were not computed.

The measurements described on pages 213–214 were made at the Wihuri Physical Laboratory with the assistance of Miss Leila Kaunisto and Mr. Esko Kojo. The rest of the work was done at the Argonne National Laboratory with the efficient help of Mr. Pat Roach. The author wishes to express his sincere thanks to these persons. He is also indebted to the Emil Aaltosen Säätiö and the University of Turku for scholarships. The work on which this paper is based was performed in part under the auspices of the U.S. Atomic Energy Commission.

REFERENCES

1. Keesom, W. H., and Keesom, A. P. *Physica* **1**, 161 (1933)
2. Keesom, W. H., and Keesom, A. P. *Physica* **1**, 128 (1933)
3. Hercus, G. R., and Wilks, J. *Phil. Mag.* **45**, 1163 (1954)
4. Lounasmaa, O. V., and Kojo, E. *Ann. Acad. Sci. fenn.* **AVI**, No. 36 (1959)
5. Hill, R. W., and Lounasmaa, O. V. *Phil. Trans.* **252**, 357 (1960). For a more detailed account see: Lounasmaa, O. V. *Thesis* (Oxford, 1958)
6. Keesom, W. H., Bijl, A., and Monté, L. A. J. *Appl. sci. Res., Hague* **A4**, 25 (1953)
7. Brickwedde, F. G. *Physica* **24**, 128 (1958)
8. Lounasmaa, O. V., and Kaunisto, L. *Ann. Acad. Sci. fenn.* **AVI**, No. 59 (1960)
9. Edeskuty, F. J., and Sherman, R. H. *Low Temperature Physics and Chemistry: Proc. 5th Intern. Conf. on Low Temp. Phys. and Chem.* (Madison, Wisconsin) p. 102 (1958)
10. Fairbank, W. M., Buckingham, M. J., and Kellers, C. F. *Low Temperature Physics and Chemistry: Proc. 5th Intern. Conf. on Low Temp. Phys. and Chem.* (Madison, Wisconsin) p. 50 (1958)
11. Kramers, H. C., Wasscher, J. D., and Gorter, C. J. *Physica* **18**, 329 (1952)
12. Clement, J. R. *P.V. Com. int. Poids Més.* **26A**, Annexe T 21 (1959)
13. Hill, R. W., and Lounasmaa, O. V. *Phil. Mag.* **2**, 143 (1957)
14. Edwards, M. H. *Canad. J. Phys.* **36**, 884 (1958)

A Precision Laboratory Cryostat for Studying the Electrical and Elastic Properties of Crystals

V. A. Koptsik, B. A. Strukov, and L. A. Ermakova
Physical Faculty, Moscow State University

Received 8 March 1961†

A LARGE number of different types of cryostat which can be used for physico-chemical studies of matter has been described in the literature.[1–9] Without going into constructional details, we can distinguish the following main components of any present-day cryostat; thermostatted chamber, heater, coolant, temperature regulating system (manual or automatic), and temperature measuring arrangement. Most such equipments have disadvantages making it difficult to use them for studying the electrical properties of crystals at different temperatures. The limiting accuracy of the temperature control ($\pm 0{\cdot}5$–1°C) and the complexity of construction are such drawbacks. The existing methods of automatic temperature control come down, in the main, to two types. In one the constant temperature is maintained by a photoelectric regulator which controls the current through a heater, while in the other the heating is determined by a thyratron regulator. These methods achieve temperature control with an accuracy of $\pm 0{\cdot}01^\circ$C.

Sarakhov[2] has obtained an accuracy in temperature control of $\pm 0{\cdot}005^\circ$C in his cryostats. A resistance thermometer, included in a bridge circuit, is used as the temperature pick-up. The out-of-balance signal, arising from overheating or undercooling, is amplified and rectified and controls the current through a heater. The absence of a phase-sensitive stage is an inconvenience, making necessary an additional control on the cryostat temperature. Wilson and Stone[9] developed this system in 1957, introducing a phase-sensitive stage. The heater was incorporated as the anode load of the output power stage. The magnitude of the current through it depends on the relative phases of the voltage applied to the bridge and of the out-of-balance signal. Vasil'ev[1] used this circuit, connecting it with the heating current control, thereby increasing still further the accuracy of temperature regulation. The present authors have used Vasil'ev's circuit as the basis for constructing a precision laboratory cryostat for studying the electrical and elastic properties of crystals in the region of polymorphic phase transitions.

† Received by PTÉ Editor 30 December 1959. *Pribory i Tekhnika Éksperimenta* No. 1, 180 (1961).

The nature of ferroelectric and piezoelectric measurements make further demands on the cryostat.

(1) It must make possible the attainment of stable temperatures at intervals of 0·1 to $0{\cdot}2^\circ$C (this is essential for measurements in the region of phase transitions).

(2) Temperatures must be stable to better than $\pm 0{\cdot}005^\circ$C for the time required to carry out in full complex electrical measurements at each point (30–60 min).

(3) The specimen must be in a vacuum or in a dry atmosphere to prevent condensation, and the accompanying changes in electrical properties.

(4) The arrangement of electrical leads must not introduce temperature gradients in the thermostatted chamber.

Other important points relate to convenience in changing specimens, the reliability of the electrical contacts, and the ease in going from one temperature to another. Considerable cooling should last for 6–7 hr.

The experimental arrangement

The apparatus consists of the cryostat, the electrical circuit, which controls the temperature to the necessary accuracy, the vacuum system, and the potentiometric circuit for measuring the temperature.

The thermostatted cryostat. This consists of a block of copper 9 (Figure 1), 180 mm long and 45 mm in diameter. Two cylindrical channels are drilled in the cylinder and extend over three-quarters of its whole length. One of the channels is for the thermocouple and the other for the ampoule containing the specimen. There is a four-start thread on the surface of the cylinder, of 67 turns with 1·5 mm spacing and 1 mm deep. The heater of nichrome wire (0·1 mm diameter) is wound in two of the channels, and a platinum resistance thermometer (0·03 mm diameter, 'extra' platinum) in the other two. The thread is covered with a layer of polymerized Bakelite varnish to insulate the wires from the copper block. At 250 V this insulation resistance is $\sim 10^{10}\ \Omega$. The heater has a resistance of 1 kΩ and the thermometer 300 Ω. When the temperature is being controlled automatically, it is the surface of the copper block which is maintained at

constant temperature. Because of the high heat conductivity of copper, the same temperature is reached after a certain time (10–15 min) in the space for the specimen container.

The system for cooling the thermostatted chamber. Regulation of the flow of cold to the copper block is achieved in the following way (Figure 1). The copper block 9, covered with the aluminium shield 10, is contained in a cylindrical double-walled glass vessel 11. The space between the walls is connected to a vacuum system by the glass tube 7. The glass vessel is fixed into the cap 2 made of porous plastic PS-4, and is bathed in liquid nitrogen contained in the large Dewar 3. An ebonite stopper 6 is screwed on to the aluminium shield, with openings for the heater and resistance thermometer leads. The flange of the stopper rests on the Textolite cover and thus carries the whole weight of the thermostat.

The whole structure is housed in a sheet iron case 4 for protection against breakage and for rigidity. The outer Dewar is insulated from the casing by a rubber washer in the form of a ring. A wooden support 5 is placed at the bottom of the case. For a pressure of 10^{-2} to 10^{-3} mm Hg between the walls of the inner Dewar 11, the influx of cold can be compensated by a low power heater (1 kΩ, 8 mA).

The electronic regulating circuit. The temperature sensitive element of the circuit is a platinum resistance thermometer R_p, wound on the copper block and incorporated into an equal arm bridge (Figure 2). The other arms are manganin resistors r_1 and r_2, each of 250 Ω,

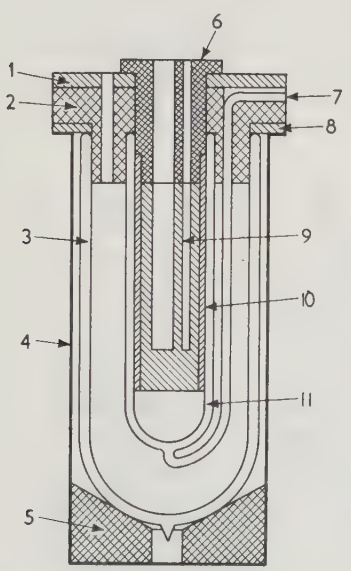

1: Textolite lid
2: Porous plastic PS-4 lid
3: Outer Dewar
4: Sheet iron protective case
5: Wooden support
6: Ebonite stopper
7: Glass connecting tube to pump
8: Rubber ring
9: Copper block
10: Aluminium shield
11: Inner glass vessel

Figure 1. Construction of the cryostat

and a non-inductive resistance box R, which serves to establish the required temperature. The bridge is balanced when $R_p(T) = R$.

If a voltage $u = u_0 \sin \omega t$ is applied to the bridge, then for $R_p > R$

$$u_{\text{out of balance}} = \left(\frac{u_0}{2} - \frac{u_0 R}{R_p + R}\right) \sin \omega t$$

while $uR/(R_p + R) > \frac{1}{2}u_0$.

For $R_p = R$ we have $u_{\text{out of balance}} = 0$

For $R_p < R$ we obtain

$$u_{\text{out of balance}} = \left(\frac{u_0}{2} - \frac{u_0 R}{R_p + R}\right) \sin \omega t$$

while $u_0 R/(R_p + R) < \frac{1}{2}u_0$.

The phase of the out-of-balance signal therefore changes by 180 degrees depending on which of the conditions $R_p > R$ or $R_p < R$ is fulfilled. The electrical circuit is required to arrange automatically that an amount of heat should be applied to the sensitive element so that the resistance of the platinum should be kept equal to the resistance of the box.

The fixed frequency 2 kc/s oscillator is made from two 6N8 triodes, the first of which, V_1, is a self-oscillator and the second, V_2, is a tuned amplifier. Two voltages of 2 and 40 V are tapped off the transformer T_2; the first supplies the bridge and the second is the reference for the phase detector V_7. The reference phase can be changed by the phase shifting circuit, 300 kΩ—150 kΩ—470 pF. The supply to the oscillator is stabilized by the stabilizer SG-4 and the supply to the whole circuit except the final valve V_9 is provided by a separate rectifier with electronic stabilization.

The amplified bridge out-of-balance signal is fed to the three valves V_3–V_5. By using a filter of two RC circuits, the 50 c/s background and the high frequency noise can be completely suppressed. (The filter is described by Henshaw.[10]) The maximum amplification of the circuit, 5×10^5, makes the amplifier sensitive to out-of-balance voltages of tens of microvolts. The amplified out-of-balance voltage is fed to the limiter V_6, working in the diode region, so that there is only a positive half-wave out-of-balance voltage on the anode of the next triode V_7. The reference voltage is applied to the grid of V_7 through a limiting resistance of 1 MΩ. When the reference voltage is in phase with the amplified out-of-balance voltage, a high current flows through valve V_7 and a very small positive voltage is obtained at the input to the d.c. restorer (the diode 6B8S). If the out-of-balance voltage is opposite in phase to the reference voltage then the whole voltage is passed to the next stage.

The output voltage of the phase detector (which is different in magnitude for in-phase and out-of-phase voltages) is applied to an integrating circuit, 3 MΩ—2 mμF, and then to a d.c. restorer. As a result, a d.c. voltage of magnitude determined by the magnitude and phase of the out-of-balance signal is applied to the control grid of 6B8S.

The amplified d.c. voltage is applied to the grid of the power amplifier V_9 and the nichrome heater is the anode load of this valve. This amplifier is fed from a 300 V rectifier. The cathode of V_9 is given a positive bias of +70 V, which is sufficient to cut-off the valve when the signal applied to the grid of V_8 corresponds to the voltages from the oscillator and from the out-of-balance signal being in-phase. The overall amplification of the circuit and the magnitude of the bias applied to V_9 are chosen so that a change of 0·2 Ω in the resistance R from the balance position of the bridge produces a current of 100 mA through V_9 and the heater. The power dissipated in the heater is then ~10 W. The reduction of R to any value below that corresponding to balance does not lead to a current through the heater. The chamber is cooled during that time until the bridge is unbalanced. As soon as the platinum resistance becomes slightly less than R, current flows through the heater, maintaining a very constant value for the resistance R_p.

The temperature of the thermostatted space was checked by the magnitude of the platinum resistance and also with the help of a triple copper–constantan thermocouple, housed in a hole in the copper block.

The vacuum system. This is shown diagrammatically in Figure 3. It consists of two main sections, through one of which the inner Dewar of the cryostat is pumped (the two-way tap 10, inner Dewar 8, and thermocouple gauge 2 for measuring the vacuum), while the other allows the glass tube with specimen holder to be pumped and also filled with dry air (tube 5, mercury manometer 4, tube with drying agent 3, and three-way tap 9). The pumping system includes a fore vacuum pump 7, oil vapour trap 6, three-way tap 11, and a fore vacuum bottle 1. The electrical leads in the specimen tube are made of fine wire and the heat flow along them is negligible.

Operation of the cryostat

The attainment of the required temperature and its maintenance to the necessary accuracy reduces to the following:

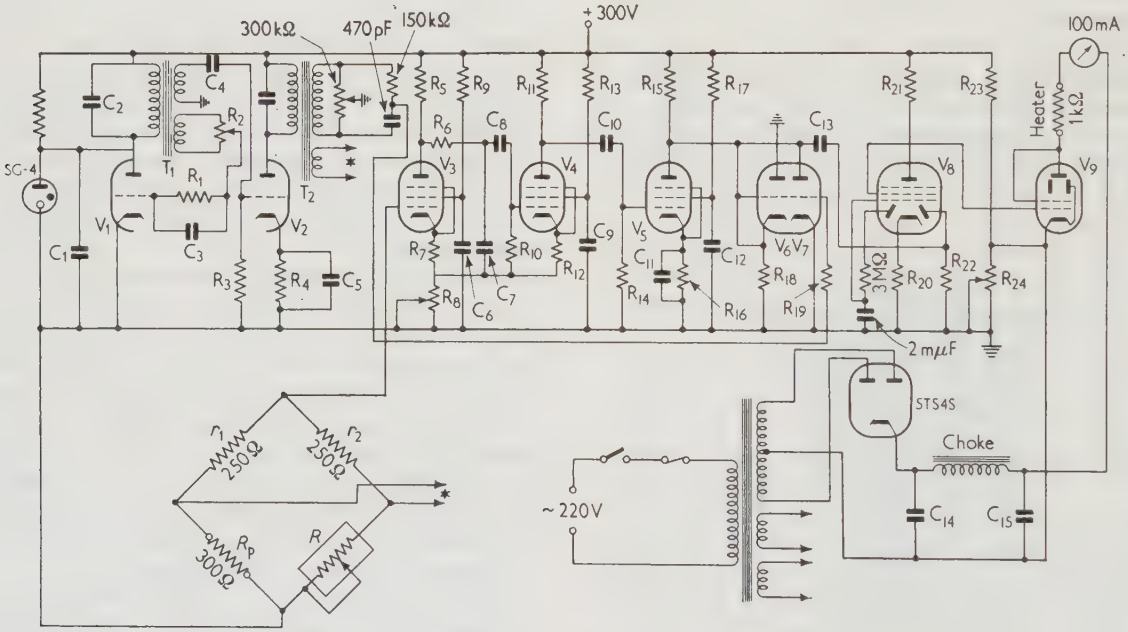

V_1, V_2: 6N8 — V_3, V_4, V_5: 6Zh8 — V_6, V_7: 6N8 — V_8: 6B8S — V_9: 6P3

R_1: 82 kΩ; R_2: 22 kΩ; R_3: 0·5 MΩ; R_4: 300 Ω; R_5: 100 kΩ; R_6: 150 kΩ; C_1: 20 μF; C_2: 10 mμF; C_3: 0·05 μF

R_7: 2·5 kΩ; R_8: 2 kΩ; R_9: 2 MΩ; R_{10}: 0·5 MΩ; R_{11}: 100 kΩ; R_{12}: 2·5 kΩ; C_4: 5 mμF; C_5: 10 μF; C_6: 0·1 μF; C_{13}: 50 mμF

R_{13}: 2 MΩ; R_{14}: 0·5 MΩ; R_{15}: 100 kΩ; R_{16}: 2·5 kΩ; R_{17}: 2 MΩ; R_{18}: 3 MΩ; C_7: 750 pF; C_8: 750 pF; C_9: 0·1 μF; C_{14}: 20 μF

R_{19}: 1 MΩ; R_{20}: 700 Ω; R_{21}: 27 kΩ; R_{22}: 0·9 MΩ; R_{23}: 0·5 MΩ; R_{24}: 330 kΩ; C_{10}: 50 mμ; C_{11}: 5 μF; C_{12}: 0·1 μF; C_{15}: 20 μF

Figure 2. Electronic circuit of automatic temperature regulator

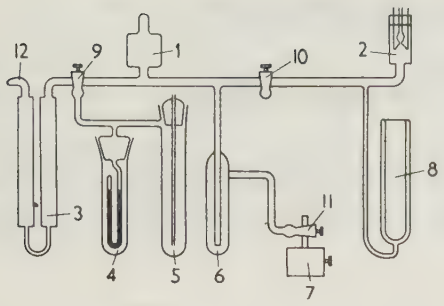

1: Fore vacuum bottle
2: Thermocouple gauge
3: Drying tube
4: Mercury manometer
5: Tube with specimen
6: Oil vapour trap
7: Fore vacuum pump
8: Inner Dewar
9: Three-way tap
10: Two-way tap
11: Three-way tap
12: Capillary

Figure 3. Vacuum system

(1) The copper block and specimen holder are put into the cryostat Dewar;
(2) Liquid nitrogen is poured into the outer Dewar and the automatic nitrogen level device[11] put into operation. Cooling starts at a rate of approximately 0·5 deg.C/min;
(3) Within 3–4°C of the required temperature the inner Dewar is pumped and the pressure reduced to 10^{-3} mm Hg. The rate of cooling is rapidly reduced;
(4) The bridge is balanced by means of the resistance box;
(5) The automatic temperature control circuit is switched in.

Further reduction in the temperature is produced in discrete steps using the resistance box.

As has already been mentioned, the accuracy of the stabilization is checked by measuring the e.m.f. of the copper–constantan thermocouple which has a sensitivity ~0·1 mV/deg.C. The temperature changed by less than 0·005°C over a period of 60 min.

The operation of the cryostat was checked over a period of two years. The temperature dependence of a number of piezoelectric[12] and ferroelectric[13] crystals was obtained in the region of the ferroelectric phase transitions.

In conclusion we express our grateful thanks to B. N. Vasil'ev for suggesting the system and for practical advice on the cryostat construction, and to A. F. Solov'ev for help in setting up the electrical circuit.

REFERENCES

1. Vasil'ev, B. N. *Cryostat With Automatic Temperature Control* (VINITI Society, Suppl. 11, 59101/2)
2. Sarakhov, A. I. *Thesis* (Physico-chemical Institute, Academy of Sciences, U.S.S.R, 1953)
3. Sreedhar, A. K. *Proc. Indian Acad. Sci.* **36,** 141 (1952)
4. Peshkov, V. P. *J. exp. theor. Phys.* **14,** 514 (1944)
5. Ure, R. W. *Rev. sci. Instrum.* **28,** 836 (1957)
6. Andrews, D. H. *J. Franklin Inst.* **206,** 285 (1928)
7. Southard, J. C., and Andrews, D. H. *J. Franklin Inst.* **207,** 323 (1929)
8. Taylor, C. A. *Appl. Sci. Res.* **B4,** 271 (1955)
9. Wilson, W., and Stone, N. W. B. *J. sci. Instrum.* **34,** 327 (1957)
10. Beattie, J. R., and Conn, G. K. T. *Electron. Engng* **25,** 299 (1953)
11. Henshaw, D. E. *J. sci. Instrum.* **34,** 207 (1957)
12. Koptsik, V. A., and Ermakova, L. A. *Fiz. tverdogo Tela* **2,** 697 (1960)
13. Koptsik, V. A., Strukov, B. A., Sklyankin, A. A., and Levina, M. E. *C. R. Acad. Sci. U.S.S.R. (Fiz.)* **24,** 1228 (1960)

EDITORIAL NOTE

Included in this issue of CRYOGENICS for the first time are translations of papers concerning low temperature topics from the Russian journal *Pribory i Tekhnika Éksperimenta.* We have received these through the courtesy of the Soviet editors. By arrangement with the Soviet authorities, a cover-to-cover translation of PTÉ is published under the title *Instruments and Experimental Techniques* by Consultants Bureau Inc. for the Instrument Society of America, by whose permission these articles are printed in CRYOGENICS.

The Velocity of Sound in Liquid Argon and Liquid Nitrogen at High Pressures

A. Van Itterbeek and W. Van Dael

Instituut voor Lage Temperaturen en Technische Fysica, Louvain

Received 24 January 1961

DURING the last few years we have carried out some measurements on the velocity of sound in liquid argon, liquid oxygen, and liquid nitrogen[1–3] in order to obtain thermodynamic data. The earlier experimental arrangement, consisting of an interferometer with variable path length, limited the allowable pressure to about 75 kg/cm^2. In that range the pressure dependence was nearly linear. In order to extend this pressure range appreciably we developed a new apparatus with a fixed path resonator, and new measurements were carried out in liquid nitrogen and liquid argon. These results are compared with those obtained by other authors.

Experimental method

The acoustical resonator is shown in Figure 1. Two transducers K_1 and K_2 of barium titanate, with almost identical dimensions and properties, are separated by a brass tube (a) with accurately parallel ends (length 8 cm, diameter 2·3 cm). This tube is connected to the inner electrodes e_1 and e_2 of the crystals and to earth; b_1 and b_2

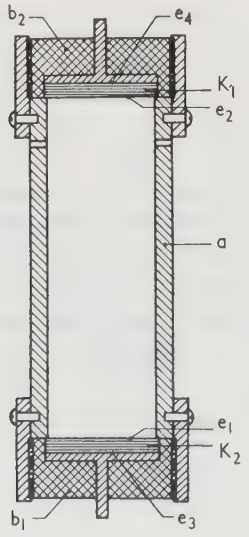

Figure 1. Acoustical resonator

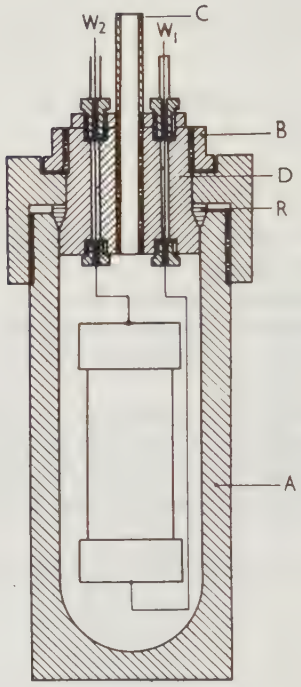

Figure 2. High pressure container

are pieces of Plexiglass pressing the transducers to the ends of the tube a. The electrode plates e_3 and e_4 are connected by means of insulated and screened lines to the electronic devices. The acoustical system is placed in a high pressure container (Figure 2).

This brass high pressure vessel is of a self-tightening type. The inside pressure compresses the aluminium packing ring R between the cylinder A and the cover D. The screw ring B is used to exert a preliminary pressure on the packing ring. The gas to be condensed is admitted through the stainless steel tube C which is screwed and hard soldered into the cover D. The connection wires W_1 and W_2 are insulated from D by a packing system filled with a resin plastic (Stycast 2850 GT) which resists very well the high pressures and low temperatures.

During a preliminary investigation we compared different measuring methods, using the properties of

standing waves and those of pulsed signals. The most accurate results are obtained by measuring, with an electronic counter, the pulse repetition frequency needed for interference of a pulse with the echoes of the preceding ones. The pulse width is about 20 μsec and the ultrasonic frequency 1 Mc/s. We estimate the precision in determining the pulse resonance frequency to be one part in a thousand. The block diagram of the electronic equipment is given in Figure 3.

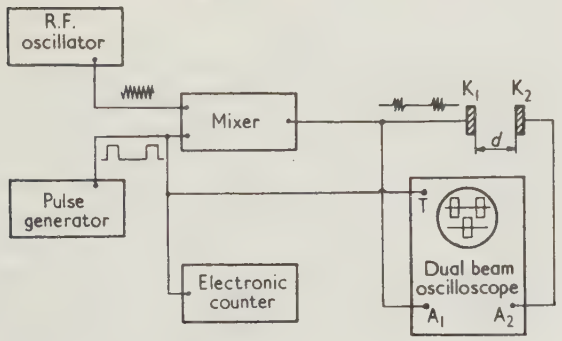

Figure 3. Block diagram of the electronic equipment

Table 1. Velocity of Sound in Liquid Nitrogen

90·1° K		87·3° K		77·4° K	
p (kg/cm²)	W (m/sec)	p (kg/cm²)	W (m/sec)	p (kg/cm²)	W (m/sec)
201·0	897·0	200·0	912·6	201·0	988·2
191·0	890·5	191·0	908·4	186·0	981·0
181·0	882·2	176·0	899·4	170·0	970·1
166·5	872·1	160·0	888·1	153·5	960·8
151·5	858·3	145·5	877·9	141·0	952·8
136·5	849·4	131·0	865·5	126·0	943·6
121·5	837·2	115·0	854·4	110·0	932·8
105·5	824·8	101·0	842·5	95·0	921·9
90·5	812·0	85·5	830·2	80·5	913·4
75·0	798·2	70·5	816·8	66·0	902·2
60·5	784·2	55·5	802·5	50·0	890·8
46·5	767·0	36·0	784·2	30·5	876·6
32·0	752·8	23·0	770·6	18·5	865·5
18·5	738·4	7·5	753·1	6·0	857·0
6·5	724·5	4·5	748·0		

Results

In Tables 1 and 2 the experimental results in liquid nitrogen and liquid argon at pressures up to 200 kg/cm² are given. From the graphs in Figures 4 and 5 we see clearly that at the highest pressures a deviation from linearity appears.

Finally, we compared our experimental results with the recently published data of Dobbs and Finegold.[4] They measured, up to 135 atm, the resonance frequencies of a barium titanate cylinder filled with the same liquids as in our experiments. From these measurements they calculated the most probable value of the velocity W by means of the equation

$$W = W_0 + ap + bp^2$$

For the values of W_0, a, and b we refer to Table 3. In Figures 4 and 5 we have given our experimental results together with the curves representing the equations established by Dobbs and Finegold. Two conclusions can be drawn:

(1) The absolute value of the velocity depends directly on the precision in determining the dimensions of the resonator. Taking into account the thermal expansion of the tube and the correction of the ends of the resonator we calculated an effective path length. The results obtained in this way agree with the data in the literature. The discrepancy of about 0·5 per cent with the results of Dobbs and Finegold can be explained, as they suggest in their paper, by the presence of a systematic error, probably related to the effective diameter of their barium titanate resonator.

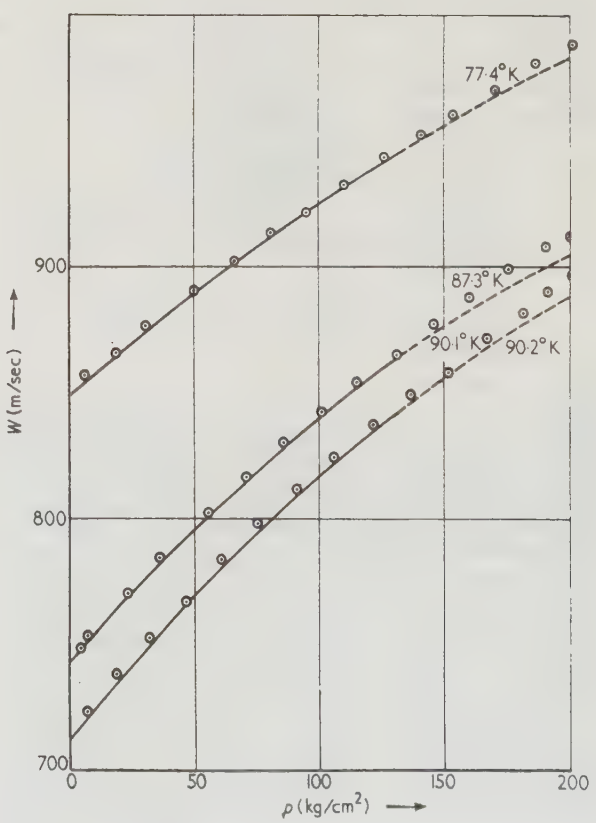

Figure 4. Velocity of sound in liquid nitrogen

Table 2. Velocity of Sound in Liquid Argon

90·3° K		87·3° K	
p (kg/cm²)	W (m/sec)	p (kg/cm²)	W (m/sec)
201·5	908·4	144·0	904·1
189·5	904·9	136·0	901·0
176·0	899·6	120·0	895·4
161·0	894·2	103·0	889·4
142·5	887·3	83·0	881·1
127·0	879·9	62·5	870·5
111·0	872·7	42·0	860·4
95·0	866·2	24·0	853·9
80·5	859·6	13·5	846·8
65·5	852·3	3·0	843·0
52·0	846·2		
37·0	839·0		
27·0	833·2		
14·0	827·3		
3·5	821·4		

(2) The pressure dependence of W in both sets of measurements is quite the same. It appears from the extrapolation of the $W(p)$ curves to 200 kg/cm² that in the case of nitrogen the influence of the quadratic term b is overestimated. A decrease in the absolute value of the negative term b should be compensated by a decrease in the positive value of a. We calculated again, going out from our experimental results, the most probable value of a and b (Table 3). As pressure units we have adopted kilograms per square centimetre.

Table 3

		Van Itterbeek/Van Dael up to 75 kg cm² (references 1–3)		*Dobbs/Finegold up to 135 kg cm² (reference 4)*			*Actual results up to 200 kg/cm²*		
		W_0 (m/sec)	$a(b=0)$	W_0 (m/sec)	a	$b.10^4$	W_0 (m/sec)	a	$b.10^4$
N_2	90·3	725·0	1·078						
	90·2			712·8	1·207	−16·3			
	90·1						717·4	1·164	−13·7
	87·3			743·5	1·134	−16·1	744·1	1·109	−13·4
	77·4	857·4	0·716	849·2	0·848	− 8·9	851·9	0·804	− 6·2
A	90·3	819·6	0·54				819·6	0·533	− 4·5
	90·1			816·2	0·529	− 4·1			
	87·3						840·7	0·523	− 5·7
	87·2			836·2	0·498	− 3·6			
	87·1	841·0	0·48						

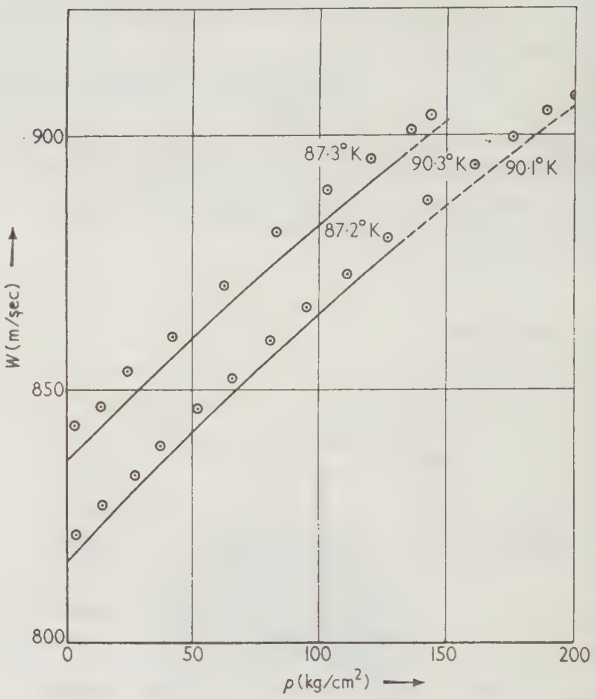

Figure 5. Velocity of sound in liquid argon

This study is a part of the research programme carried out with Dr. L. Deffet, Director of the Institut Belge des Hautes Pressions, on the equation of state of fluids. It was financially supported by the Institut pour l'Encouragement de la Recherche Scientifique dans l'Industrie et l'Agriculture, to which we express our sincere thanks. We also thank Dr. G. Forrez for his advice and help during the construction of the apparatus.

REFERENCES

1. Van Itterbeek, A., and Van Dael, W. *Bull. Inst. int. du Froid.* Suppl. Annexe 1–1958, 295–306.
2. Van Itterbeek, A., Van Dael, W., and Grevendonk, W. *Physica* **25**, 640 (1959)
3. Van Itterbeek, A., Grevendonk, W., Van Dael, W., and Forrez, G. *Physica* **25**, 1225 (1959)
4. Dobbs, E. R., and Finegold, L. *J. acoust. Soc. Amer.* **32**, 10, 1215 (1960)

A Direct Reading Constant Volume Gas Thermometer

J. K. Hulm and R. D. Blaugher *Westinghouse Research Laboratories, Pittsburgh, Pa.*

Received 26 January 1961

In recent studies of superconducting materials, the need arose for fairly accurate and rapid temperature determination between 4·2° K and 20° K. An instrument frequently employed for this temperature range is the constant volume helium gas thermometer, which utilizes the variation of pressure with temperature at constant volume. This type of thermometer has a major advantage in that it needs to be calibrated only at one temperature, since the equation of state for helium gas is known very accurately.

In the usual mode of operation of gas thermometers, the pressure is determined on a special mercury-in-glass manometer. This manometer is arranged so that the mercury meniscus on the helium side can be adjusted to touch a fiducial pointer in order to maintain a constant dead space volume. Unfortunately, this technique is quite laborious, requiring a series of time-consuming volume adjustments for each pressure reading. When some of our experiments required the rapid determination of a large number of different temperatures, the adjustment of the mercury column for each reading became impractical. Because of its ease of calibration, we were reluctant to abandon the gas thermometer, and we therefore sought a more rapid method of measuring pressure. The problem was solved by adopting a modified aneroid-type pressure gauge constructed by Wallace and Tiernan, Belleville, New Jersey, from their basic Precision Dial Manometer Model FA 145.

The FA 145 pressure gauge has a custom calibrated pressure gauge scale from 0 to 800 mm Hg. The pressure sensitive element will respond to pressure changes of one part in 10,000 of the scale range with an accuracy of one part in 1,000. The reproducibility is extremely good and can be attributed partly to the reduction of any hysteresis effect to one part in 500 for a full range in pressure. The casing surrounding the pressure sensitive capsule can be evacuated, converting the instrument to an absolute pressure measuring device. At our request, the FA 145 was modified by the Wallace and Tiernan Company to minimize the dead space of the pressure sensitive capsule and its internal connecting tube. The resultant dead space amounted to about 9·2 cm^3 at zero gauge pressure, with an increase of approximately 0·5 cm^3 for a full scale (0–800 mm Hg) change in gauge pressure.

The pressure gauge was connected by approximately 220 cm of 1 mm inside diameter cupro-nickel capillary tube to the actual gas thermometer bulb. The system could be evacuated or filled through a modified Hoke needle valve which was inserted in the capillary line in the manner shown in Figure 1. This needle valve was fitted with sleeve inserts in order to minimize its dead space contribution.

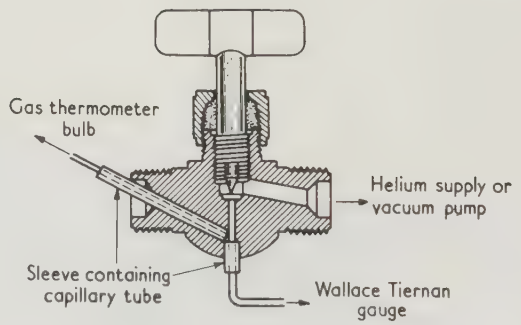

Figure 1. Modified Hoke needle valve

The actual volume of the capillary tube plus the needle valve was about 2·0 cm^3. However, in calculating the dead space correction, allowance had to be made for the fact that part of the capillary tube was at low temperature within the cryostat. The contribution of this low temperature region was measured directly as a function of the temperature at the lower end in a separate experiment in which the capillary was sealed off at the point of entry to the thermometer bulb. If we refer all dead space volumes to room temperature (296° K), the 'effective' volume of the capillary tube and needle valve amounted to 4·8 cm^3 with the lower end of the capillary at 4° K. Under these conditions, the combined effective volume of pressure gauge, needle valve, and capillary tube was 14·0 cm^3 (+0·5 cm^3 for full scale gauge reading) compared to 9·0 cm^3 in the gas thermometer bulb itself.

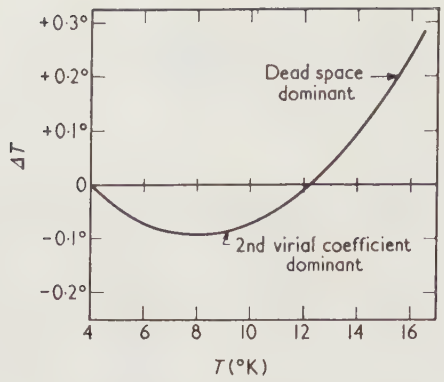

Figure 2. Correction to law $p = aT$ for thermometer pressure 150 mm Hg at 4° K

The practice was followed of calibrating the gas thermometer at one fixed temperature (usually 4° K) with the bulb and part of the capillary tube immersed in liquid helium. The bulb temperature was determined from the helium vapour pressure,[1] with suitable correction for the hydrostatic head of the liquid helium. The thermometer pressure was also corrected for the immersed portion of the capillary tube. In practice, both these corrections were determined experimentally by measuring the thermometer pressure as a function of liquid level at constant bath pressure.

For measurements above 4·2° K, with both the thermometer bulb and the capillary tube well above the surface of the liquid helium, the principal corrections arose from dead space and deviations from ideal gas behaviour. By starting with the same initial conditions of pressure and temperature (usually 150 mm at 4° K), a standard correction curve could be used in all experiments. This standard curve showing ΔT as a function of T is shown in Figure 2. Other corrections such as thermomolecular pressure, external temperature variation, gauge hysteresis, etc., had a negligible influence on ΔT under the conditions of our experiments. With the system described, temperatures between 4·2 and 20° K could be measured with an estimated accuracy of 0·02° K.

REFERENCE

1. Brickwedde, F. G., van Dijk, H., Durieux, M., Clement, J. R., and Logan, J. K. *J. Res. nat. Bur. Stand.* G4A, 1 (1960)

CONFERENCE

A *Symposium on Electric and Magnetic Properties of Thin Metallic Layers* is to be held on 4–7 September, 1961 at Louvain, Belgium, sponsored by the International Union of Pure and Applied Physics and the Flemish Academy of Sciences. Details may be obtained from: Prof. A. Van Itterbeek, Instituut voor Lage Temperaturen en Technische Fysika, Naamsestraat 61, Leuven, Belgium.

The Clarendon Laboratory Helium Liquefier

A. J. Croft and B. R. Bligh *Clarendon Laboratory, Oxford*

Received 1 March 1961

ALTHOUGH several small liquefier–cryostats are still in use at the Clarendon Laboratory, most cryostats are now supplied with liquid helium from an external source. In 1950 a Simon helium liquefier was built which produced 1 l. per hour of 'free' liquid helium[1] but it had become clear by 1955 that a liquefier of much greater output was needed. We decided to plan for an output of 50 l. per week made in one run by a liquefier of about 10 l. per hour output feeding a storage vessel of 100 l. capacity.

Choice of type

We considered the following courses:

(1) To buy a Collins expansion engine liquefier;
(2) To build a larger Simon liquefier;
(3) To build a Linde liquefier.

The latter two possibilities were open to us because of our possession of a hydrogen liquefier producing 18 l./hr.[2,3] We did not feel able to undertake the design and building of an expansion engine.

Although our experience of the Simon liquefier had been good, it would not have been practicable to build one on a ten times larger scale. Moreover, even with the improvement suggested by Simon and Ahlberg,[4] the liquid hydrogen consumption would have been excessive.

After consultation with colleagues in other laboratories, we decided to build a Linde liquefier. This proceeded less from financial considerations than from a conviction that reliability and light demands on skilled maintenance should be put first. The machinery associated with a Linde liquefier is of conventional design and works at room temperature: a thorough annual overhaul is generally enough to give reliable service with negligible attention at other times. An expansion engine on the other hand needs more frequent, more lengthy, and more skilled maintenance. Our experience in the four years during which this liquefier has been operating regularly has confirmed this view.

Design

The basis of our design was as follows: output—about 10 l./hr; output in one run—not less than 50 l. (this determines the gas-storage facilities and the capacity of the cleaning stages); liquid hydrogen consumption not above 18 l./hr (so that our hydrogen liquefier could keep pace). We decided to use a two-stage Reavell CSA 6 compressor which delivers 30 ft^3/min at 400 lb/in^2 running at 450 rev/min—this is in fact an air-compressor about 50 per cent under-run to allow for the higher γ of helium. It is driven by a 15 h.p. slip-ring motor. The liquid hydrogen pump is the Pulsometer Type 12: swept volume 3,480 l./min taking 6 h.p. (The 1955 costs of these machines with motors were £500 and £420, respectively.)

We followed these principles in settling the remaining features: the liquid hydrogen bath to work as near to the triple point as possible; the pressure over the liquid helium bath to be less than 0·2 atm; the liquid hydrogen bath not to need refilling more frequently than twice per hour; liquid helium not to need drawing off more frequently than three times per hour.

The circuit decided on is shown in Figure 1. The enthalpy of the major fraction of the incoming helium gas is absorbed by the returning unliquefied fraction in one exchanger working between 14° K and room temperature (this is the YZ exchanger in the Figure). The minor fraction is cooled partly by the liquid hydrogen in the bath at 14° K and also in a heat exchanger carrying the hydrogen vapour (YH in the Figure). Some additional preliminary cooling is needed and this is provided by a liquid air bath which can be by-passed by a valve—no attempt is made to make use of the 'cold' of the small amount of evaporated air. This bath is also used to cool the entire liquefier to liquid air temperature.

Efficient purification of the gas is essential if the liquefier is to be capable of long runs. Before being stored under pressure, the helium gas is cleaned with charcoal at liquid air temperature. After the compressor there is an oil and water droplet separator (a column packed with granite chips obtained from an undertaker), a column of activated alumina to remove residual water and oil vapour, a 2 l. charcoal vessel incorporated in the X-stage, and a 200 cm^3 charcoal vessel in the liquid hydrogen bath to deal with small traces of hydrogen and neon. (The heat exchanger in the X-stage is to restore the gas stream leaving the cleaner to room temperature.)

Heat insulation is achieved mainly by the use of large glass Dewar vessels in metal cases and partly by the use of high vacuum. (Since 1955, heat insulation techniques have improved and one would probably now design differently.) The glass Dewar vessels are similar to those used with success in the hydrogen liquefier and elsewhere. They are made by J. Jobling Limited and are 8 in.

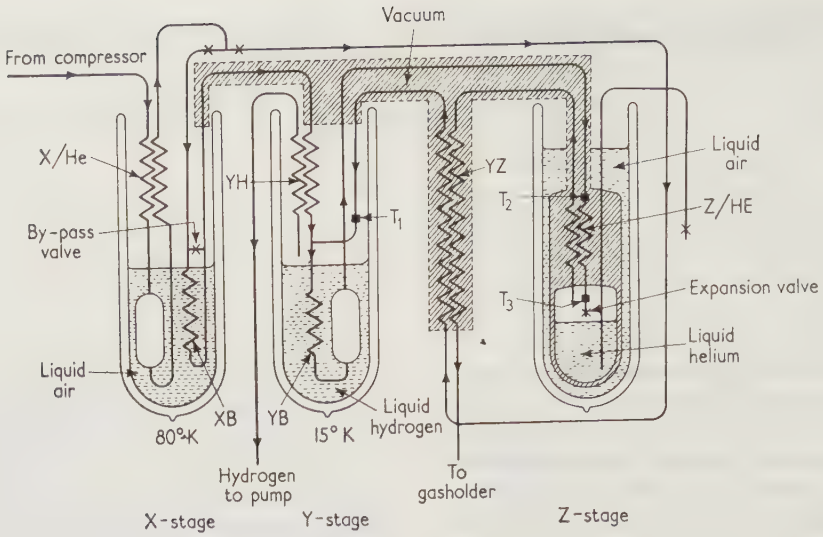

Figure 1. Flow diagram

internal diameter by 36 in. deep. Three are used: for the pre-cooling liquid air in the X-stage, for the liquid hydrogen bath in the Y-stage, and for the liquid air Dewar which surrounds the liquefaction stage. An unsilvered strip and portholes in the surrounding case enable the level of the liquid hydrogen to be seen. The final heat exchanger, the liquid helium vessel, the YZ heat exchanger, and the transfer tubes between the four sections are in a common high vacuum. The liquid air, hydrogen, and helium transfer tubes are permanently evacuated and sealed off.

The heat exchangers are of the type first used in the rebuilt hydrogen liquefier.[3] In this type, the high pressure gas flows in about eight copper tubes which are built up into a mass of alternately right- and left-handed multi-start coaxial helices which fits tightly into a cupronickel tube, itself wound into a helix. This construction has been found to give a relatively high efficiency due partly to the increased surface area and also to the fact that the surfaces present an angle of about 30–45 degrees to the direction of low pressure flow—a rather distant approximation to the cross-flow type of exchanger. These exchangers are easy to make from readily available materials. They were designed so far as pressure drop was concerned by extrapolating from measurements on test lengths at room temperature. We have found that the usual methods of calculating heat transfer coefficients can be applied satisfactorily. Figure 2 shows a sample of the type used in exchangers YH and YZ. Details of the heat exchangers are available from the Clarendon Laboratory.

The general arrangement is shown in Figure 3. There is a diagram showing the circuit of the liquefier facing the operator on which all the valves and gauges appear in their correct positions—this greatly simplifies operation. Below the liquefier is a pit 4 ft deep to allow the Dewar cases to be lowered.

The instruments provided are as follows: Three helium gas thermometers in the positions marked T in Figure 1, a Rotameter flowmeter in the low pressure return line, a liquid helium level indicator which uses a chain of carbon resistors, and a Philips vacuum gauge.

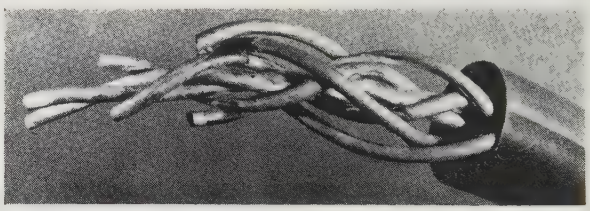

Figure 2. Sample of heat exchanger. The outer tube is 1 in. outside diameter

The 'make-up' helium gas is stored in a high pressure cylinder which at 120 atm holds 43 m^3 of gas at n.t.p. For as long as the pressure in this bottle is above 27 atm, the make-up gas passes through a reducing valve into the high pressure stream from the compressor, adding about 20 per cent to its output.† At lower pressures, the make-up gas goes straight to the gasholder. The valves controlling both these flows of make-up gas are controlled by gasholder height through an arrangement of cords, pulleys, and weights. An automatic high pressure by-pass is operated by an air-operated servomechanism.

It may be of interest to note that the liquefier itself was built in our workshops at the expense of 1·5 skilled man-years. The work of installation took about 0·5 man-years.

† We are grateful to Professor C. A. Swenson of Iowa State University for this suggestion.

Safety

The principal source of danger in this plant lies in the use of hydrogen. A leakage of air into the hydrogen system can be guarded against by careful design and is tested for regularly. However, there remains the possibility of breakage of the Y-stage Dewar while it contains liquid hydrogen. (We have never in fact had a case of a Dewar's breaking while cold, although there have been cases of spontaneous breakage when a badly made Dewar was warming up.) Against this possibility we have provided a 2 in. diameter by 12 ft long pipe to the open air with a disk blow-off on the end, and we have estimated that with this the release of 10 l. of liquid hydrogen into the case containing the Dewar would not give rise to a pressure greater than a few atmospheres. Since the case was hydraulically pressure-tested to 10 atm, we feel that we have adequately provided against this contingency. As a further precaution, the top, front, and side panels of the liquefier are solidly made and the back is left open. The electricity supply to the whole system can be cut off at several places and any consequent dangers are provided against. The operators wear safety spectacles. Pressure relief valves—mostly the spring-loaded disk type—are provided wherever excessive pressures might build up.

Very little hydrogen escapes into the atmosphere during liquid hydrogen transfers and a normal exhaust fan is adequate to deal with it. When built, the liquefier was installed in a research room for lack of other accommodation but Figure 3 shows it in the new quarters, near the hydrogen liquefier, into which it was moved in 1960. A large blow-out hatch is provided in the roof and flame-proof heating and lighting are installed.

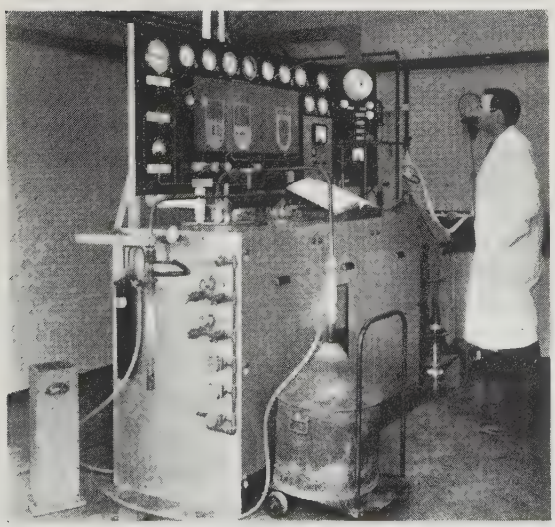

Figure 3. The Clarendon Laboratory helium liquefier in operation

Operation

The liquefier is run by one man (not including the staff belonging to the hydrogen liquefier) with help during starting up and in fetching liquid air and liquid hydrogen. Before a run, the charcoal cleaner in the X-stage is reactivated at 200° C under vacuum; the Y-stage cleaner is not heated above room temperature but is also pumped out.

We now give the timetable for a typical run—the unusually rapid starting up time should be noted.

9.30 a.m. High vacuum system, helium compressor, and hydrogen pump started: tests made for leaks from the high pressure helium system and for leaks into the hydrogen system. Transfer tube from liquefier to 100 l. vessel inserted.

10.00 a.m. X-stage and Z-stage Dewars filled with liquid air. Helium gas flow started—at this stage the whole flow passes through the X-stage and the low pressure return path is partly by-passed so as to avoid an excessive pressure in the liquid helium space.

10.30 a.m. The thermometers will by now show that all relevant parts of the liquefier are at about 80° K. One 12 l. metal Dewar of liquid hydrogen is then brought in and transferred into the Y-stage. The return path is now almost completely by-passed.

10.35 a.m. The thermometer at the expansion valve will by now be reading 30° K or less. The low pressure by-pass is then shut off and the high pressure valve leading to the YZ heat exchanger is opened and adjusted so that the helium gas leaving this exchanger is at about 20° K. The high vacuum system can now be shut off. (Unless the low pressure by-pass is kept open until the expansion valve is below the inversion point, the liquefier will not cool down. This is indicative of high efficiency of the final exchanger.)

10.40 a.m. Liquefaction will by now have started. A second 12 l. Dewar is transferred and this leaves the Y-stage Dewar full. (From this point, the assistant operator is needed only intermittently.)

10.50 a.m. The liquid helium container in the liquefier is now full and the first 3 l. are transferred. (The evaporating helium gas is returned to the low pressure gasholder belonging to the liquefier.) From now on, liquid helium transfers are made about every 15 min and liquid hydrogen transfers about every 40 min.

Performance

Liquefaction rate—maximum internal: 14·6 l./hr from 14·4° K and 24 atm.

Liquefaction efficiency: 0·20 taking the measured value of 54 m^3/hr for the compressor output. *Allowing for the displacement of vapour*, Keesom's data gives a figure of 0·22. (Note: since the ratio of the densities of liquid and gaseous helium at 4° K is only 8, it is important not to ignore the vapour displaced by the liquid.)

Liquefaction rate—long-term external: 10·5 l./hr. The reduction is accounted for by transfer losses, including the 'flash' loss (6 per cent) and reduction of output during liquid hydrogen replenishment.

Total pressure drop on low pressure side: 0·24 atm.

Consumption of liquid refrigerants

Liquid air—initial: 15 l.
—when in equilibrium:
3·2 l./hr or 0·30 l. per litre of liquid helium

Liquid hydrogen—initial: 10 l.
—when in equilibrium:
internally 17·5 l./hr (1·20 l./l.)
externally 18·5 l./hr (1·27 l./l.)

The calculated figure for internal consumption is 0·9 l./l.

Heat leaks—in Y-stage: 0·76 l. of liquid hydrogen per hour
—in Z-stage: 0·26 l. of liquid helium per hour

It will be seen that the performance is satisfactory except as regards the consumption of liquid hydrogen. Experiment has shown that this is due to the inadequacy of the YZ heat exchanger. It was known that this was under-dimensioned when the liquefier was designed, but we were unable to do any better at the time. Now that suitable finned tubing is available, we hope to remake this exchanger in the Collins form. This would also reduce the pressure drop on the low pressure side.

The liquefier has been in regular weekly use since early in 1957 and has proved stable and easy to operate. It has produced up to 85 l. in one run with no trace of blocking. (In most of the weekly runs we produce about 50 l.) Blocking has occurred on a few occasions when an excessive quantity of hydrogen was accidentally let into the general laboratory helium system, and also once when the cleaners became contaminated and neon built up in the system. A leak into the high vacuum system gradually developed during the first few months of use. It was eliminated by a partial reconstruction, being of the sort that is impossible to find at room temperature even with a mass-spectrometer leak detector. The system now remains at less than 10^{-5} mm Hg when cold, without the aid of the pumps.

This work was undertaken at the request of the late Professor Sir Francis Simon and the writers were very grateful for his interest and encouragement. A few days before his untimely death, they had the satisfaction of being able to report to him that the liquefier was functioning. We thank many of our colleagues in Oxford and elsewhere for their help. In particular we thank Mr. E. R. Tilbury and others of our technical staff without whose skill and enterprise the liquefier could never have been built.

REFERENCES

1. Croft, A. J. *J. sci. Instrum.* **29**, 388 (1952)
2. Jones, G. O., Larsen, A. H., and Simon, F. E. *Research, Lond.* **1**, 420 (1948)
3. Croft, A. J., and Simon, F. E. *Bull. Inst. int. du Froid* p. 81, Annexe 1955–2
4. Simon, F. E., and Ahlberg, J. E. *Z. Phys.* **81**, 817 (1933)

White, G. K. *Experimental Techniques in Low Temperature Physics* (Clarendon, Oxford, 1959)
Scott, R. B. *Cryogenic Engineering* (Van Nostrand, Princeton, 1959)
Croft, A. J. 'Helium liquefiers.' *Progress in Cryogenics 3* (Heywood, London; Academic, New York, 1961)

B. R. Bligh is now with Imperial Chemical Industries Ltd.

Research and Technical Notes

THE PREPARATION OF MINIATURE CARBON RESISTANCE THERMOMETERS FOR LOW TEMPERATURES

N. V. Zavaritskii and A. I. Shal'nikov

Institute for Physics Problems, Academy of Sciences, U.S.S.R.

Received 8 March 1961†

For measurements at low temperatures it is often essential to have miniature thermometers with small inertia. Although thermocouples can be applied above 10° K, they are insufficiently sensitive at lower temperatures. Carbon film thermometers, which are suitable in this temperature region, have been known for 20 years,[1] but the established methods of making them have not been described until now. Here we describe a means of preparing resistance thermometers of very small dimensions, suitable for measurements from 0·1 to 10° K.

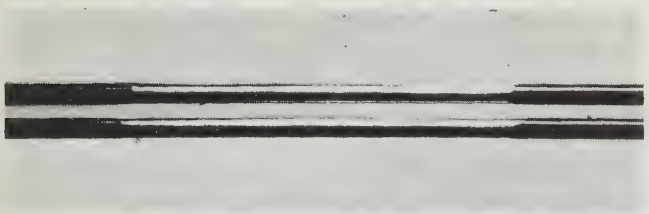

Figure 1. 110 microns diameter wire with enamel removed

Two varnished copper wires of diameter 0·03–0·2 mm and length about 100 mm are stretched between fixed pins parallel to one another, about 0·5 mm apart, by a weak spring. The insulating layer is removed from both wires over a length of about 1 mm. For this purpose, the wires are dipped into a drop of fused alkali, potassium hydroxide, in which the varnish completely dissolves within 2–3 sec. There is then a sharp boundary between the cleaned and uncleaned part of the wire (Figure 1).‡ A special tool (Figure 2) is used for this operation consisting of a nickel or stainless steel wire of diameter 0·3–0·4 mm,

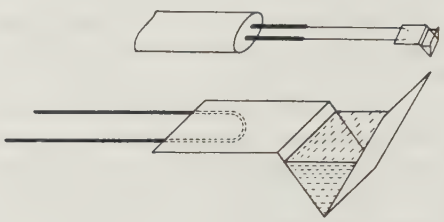

Figure 2. Instrument for removing enamel

bent into a loop.§ The loop is fixed to the current leads in a light handle and is heated by current from a variable step-down transformer. A piece of caustic potash (about 1 mm^3) is placed on the loop and this first boils on heating and then, on losing its water of crystallization, melts and remains liquid at temperatures above 360° C. The part of the varnished wire from which the insulating layer is to be removed is placed in this molten drop (the drop must remain liquid on the wire!). The alkali remaining on the wire is removed by wet cotton wool. The bare copper core is quite clean and unannealed.

The two wires are brought together so that their insulation layers are in contact by means of two threads of wire. A drop of adhesive BF-6 is placed on either side of the bared parts of the wires and the part of the wire covered with adhesive is heated with the instrument described until the adhesive polymerizes, after which a paste of colloidal graphite mixed with glycerine is applied to the bare part. After the glycerine has been removed by heating, the graphite layer is covered with a cellulose varnish, dissolved in amyl acetate. When the varnish has dried, the thermometer is ready for use (Figure 3) and can be fixed to the surface of the specimen.

† Received by PTÉ Editor 3 December 1959: *Pribory i Tekhnika Éksperimenta* No. 1, p. 189 (1961).

‡ The removal of the insulation from varnished wires is known to be a very difficult operation. The method suggested for removing any insulation by caustic potash completely solves this problem. The insulation from wires of diameter up to 0·2 mm can be removed easily by the instrument described here; larger wires are dipped into a nickel crucible containing molten alkali.

§ If it is essential to remove the insulation from an exactly defined portion, a strip of nickel foil is welded to the loop, bent as shown in Figure 2.

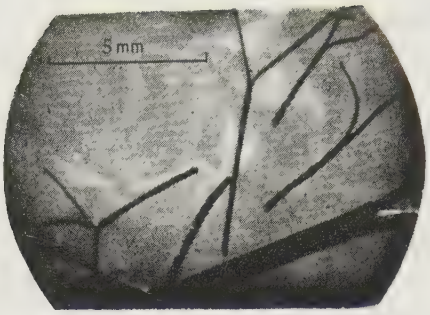

Figure 3. Carbon thermometers prepared from wires of 200 microns, 60 microns, and 45 microns diameter

In the case of a cylindrical specimen the thermometer can be prepared directly on its surface. A spiral of two 30 microns uninsulated copper wires is wound on to the surface of the specimen which has been covered with polymerized adhesive BF. The ends of the spiral are fixed with a thick cellulose lacquer. After checking for the absence of contact between the wires, the spiral is covered with an aqueous mixture of graphite or with a liquid paste of graphite mixed with glycerine. The graphite covering is dried. In the case of a glycerine paste, the specimen must be heated at about 50°C for about 20 min in a vacuum of the order of 10^{-4} mm Hg. The thermometer is covered with cellulose varnish. By this method thermometers of width down to even 0·1 mm can be prepared (Figure 4).

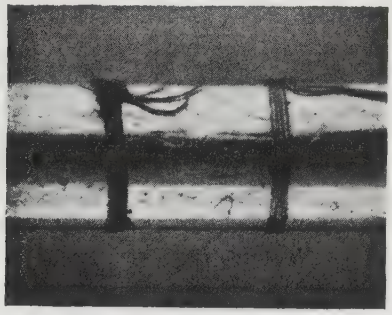

Figure 4. Thermometers on a 2 mm diameter specimen. Right: spiral before filling with carbon; Left: finished thermometer

The characteristics of the thermometers are determined by the graphite particle size.[2] Graphite prepared in a ball mill, and reduced to $(2–5) \times 10^{-6}$ cm is suitable. The paste for the thermometers is made up of one part dry graphite to two parts glycerine.

An example of the temperature dependence of the resistance of the finished thermometers is shown in Figure 5. A 1 mm long wire thermometer has an absolute resistance of 5–15 Ω at 20°C. The value of $d(\log R)/d\log T$ can vary by about 30 per cent for different specimens of thermometer. The resistance decreases for an appreciable

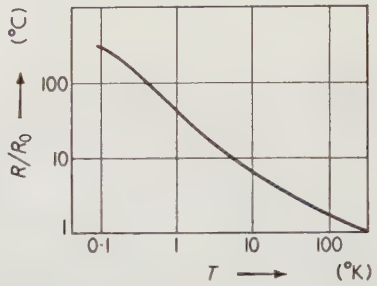

Figure 5. A typical temperature–resistance curve of the thermometers

increase in measuring current in the helium region and at lower temperatures (this effect is not produced by overheating of the thermometer). There is only an insignificant reduction of resistance in a magnetic field, e.g. about 0·4 per cent at 4·2°K in a field of 15 koersteds.

The non-reproducible resistance change when a thermometer is cooled to 4·2°K and heated to a little below 0°C many times is less than 1 per cent. Even a single warming above 0°C can produce a considerable change in resistance. The cellulose covering easily swells in a damp atmosphere, producing mechanical strains in the graphite layer and changes in resistance. The resistance is restored on drying. The thermometer calibration must therefore be checked after warming up.

REFERENCES

1. Giauque, W. F., Stout, J. W., and Clark, C. W. *J. Amer. chem. Soc.* **60**, 1053 (1938)
2. Geballe, T. H., Lyon, D. N., Whelan, J. M., and Giauque, W. F. *Rev. sci. Instrum.* **23**, 489 (1952)

THE SEALING OF GLASS VIEWING PORTS IN LIQUID HYDROGEN BUBBLE CHAMBERS

V. A. Beketov, Ya. M. Selektor, S. M. Zombkovskii, and M. S. Ainutdinov

Received 8 March 1961†

ONE of the greatest difficulties met in the construction of liquid hydrogen bubble chambers is the achievement of a reliable vacuum seal at low temperatures between the body of the camera and the glass viewing ports, through which the illumination and photography take place. The methods of sealing described in the literature[1,2] are either insufficiently reliable, even for a camera diameter of 25 cm, or require replacement of the washer after one or two successive coolings of the camera.

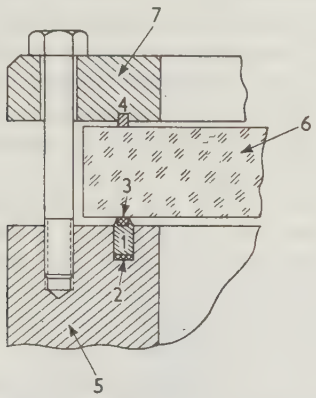

1: Copper washer
2, 3: PTFE washers
4: Copper ring
5: Camera casing
6: Glass
7: Pressure flange

Figure 1

We have carried out a number of experiments using PTFE, squeezed in an enclosed space, in order to produce a reliable seal which could be used many times. The best results were obtained with the seal shown in Figure 1.

The copper washer 1 is sealed into a groove in the camera by means of the PTFE ring 2. There is a rectangular channel in the upper part of the copper washer, into which the PTFE ring 3 is pressed. On tightening the seal the copper is compressed, squeezing out the PTFE which in turn produces a reliable vacuum seal with the glass. Brass bolts are used to tighten up the seal; because of the difference between the coefficients of expansion of the glass and brass, there is a further tightening on cooling the camera. There is a washer 4 of annealed copper between the glass and the compression flange in order to transmit the pressure evenly over the glass. This kind of seal has been used for a long period in a 25 cm diameter liquid hydrogen bubble chamber in action. The body of the camera was made of brass. The copper washer used was 3·1 mm wide and 7·5 mm high and the corresponding dimensions of the PTFE ring 3 were 1 and 1·8 mm. The seal was tightened by 22 brass M12 bolts tightened to a tension of 1·5 kg. Under these conditions an absolutely reliable seal for the front glass of the camera was obtained which allowed a number of consecutive coolings of the camera. The reliability of the seal is comparable with that of the usual vacuum rubber seal at room temperature. Another advantage of the seal described is the possibility of repeated use in re-sealing the chamber. The limiting diameter of glass ports which can be sealed by such a washer is determined by the allowable relative movement of the glass and washer when deformed thermally. From these considerations it seems possible to use the washers in stainless steel chambers with glass diameters of up to 40–50 cm.

† Received by PTÉ Editor 10 December 1959: *Pribory i Tekhnika Éksperimenta* No. 1, p. 182 (1961).

REFERENCES

1. PARMENTIER, D., Jr., and SCHWEMIN, A. J. *Rev. sci. Instrum.* **26**, 954 (1955)
2. KOLGANOV, V. Z., LEBEDEV, A. V., NIKITIN, S. YA., and SMOLYANKIN, V. T. *Prib. i Tekh. Éksper.* No. 1, p. 31 (1958)

A METAL CRYOSTAT FOR OPTICAL INVESTIGATIONS ON SOLIDS AT LOW TEMPERATURES

E. N. Lotkova and A. B. Fradkov
Physical Institute, Academy of Sciences, U.S.S.R.

Received 8 March 1961†

A METAL cryostat with plane parallel windows has been designed for carrying out optical investigations at low temperatures. The plan of construction is shown in Figure 1. The vessel 4 for the liquid coolant (helium or hydrogen) is suspended inside the cylindrical case 1 by a stainless steel tube and to it is attached the conductor of cold. Two windows of diameter 30 mm are mounted on the lower part of the casing. The glass of the windows, made of potassium bromide or sodium chloride, is sealed to the case by steel flanges with rubber washers. The thermal insulation for the cryostat—a high vacuum—is produced by pumping through the vacuum valve 7 before the cooling liquid is poured in, and is maintained by adsorption on activated charcoal which is in contact with the inner vessel. There is a nitrogen bath 2 in the upper part of the cryostat, and the shield 3 surrounding the inner vessel and the conductor to reduce the radiation heat influx. The nitrogen bath is suspended from the lid of the case by two thin-walled stainless steel tubes, through which the liquid nitrogen is fed in and the evaporating gas escapes. The case, nitrogen bath, shield, and inner vessel are of copper, and their surfaces in contact with the vacuum space are carefully polished. The case, inner vessel, and nitrogen bath must have joins of good quality. These were tested by a leak detector PTI-4.

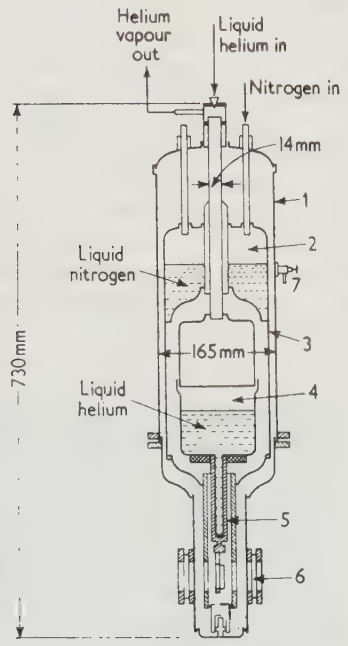

1: Case
2: Nitrogen bath
3: Shield
4: Helium bath
5: Conductor of cold
6: Window for illuminating the specimen
7: Tap for evacuation

Figure 1. Cryostat for optical investigations

The lower part of the case and the shield are made detachable so that specimens can be changed. The solid specimen with dimensions 25 mm × 10 mm × 2 mm is fixed by adhesive BF-2 to the plane end of the conductor 5 with an opening 20 mm × 5 mm for transparency. Using this method of attachment, the temperature of the specimen is 14° K without illumination and 18° K with illumination of the specimen by the focused light from a Globar. With liquid nitrogen in the inner vessel, the temperature of the specimen is the same with and without illumination. The temperature is measured with a carbon resistance thermometer. The attainment of a good contact between the specimen and the conductor is extremely important, since the temperature difference between specimen and liquid coolant depends on it.

The cryostat is pumped to 10^{-4} mm Hg before liquid helium is introduced and is then disconnected from the vacuum system. The nitrogen bath is filled with liquid nitrogen and the inner vessel with gaseous helium. The cryostat is kept in this state for 2–3 hr.

The inner vessel holds 1·3 l. of liquid and requires about 1 l. for cooling. The cryostat is as useful for working with liquid helium as with liquid hydrogen and liquid nitrogen. Liquid helium lasts for 8 hr with a mean evaporation rate of 2 l./min of gas. Liquid hydrogen lasts for 72 hr with an evaporation rate of 0·2 l./min of gas. This period is halved if the cryostat is placed in front of the entrance slit of a two beam infra-red spectrometer IKS-14 and its window illuminated with light from a Globar. The cryostat is very convenient and safe as it is constructed of metal and does not require continuous pumping.

† Received by PTÉ Editor 21 January 1960: *Pribory i Tekhnika Éksperimenta* No. 1, p. 188 (1961).

A HIGH PRESSURE BOMB FOR OPTICAL STUDIES AT LOW TEMPERATURES

A. K. Tomashchik

Institute of Physics, Academy of Sciences, Moscow

Received 8 March 1961†

A STUDY of the effect of hydrostatic compression on the optical and photoelectric properties of crystals at low temperatures is of scientific and, sometimes, practical interest. Such investigations have been hampered by the lack of substances which are transparent and can transmit pressure at low temperatures. In this work we describe the construction of a high pressure vessel for optical and photoelectric studies at low temperatures.

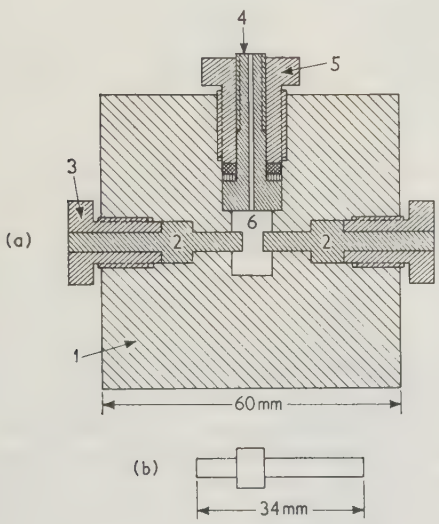

1: Body
2: Windows
3: Sealing screw
4: Mushroom
5: Nut
6: Working space

Figure 1. (a) High pressure bomb; (b) Methyl methacrylate windows

The method of freezing water in a constant volume bomb[1] is used for obtaining the pressures. The bomb is made of beryllium bronze and has methyl methacrylate windows (an organic glass). The bomb and windows are shown in Figure 1. The windows are 8 mm in diameter, 6 mm thick, and have two 4 mm diameter projections. One of these goes into the working space 6 and reduces the scattering path of the light in ice. The other fills the closing screw, allowing working directly in the coolant liquid. In unfortunate cases the hydrogen or helium boiling off collects in the screw and it becomes impossible to make observations. All packings are made on the unsupported area principle.[2] The specimen is fastened to the mushroom 4 which has a metal diaphragm and a hole for electrical leads.

To improve the filling of the bomb it is put in boiling distilled water with the specimen before being put together. It is assembled in the water after cooling, tightened up, and hung on a special rod in the cryostat,[3] after which the cryostat is cooled. The water, freezing first in the hole of the mushroom seals off the working space in a reliable way. According to Lazarev and Kan[1] the pressure in a constant volume bomb at 20° K is 1,750 atm.

As an example the absorption spectra of a single crystal of cadmium sulphide are shown in Figure 2 under pressure and without pressure at 20° K, obtained with a KS-55 spectrograph with a GSVD-120 lamp, spectral slit width approximately 0·4 Å, and exposure 20 min. It can be seen that the absorption band edge moves 170 cm^{-1} towards the short wave end, or $\sim 0{\cdot}1$ cm^{-1}/atm (0·022 Å/atm). A similar shift (0·02 Å/atm) was found in cadmium sulphide for a pressure of 500 atm.[4] This shows agreement between the pressure in the bomb and Lazarev's measurements.[1] The largest absorption edge shift found by Broude et al.[5] under a non-uniform deformation of a cadmium sulphide crystal in a mechanical press is 250 cm^{-1}. A linear extrapolation gives the maximum pressure in the press as about 2,500 atm.

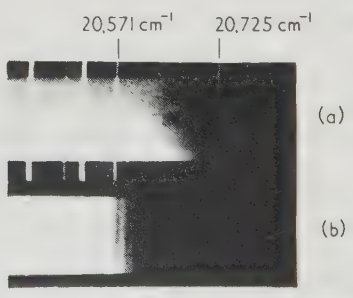

Figure 2. (a) Spectrum of cadmium sulphide single crystal under pressure at 21° K; (b) The same spectrum without pressure

† Received by PTÉ Editor 8 January 1960: *Pribory i Tekhnika Éksperimenta* No. 1, p. 193 (1961).

The bomb works very reliably and, ignoring a certain residual deformation of the windows, none of its components, including the windows, has ever failed. A simple method has thus been developed for studying optical and photoelectric properties at high pressures at temperatures of 220–230°K (the phase transition point of ice) down to helium temperatures.

The author expresses his thanks to A. F. Prikhot'ko and V. L. Broude for their interest in the work and valuable advice.

REFERENCES

1. Lazarev, B. G., and Kan, L. S. *J. exp. theor. Phys.* **14**, 439 (1944)
2. Bridgman, P. W. *The Physics of High Pressures* (1935)
3. Babenko, V. P., Broude, V. L., Medvedev, V. S., and Prikhot'ko, A. F. *Prib. i Tekh. Éksper.* No. 1, p. 115 (1959)
4. Höhler, G. *Ann. Phys.* **4**, 371 (1949)
5. Broude, V. L., Eremenko, V. V., Medvedev, V. S., Pakhomova, O. S., and Prikhot'ko, A. F. *J. phys. Ukr.* No. 2, p. 232 (1958)

A STABILIZER FOR LOW TEMPERATURES IN HELIUM CRYOSTATS

A. N. Vetchinkin

Institute for Physics Problems, Academy of Sciences, U.S.S.R.

Received 8 March 1961†

It is not possible, by regulating the pumping speed, to achieve the necessary accuracy in maintaining the temperature for a number of experiments at temperatures obtained by pumping off helium. Regulators with carbon monitors and wire heaters are used for temperature stabilizing.[1,2]

The method described stabilized the temperature of a helium bath to an accuracy of 10^{-5}°K below 2·18°K. It consists of a monitor—a bronze thermometer, an amplifier, and a heater (Figure 1). The bronze thermometer R_2 is in one arm of a bridge supplied from an accumulator. The other arm R_3 is a variable resistance which balances the bridge at a given temperature. By using a phosphor-bronze monitor, the temperature can be fixed beforehand by the magnitude of R_3 since the characteristics of the monitor do not change from experiment to experiment. In the construction of the bridge one must prevent any instability in the current through the monitor in order to achieve high temperature stability.

The amplifier consists of a photocell amplifier F-17/1,[3] made by the 'Vibrator' factory (in Leningrad), a valve amplifier, and a d.c./a.c. converter. The converter supplies the heater which is in the helium bath with the bronze monitor. The heater is supplied with alternating current to prevent the effect of leakage currents between the monitor and the heater. This is essential as the amplifier is sensitive to voltages of several millimicrovolts.

The amplifier circuit is shown in Figure 2. The photocell amplifier F-17/1 is connected to a two-stage constant current amplifier using 6N2P. F-17/1 and the first stage

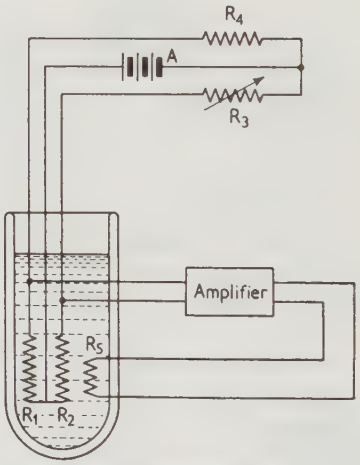

R_1: 100 Ω, constantan
R_2: 35 Ω, phosphor-bronze
R_3: Resistance box, 0–3,000 Ω
R_5: 200 Ω, constantan
A: 6 V accumulator

Figure 1. Arrangement for helium bath temperature control

of the amplifier are connected in frequency-dependent internal feedback to obtain a frequency response of the circuit providing steady operating conditions for the stabilizer even for a very large regulation factor. The valve V_3 which supplies the heater through the output transformer is the current converter. The anode circuits of the triodes are supplied with alternating current from the secondary windings of the power transformer. The

† Received by PTÉ Editor 3 December 1959: *Pribory i Tekhnika Éksperimenta* No. 1, p. 192 (1961).

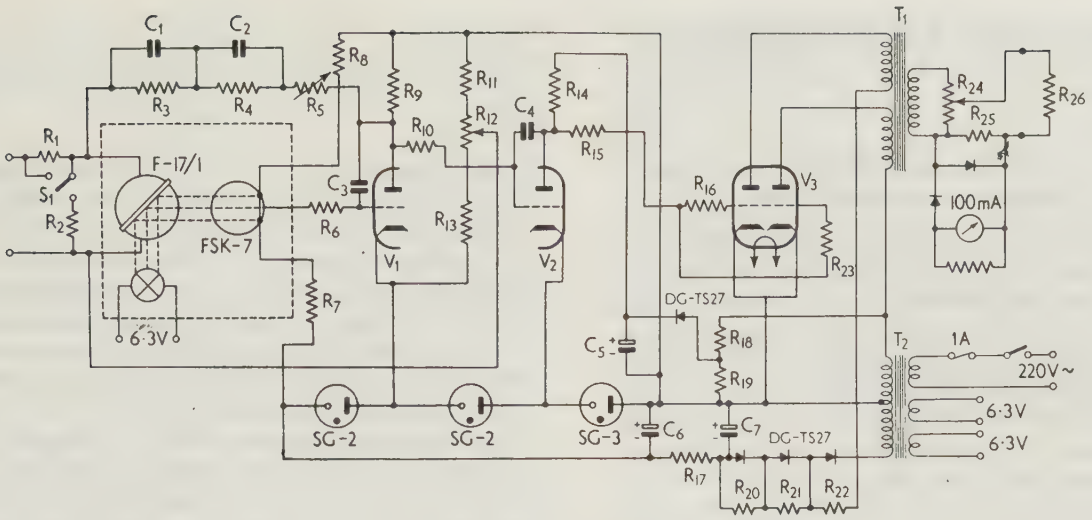

V_1: 6N2P V_2: 6N2P V_3: 6N3P

R_1: 10 kΩ	R_7: 20 kΩ	R_{13}: 62 kΩ	R_{19}: 27 kΩ
R_2: 51 Ω	R_8: 20 kΩ	R_{14}: 430 kΩ	R_{20}: 91 kΩ
R_3: 33 MΩ	R_9: 100 kΩ	R_{15}: 2·4 kΩ	R_{21}: 91 kΩ
R_4: 10 MΩ	R_{10}: 120 kΩ	R_{16}: 430 Ω	R_{22}: 91 kΩ
R_5: 2·7 MΩ	R_{11}: 150 kΩ	R_{17}: 5 kΩ	R_{23}: 430 Ω
R_6: 36 kΩ	R_{12}: 150 kΩ	R_{18}: 87 kΩ	R_{24}: 1 kΩ
	R_{25}: 50 Ω	R_{26}: 200 Ω	

C_1: 100 mμF C_3: 150 pF C_5: 30 μF
C_2: 1 μF C_4: 300 pF C_6: 30 μF
C_7: 30 μF

Transformer details: T_1: 2 × 6,000 : 600
T_2: 3LS–2

Figure 2. Amplifier circuit

two sections of the primary winding of the output transformer are connected so that its core is not magnetized by the d.c. component of the anode current, considerably increasing the conversion factor. The outpuf transformer is designed for a heater resistance of 200 Ω. The maximum current through the heater of 100 mA can be reduced by a variable 1 kΩ resistance. The current is measured by a milliammeter.

The establishment of the operating conditions of the stabilizer on switching on the system is considerably eased if the regulation factor is reduced before balancing the input bridge. The switch S_1 is provided for this purpose.

The author thanks V. P. Peshkov for his help with the work and K. A. Zhdanov who took an active part in developing the apparatus.

REFERENCES

1. Boyle, W. S., and Brown, J. B. *Rev. sci. Instrum.* **25,** 359 (1954)
2. Forstat, H., and Novak, J. R. *Rev. sci. Instrum.* **29,** 733 (1958)
3. Seliber, B. A., and Rabinovich, S. S. *Automat. i Telemekh.* No. 8 (1956)

Letters to the Editors

Studies of the Electrocaloric Effect of Ferroelectric Ceramics at Low Temperatures

It can be expected that, analogous to the magnetocaloric effect, the electrocaloric effect can also be utilized for obtaining low temperatures. Ferroelectric ceramics, having a high dielectric constant at low temperatures, as has been previously reported by the author,[1] seem to be particularly suitable for this purpose. In this connection, special attention should be given to pure strontium titanate because of its abnormal dielectric behaviour.

Measurements by Gränicher[2] and Weaver[3] on strontium titanate monocrystals indicated that this material does not yet become ferroelectric at 2° K. Their dielectric constant, however, has a high field dependence. We have also found such a dependence in the region from 14 to 20° K with a strontium titanate ceramic.[1]

Up to now, no papers concerning experimental research on the electrocaloric effect of ferroelectric ceramics at low temperatures have been published. Only some theoretical considerations by Gränicher[2] exist, based on his measurements.

We have now measured the electrocaloric effect of some ferroelectric ceramics at the temperatures obtainable with liquid nitrogen or liquid hydrogen. The measurements were made in an adiabatic vacuum calorimeter with a mechanical heat switch. The apparatus was designed in such a manner that it was possible to measure the dielectric constant and the loss angle ($\tan\delta$), as well as the dependence of these on a superimposed electric d.c. field, the hysteresis behaviour, the specific heat, and the electrocaloric effect on the same sample.[4]

The samples tested had a diameter of about 20 mm and a thickness of 3–5 mm, corresponding to about 0·02 mole. The sample was suspended in the calorimeter on thin Perlon threads, and the temperature was measured with the aid of platinum or lead resistance thermometers, directly attached to the sample.

For the study of the electrocaloric effect, the samples were placed in a d.c. field. When switching on the d.c. field, the heat switch was closed in order to carry away the heat of polarization, then the heat switch was opened, and the electric field switched off. The resulting changes in temperature could be observed by means of a sensitive galvanometer.

Figures 1 and 2 show the cooling effects occurring in strontium titanate and cadmium titanate ceramics, respectively, as a function of the field strength and the temperature.

According to our measurements of the specific heats (θ about 400°), it could be expected that cooling effects in this temperature region would not be large, because the lattice entropy is still high. However, Figure 1 shows clearly that in the case of strontium titanate the effect increases with decreasing temperature, and with a field strength of 8 kV/cm at a temperature of about 17·5° K we observed a cooling effect of about 0·06° K.

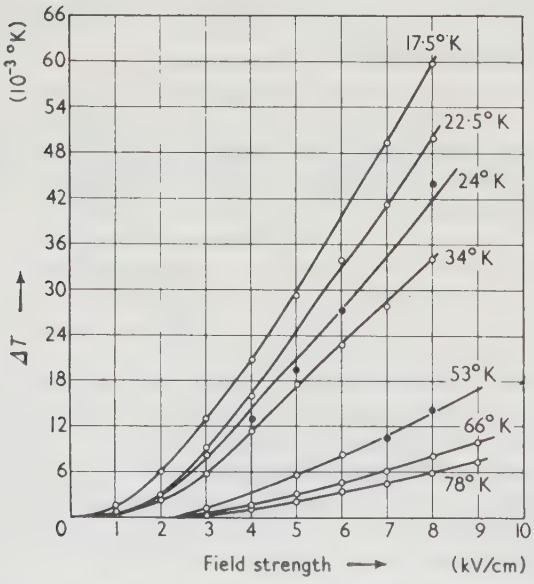

Figure 1. Cooling by the electrocaloric effect in strontium titanate ceramic as a function of temperature and field strength

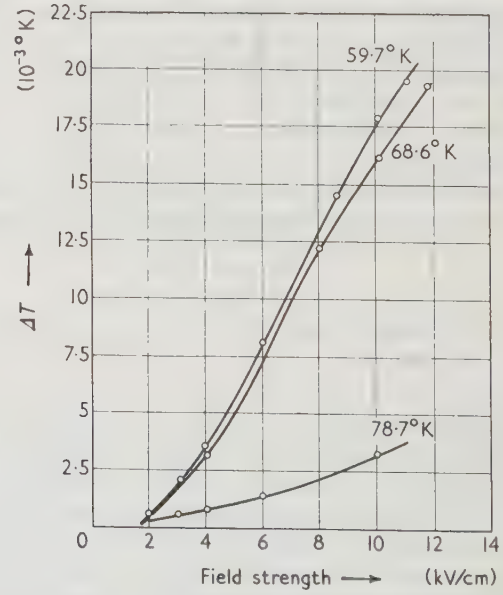

Figure 2. Cooling by the electrocaloric effect in cadmium titanate ceramic as a function of temperature and field strength

The increase of the electrocaloric effect with decreasing temperature can also be understood from the behaviour of the dielectric constant of strontium titanate in a superimposed d.c. field.[1] Whereas near 70° K the initial value of the dielectric constant of 1,750 at 0 kV/cm only decreases by about 220 in a field of 8 kV/cm, the dielectric constant decreases near 20° K from 5,000 at 0 kV/cm to 2,500, i.e. the change at 20° K is about ten times as large as at 70° K.

Above its Curie point at about 52° K, cadmium titanate also shows a similar behaviour of the dielectric constant in a superimposed d.c. field.[1] As can be clearly seen from Figure 2, with this material the electrocaloric effect increases as the Curie point is approached. Here, also, the absolute value of the effect is not very high, because in this case too the lattice entropy is still rather high, as is shown by the results of our measurements of the specific heat. Similar effects were further found in solid solutions of strontium titanate and barium titanate, the Curie points of which lie in the low temperature region.

A more detailed discussion is being deferred until measurements in the region of liquid helium become available.

The author wishes to thank Professor L. Bewilogua for his valuable advice and suggestions.

E. Hegenbarth

Deutsche Akademie der Wissenschaften zu Berlin,
Forschungsgemeinschaft,
Arbeitsstelle für Tieftemperaturphysik,
Dresden.

(6 March 1961)

REFERENCES

1. Hegenbarth, E. *Mber. Tdd. Dt. Akad. Wiss.* **1**, 411 (1959)
2. Gränicher, H. *Helv. phys. acta*, **29**, 211 (1956)
3. Weaver, H. E. *J. Phys. Chem. Solids* **11**, 274 (1959)
4. A detailed paper describing the apparatus is in preparation.

The Problem of the Superconducting Solenoid for the Production of Very High Magnetic Fields

The recent discovery[1] that suitably prepared specimens of the compound Nb_3Sn ($T_c = 18°$ K) remain superconducting in fields as high as 88 kG at temperatures below 4·2° K reopens the possibility of constructing solenoids for producing very high magnetic fields without any dissipation of power. It is the purpose of this note to analyse this possibility.

It is unlikely that pure strain-free Nb_3Sn has a critical field at 0° K greater than 10,000 gauss. The persistence of superconductivity at much larger fields is due to the existence of strain or inhomogeneity in the material leading to regions in which the normal–superconducting surface energy is negative.[2] This favours the breaking up of the specimen into numerous thin filaments of superconducting material imbedded in a normal matrix, and, provided the diameter of these filaments is small compared with the penetration depth, their critical field will be appreciably greater than the bulk value. The size of the filament is probably closely related to the normal state mean free path, or in other words to the density of 'impurities' (chemical or physical). For optimum performance, therefore, this density should be as high as possible.

Critical fields and critical currents

The critical field H_c' of a filament thin compared with the penetration depth is given by a relation of the form

$$\frac{H_c'}{H_c} = \frac{\beta\lambda}{d} \qquad \ldots(1)$$

where H_c is the bulk critical field, λ is the penetration depth, d the diameter of the filament, and β a dimensionless parameter of the order of unity. Since we want to make H_c'/H_c as large as possible (~ 10, say) we must have $d/\lambda \sim 0{\cdot}1$ or $d \sim 100$ Å.

The supercurrent-carrying capacity of the filament is also related to its diameter. There is no satisfactory theory of the destruction of superconductivity by a current in specimens small compared with the penetration depth, but it is known that in such specimens the current density is likely to be uniform and has a critical value less than that of the bulk superconductor. This bulk critical current density is given to a high degree of accuracy by the London equations, and has the value $j_s = H_c/4\pi\lambda$. We may therefore assume that the critical current i_c of the filament is given by a relation of the form

$$i_c = \gamma . \pi d^2 H_c/4\pi\lambda \qquad \ldots(2)$$

where γ is a dimensionless factor less than unity.

Theory of the solenoid

We are now in a position to discuss the operation of a superconducting solenoid. Since the field obtainable from such a solenoid will be limited either by i_c or by H_c' (whichever gives the lower field), and not by considerations of

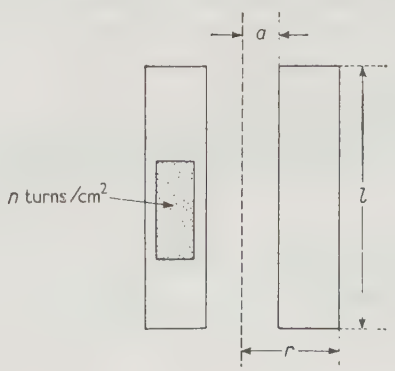

Figure 1

available power, there is no point in not making it a 'long' solenoid. In other words there is no optimum shape factor, as there is for high power water-cooled solenoids. Assume that the solenoid has the dimensions shown in Figure 1.

Suppose we have superconducting wire of cross-section A cm^2, through which run n' superconducting filaments per square centimetre, each of diameter d cm and critical current i_c. The total number of turns is thus $nl(r-a)$, and the turns per centimetre $n(r-a)$. The total supercurrent-carrying capacity of each wire is $n'Ai_c$, so the field inside the solenoid is given by

$$H = 4\pi nn'Ai_c(r-a) \qquad \ldots(3)$$

provided that $l \gg r$. Using equation (2) this becomes

$$H = \gamma . nA . n'A' . (r-a)\frac{H_c}{\lambda} \qquad \ldots(4)$$

where A' has been written for πd^2, the cross-sectional area of the superconducting filaments. nA can be written as μ, the filling factor of the wire in the solenoid, while $n'A'$ may be written as μ', the 'filling factor' of the superconducting filaments in the wire. Whereas μ may easily be as great as 0·8, it is likely that μ' will be very small.

A more illuminating form of equation (4) is obtained by eliminating A', using equation (1). This gives

$$\frac{H}{H_c} = \gamma\beta^2 . \pi . nA . n'\lambda(r-a) . \left(\frac{H_c}{H_c'}\right)^2 \qquad \ldots(5)$$

Under optimum conditions it should be possible to achieve a value of H close to H_c'. Equation (5) shows that we must then have

$$nn'\lambda(r-a)A = \frac{(H_c'/H_c)^3}{(\pi\gamma\beta^2)} \qquad \ldots(6)$$

$nn'(r-a)A$ is of course the number of 'filament turns' per centimetre length of the solenoid. Provided n' is not too small it should therefore always be possible to realize the optimum field H_c' by increasing the number of layers wound on the solenoid. Note that a large value λ is advantageous.

It is instructive to insert some plausible figures in equation (6). Assume $H_c'/H_c = 10$, $\lambda = 10^{-5}$ cm, $\beta = nA = 1$, $\gamma = 0{\cdot}1$. Then if $(r-a)$ is 3 cm we find $n' \sim 10^8$ filaments/cm^2. Thus the mean separation of the filaments must be not more than about 1 micron, which seems feasible.

Method of construction

Equation (6) shows that the cross-sectional area of the wire used is not critical, since only the filling factor nA is involved. However, if the current is not to be inconveniently large, the wire will have to be fairly thin. For example, to achieve a field of 60 kgauss, with $(r-a)$ equal to 3 cm, a current density of about 20,000 A/cm^2 is required. Thus, using wire of diameter 0·5 mm, a current of 50 A would be needed. Probably a somewhat smaller diameter would be more convenient.

The second method of preparation of the Nb_3Sn 'wire' described in reference 1 seems to be the most hopeful. The use of finely powdered niobium probably favours the existence of a high density of superconducting filaments of Nb_3Sn. It is even possible that very thin films of Nb_3Sn form over the surface of each niobium particle. Clearly the smaller the initial particle size the better—if possible, particles as small as 1 micron in diameter should be used. Heat treatment of the mixture of niobium and tin powder within the niobium capillary will presumably have to follow the winding of the solenoid, rather than precede it, since otherwise the brittle Nb_3Sn would fracture. It is likely that the niobium capillary itself will provide adequate 'insulation' between turns at the current densities used.

Alternative materials

Although Nb_3Sn has the highest observed transition temperature, there are a number of other compounds and alloys which might repay attention. These are: Nb_3Al ($T_c = 16{\cdot}8°$ K) (reference 3), V_3Si ($T_c = 17°$ K) and V_3Ga ($T_c = 16{\cdot}8°$ K) (reference 4), and, as a possibly somewhat more amenable alloy-type superconductor, an alloy of zirconium + 15 per cent rhenium ($T_c = 9{\cdot}6°$ K) (reference 5). Even the lead–bismuth eutectic alloy ($T_c = 8{\cdot}8°$ K) has been observed to have a critical field of about 16 kgauss at 4·2° K,[6] and would be an easier material to study.

Royal Radar Establishment, Malvern, Worcs.

J. M. LOCK

(23 March 1961)

REFERENCES

1. KUNZLER, J. E., BUCHLER, E., HSU, F. S. L., and WERNICK, J. H. *Phys. Rev. Lett.* **6**, 89 (1961)
2. PIPPARD, A. B. *Proc. Camb. phil. Soc.* **47**, 617 (1951)
3. CORENZWIT, E. *J. Phys. Chem. Solids* **9**, 93 (1959)
4. HARDY, G. F., and HULM, J. K. *Phys. Rev.* **93**, 1004 (1954)
5. MATTHIAS, B. T. *Progress in Low Temperature Physics*, Vol. II, p. 144 (Ed. C. J. Gorter) (North Holland, Amsterdam, 1957)
6. DE HAAS, W. J., and VOOGD, J. *Comm. Phys. Lab. Univ. Leiden* No. 208*b* (1930)

Book Reviews

Low Temperature Techniques. *F. Din and A. H. Cockett.* (*George Newnes, 1960*) *224 pages. 40s.*

It is not easy to decide on the general class of reader to whom this book is addressed. In the Preface the hope is expressed '... that the book will prove of real value to students, laboratory workers and technologists in all scientific and industrial fields'. While this is a laudable and perhaps realizable aim it is not clear whether the book is meant to serve as an introduction for these people to the type and importance of work at temperatures below zero Celsius, or as a guide to chemists, physicists, and engineers contemplating work in this field. In the topics selected for discussion, and the level at which this is carried out, the detail given often seems too much for the first purpose and too little for the latter.

Starting with an historical introduction, in which less credit than is his due has been given to Dewar for his work in producing liquid hydrogen and the wide range of his low temperature experiments, the authors proceed to deal with the production and measurement of low temperatures. Internal and external work methods of gas liquefaction are dealt with in a descriptive way but nothing is said of the efficiencies or the economics of the processes. Several pages are given to the elements of gas and electrical thermometry, most of which is not specific to low temperature work, and one wonders if it would not have been of advantage to omit much of this and deal with more specialized topics as, for instance, thermomolecular pressure differences which are not mentioned. Another surprising omission is that no consideration is given to heat exchangers since so many low temperature methods depend critically upon these devices.

The chapter on low temperature techniques in the laboratory contains useful information and the following chapter on the thermal properties of materials at low temperatures has many graphs displaying these in a convenient form. The remaining chapters dealing with gas separation and refrigeration in industry are good qualitative introductory accounts which will be read with interest by those whose main interest lies elsewhere.

The foregoing remarks are expressive perhaps of a personal disappointment that the authors have not produced a book more clearly directed to one particular class of reader, but with the rapid adoption of low temperature techniques for the most varied purposes any survey of the whole field will necessarily have shortcomings. Despite this, however, students and others will gain from a perusal of this book, for the style is very readable, both text and diagrams clearly produced, and no factual errors have been noticed.

F. E. Hoare

The Hall Effect and Related Phenomena. *E. H. Putley.* (*Butterworths, 1960*) *263 pages. 50s.*

It is well known that the major part of our present knowledge of semiconductors has been obtained from studies of the transport properties. In this work the topics discussed include the conductivity and Hall effect, magnetoresistance, thermoelectric effects, phonon drag, and thermal conductivity. The author is an authority on these subjects and has himself made many original contributions.

After a brief introduction, there is a chapter giving detailed information about methods of measurements of these properties over the temperature range from 1,200° K down to liquid helium temperatures. This is followed by a chapter on the theory relating to equilibrium carrier concentrations and transport properties. The applications of Fermi–Dirac statistics and the Boltzmann transport equation are very clearly explained and the results collected in convenient tabular form. The rest of the work is devoted to a presentation of the results obtained for some of the more important semiconductors. Results are reported for the Group IV elements and the Group III–V compounds and also for boron, tellurium, lead sulphide and telluride, silicon carbide, zinc oxide, mercury and bismuth tellurides, and magnesium–tin. A large part of this information has been available previously only in the original publications and this collection of data forms a valuable addition to the literature.

As in the case of every book, there are bound to be differences of opinion about the choice of subject matter and the emphasis to be placed on the various topics. It is rather surprising to find here only a brief reference to the classic paper of E. M. Conwell and P. P. Debye on the properties of N-type germanium and very little account of the extensive work of H. Fritzsche and collaborators. One feels that the section on impurity conduction could have been expanded and some consideration might also have been given to important experiments on 'hot' carriers. Apart from these omissions, there is nothing to criticize and this book can be strongly recommended to all physicists who are interested in semiconductors, both students and research workers and those concerned with semiconductor devices and applications.

Both the author and the publishers are to be congratulated on the excellence of the presentation, the clarity of the equations, and the convenient tabular and graphical presentation of important results.

B. V. Rollin

Helium-3. *Edited by J. G. Daunt. (Ohio State University Press, 1960) 198 pages. $4.50.*

Since the rare isotope helium-3 became available, a very active research group under Professor J. G. Daunt has been working with much success in the exciting field of investigating the properties of this substance in the liquid state. In addition he has organized symposia at Ohio State University which have become forums where the results and theories of workers all over the world have been discussed. The present book contains the papers and discussions given at the second symposium held in late August 1960. In a fast moving subject it is essential that papers presented at such meetings should be published with utmost speed and it is a further tribute to Professor Daunt that, only a little over six months after the symposium, the proceedings should be in the hands of the readers; in an attractively bound copy.

It is difficult to make a choice in mentioning some of the 32 papers contained in the volume. Probably the most exciting development is the brilliant experiment by Professor Daunt and his group on the melting curve of helium-3. Since the pioneer experiments, eight years earlier, by Weinstock, Abraham, and Osborne at the Argonne Laboratory there has been a good deal of doubt concerning their interpretation. This has now been resolved by the discovery of a minimum in the melting pressure at 0·3° K, a feature which had been predicted by Pomeranchuk as early as 1950. Another interesting paper by W. M. Fairbank and his group at Duke University deals with an extension of their nuclear resonance measurements on the solid phase down to 0·05° K. Although these observations have been carried out at pressures up to about 100 atm, no sign of the theoretically predicted antiferromagnetic or ferromagnetic transitions were found. The nuclear susceptibility of the liquid has been measured down to 0·03° K by Wheatley and his associates at the University of Illinois. Among the theoretical papers is one by Brueckner on his work together with Gammel, and a paper by Sessler applying considerations similar to the theory of superconductivity to helium-3. This leads to the prediction of a superfluid phase at very low temperatures.

While most of the work reported was carried out in the United States, some papers were read by European delegates and among these the researches by Taconis and his group at Leiden deserve special mention. Here the work on the separation into two coexistent liquid phases is of particular interest. It is most unfortunate that the Russian delegates who had hoped to attend the meeting had not succeeded in coming. A good deal of the most outstanding work on liquid helium-3, both experimental and theoretical, is being carried out in the Soviet Union.

Summarizing, one can say without reservation that this book will be of great importance to all those working on helium-3 and that it will also serve as a useful progress report for those more generally interested in low temperatures.

K. MENDELSSOHN

Expansion Machines for Low Temperature Processes. *S. C. Collins and R. L. Cannaday. 'Oxford Library of the Physical Sciences.' (Oxford University Press, 1959) 124 pages. 12s. 6d.*

The senior author of this book is of course Professor Sam Collins of M.I.T., justly celebrated all over the world as the original designer of the Arthur D. Little helium liquefier.

A most complete and scholarly account is given of the development of mechanical methods for achieving cooling by multiple expansion. Although the first name in this field is usually taken to be Claude, the historical section starts with Trevithick in 1828 followed by many other pioneers. The later work of Heylandt and Kapitza is described, followed by the development by Collins himself of the diaphragm and flexible piston-rod engines and their application to low temperature systems. The rest of the book (about a quarter) deals with expansion turbines.

It would be hard to over-praise the text of this book or the standard of its production. The figures and plates are excellent and the binding light but adequate. (It is difficult to reconcile the low price with the technical qualities of this series.)

A. J. CROFT

Bibliography

The following list of papers and letters concerning low temperature physics and engineering has been compiled from a wide range of periodicals and covers the period November 1960–March 1961. A list of recent publications will be a regular feature of CRYOGENICS.

ABRIKOSOV, A. A., and GOR'KOV, L. P. 'On the Problem of the Knight Shift in Superconductors.' *J. exp. theor. Phys.* **39,** 480 (1960), *Soviet Phys. JETP* **12,** 337 (1961)

AHERN, S. A., GOULD, P. A., and WALLING, J. C. 'Cross Relaxation Phenomena in Solid State Masers.' *J. Electron. Control* **IX,** 477 (1960)

ALEKSEEVSKII, N. E., BONDAR, V. V., and POLUKAROV, Y. M. 'The Superconductivity of Electrolytically Deposited Copper–Bismuth Alloys.' *J. exp. theor. Phys.* **38,** 294 (1960), *Soviet Phys. JETP* **11,** 213 (1960)

ALEKSEEVSKII, N. E., and GAĬDUKOV, Y. P. 'Anisotropy of the Electrical Resistance of Mg and Pt Single Crystals in a Magnetic Field at 4·2° K.' *J. exp. theor. Phys.* **38,** 1720 (1960), *Soviet Phys. JETP* **11,** 1242 (1960)

ALEKSEEVSKII, N. E., and MIKHEEVA, M. N. 'Critical Currents in Superconducting Tin Films.' *J. exp. theor. Phys.* **38,** 292 (1960), *Soviet Phys. JETP* **11,** 211 (1960)

ALIKHANOV, R. A. 'A Cryostat for Neutron Diffraction Studies.' *J. exp. theor. Phys.* **38,** 806 (1960), *Soviet Phys. JETP* **11,** 585 (1960)

ANDERSON, M. E., ZANDSTRA, P. J., and TUTTLE, T. R., JR. 'Proton Resonance Shifts in Pyrene Mononegative Ion at 4·2° K.' *J. chem. Phys.* **33,** 1591 (1960)

ANDROES, G. M., and KNIGHT, W. D. 'Nuclear Magnetic Resonance in Superconducting Tin.' *Phys. Rev.* **121,** 779 (1961)

ANON. 'IBM's New Cryogenic Memory Planes.' *Missiles and Rockets* **8,** No. 2, 25 (January 9, 1961)

ANON. 'New Helium Plant.' *Mod. Refrig.* **64,** No. 754, 91 (January, 1961)

ANON. 'Superconducting Solenoids Advance.' *Missiles and Rockets* **8,** No. 8, 35 (February 20, 1961)

ARASE, E. M., and HATCHER, R. D. 'Frequency Distribution and the Specific Heat of NaCl at Low Temperatures.' *J. chem. Phys.* **33,** 1704 (1960)

BALDWIN, S. A., and GAVRILOVSKII, B. V. 'Sealing of Windows in Work with High Pressures and Low Temperatures.' *Prib. i Tekh. Éksper.* No. 1, p. 145 (1960), *Instrum. Exper. Tech.* No. 1, p. 163 (1960)

BERMAN, R., FOSTER, E. L., SCHNEIDMESSER, B., and TIRMIZI, S. M. A. 'Effects of Irradiation on the Thermal Conductivity of Synthetic Sapphire.' *J. appl. Phys.* **31,** 2156 (1960)

BEZUGLYI, P. A., GALKIN, A. A., and KOROLYUK, A. P. 'Investigation of the Anisotropy of the Energy Gap in Superconducting Tin.' *J. exp. theor. Phys.* **39,** 7 (1960), *Soviet Phys. JETP* **12,** 4 (1961)

BHATIA, A. B., and MOORE, R. A. 'Ultrasonic Attenuation in Normal Metals at Low Temperatures.' *Phys. Rev.* **121,** 1075 (1961)

BLEANEY, B. and RUBINS, R. S. 'Explanation of some "Forbidden" Transitions in Paramagnetic Resonance.' *Proc. phys. Soc. Lond.* **77,** 103 (1961)

BOGOLYUBOV, N. N., ZUBAREV, D. N., and TSERKOVNIKOV, Y. A. 'An Asymptotically Exact Solution for the Model Hamiltonian of the Theory of Superconductivity.' *J. exp. theor. Phys.* **39,** 120 (1960), *Soviet Phys. JETP* **12,** 88 (1961)

BRANDT, N. B. 'A Device for Investigating the Anisotropy of Metals at Ultralow Temperatures.' *Prib. i Tekh. Éksper.* No. 3, p. 214 (1960), *Instrum. Exper. Tech.* No. 3, p. 473 (1960)

BRANDT, N. B. 'The Obtaining of Ultra-high Pressures at Low Temperatures.' *Prib. i Tekh. Éksper.* No. 2, (1960), *Instrum. Exper. Tech.* No. 2, p. 314 (1960)

BREWER, D. F., and MENDELSSOHN, K. 'Transfer of the Unsaturated Helium-II Film.' *Proc. roy. Soc.* **A260,** 1 (1961)

BURSTEIN, E., LANGENBERG, D. N., and TAYLOR, B. N. 'Superconductors as Quantum Detectors for Microwave and Sub-millimeter-wave Radiation.' *Phys. Rev. Lett.* **6,** 92 (1961)

CADEVILLE, M.-C., and MEYER, A. J. P. 'Propriétés Magnétiques de Fe_2P.' *C. R. Acad. Sci., Paris,* **252,** 1124 (1961)

CARERI, G., SCARAMUZZI, F., and THOMSON, J. O. 'Heat Flash and Mobility of Electric Charges in Liquid Helium. II.—Turbulent Flow.' *Nuovo Cim.* **18,** 957 (1960)

CARRUTHERS, P. 'Theory of Thermal Conductivity of Solids at Low Temperatures.' *Rev. mod. Phys.* **33,** 92 (1961)

CASWELL, H. L. 'Effect of Residual Gases on Superconducting Characteristics of Tin Films.' *J. appl. Phys.* **32,** 105 (1961)

CHALLIS, L. J., DRANSFELD, K., and WILKS, J. 'Heat Transfer between Solids and Liquid Helium-II.' *Proc. roy. Soc.* **A260,** 31 (1961)

CHANDRASEKHAR, B. S., and RAYNE, J. A. 'Limiting Value of Debye Temperature for Superconducting and Normal Indium from Low-Temperature Elastic Constants.' *Phys. Rev. Lett.* **6,** 3 (1961)

CHARI, M. S. R. 'Anomalous Conductivity and Lorenz Parameter in Dilute Silver–Manganese Alloys at Low Temperatures.' *Nature, Lond.* **189,** 824 (1961)

CHIH-CH'AO, L., and NASLEDOV, D. N. 'Influence of the Electric Field on the Electrical Conductivity, Hall Coefficient, and Magnetoresistance of n-Type InSb at Low Temperatures.' *Fiz. Tverd. Tela* **2,** 793 (1960), *Soviet Phys. Solid State* **2,** 729 (1960)

CHUENKOV, V. A. 'Electrical Conductivity of Valence Semiconductors at Low Temperatures in Strong Electric Fields.' *Fiz. Tverd. Tela* **2,** 799 (1960), *Soviet Phys. Solid State* **2,** 734 (1960)

COHEN, M. L. 'A 6-Megacycle Cryotron Ring Oscillator.' *Proc. Inst. Radio Engrs, N.Y.* **49,** 371 (1961)

DHEER, P. N. 'The Surface Impedance of Normal and Superconducting Indium at 3,000 Mc/s.' *Proc. roy. Soc.* **A260,** 333 (1961)

DRABKIN, G. M., and ZHITNIKOV, R. A. 'Production of "Supercold" Polarized Neutrons.' *J. exp. theor. Phys.* **38,** 1013 (1960), *Soviet Phys. JETP* **11,** 729 (1960)

DUPUIS, M., MAZO, R., and ONSAGER, L. 'Surface Specific Heat of an Isotropic Solid at Low Temperatures.' *J. chem. Phys.* **33,** 1452 (1960)

EGAN, E. P., JR., and WAKEFIELD, Z. T. 'Low Temperature Heat Capacity and Entropy of Bertinite.' *J. phys. Chem.* **64,** 1953 (1960)

EGAN, E. P., JR., and WAKEFIELD, Z. T. 'Low Temperature Heat Capacity and Entropy of Potassium Metaphosphate.' *J. phys. Chem.* **64,** 1955 (1960)

ELIASHBERG, G. M. 'Interactions between Electrons and Lattice Vibrations in a Superconductor.' *J. exp. theor. Phys.* **38,** 966 (1960), *Soviet Phys. JETP* **11,** 696 (1960)

EROS, S., and SMITH, C. S. 'Low-temperature Elastic Constants of Magnesium Alloys.' *Acta Metall.* **9,** 14 (1961)

ESCOFFIER, P., and GAUTHIER, J. 'Étude Thermomagnétique de Quelques Sels Minéraux Neutres et Basiques de Cuivre.' *C. R. Acad. Sci., Paris* **252,** 271 (1961)

EULER, R. D., and WESTRUM, E. F., JR. 'Heat Capacity and Thermodynamic Properties of Titanium Tetrafluoride from 6 to 304° K.' *J. phys. Chem.* **65,** 132 (1961)

FICKELSCHER, H., and ZUKALE, W. 'Ultrarotabsorption des Kupferoxyduls (Cu_2O).' *Naturwiss.* **48,** 24 (1961)

FLUBACHER, P., LEADBETTER, A. J., and MORRISON, J. A. 'Heat Capacity of Ice at Low Temperatures.' *J. chem. Phys.* **33,** 1751 (1960)

FRADKOV, A. B. 'Helium Cryostat without Cooling by Liquid Nitrogen.' *C. R. Acad. Sci. U.R.S.S.* **133,** 829 (1960), *Soviet Phys. Doklady* **5,** 888 (1961)

FRADKOV, A. B., and SHAL'NIKOV, A. I. 'A Liquid-helium Level Indicator for Metallic Containers.' *Prib. i Tekh. Éksper.* No. 3, p. 148 (1960), *Instrum. Exper. Tech.* No. 3, p. 508 (1960)

FROIS, C., and DIMITROV, O. 'Existense, dans l'Aluminium Fortement Écroui, d'un Nouveau Stade de Variation de la Résistivité Électrique entre 80 et 150° K.' *C. R. Acad. Sci., Paris* **251,** 2704 (1960); Addendum: *C. R. Acad. Sci., Paris* **252,** 276 (1961)

GALKIN, A. A., and KOROLYUK, A. P. 'Absorption of Ultrasound in Zinc at Low Temperatures.' *J. exp. theor. Phys.* **38,** 1688 (1960), *Soviet Phys. JETP* **11,** 1218 (1960)

GALKINA, O. S., and CHERNIKOVA, L. A. 'The Relation between the Temperature Dependence of Electrical Resistance at Low Temperatures and the Galvanomagnetic Effect in Strong Magnetic Fields.' *J. exp. theor. Phys.* **38,** 3 (1960), *Soviet Phys. JETP* **11,** 1 (1960)

GARBER, R. I., GINDIN, I. A., LAZAREV, B. G., and STARODUBOV, Y. D. 'Low-Temperature Recrystallization of Copper.' *Fiz. Tverd. Tela* **2,** 1096 (1960), *Soviet Phys. Solid State* **2,** 991 (1960)

GOLDMAN, M., and LANDESMAN, A. 'Polarization Dynamique Nucléaire par Contact Thermique entre des Systèmes de Spins.' *C. R. Acad. Sci., Paris* **252,** 263 (1961)

GOLDSMITH, M. 'Liquid Rockets.' *Astronautics* **5,** No. 11, 38 (1960)

GRAJCAR, L., and LEACH, S. 'Sur les Spectres d'Émission et d'Absorption vers 4,600 Å du Radical Benzyle à 77° K.' *C. R. Acad. Sci., Paris* **252,** 1014 (1961)

GRANATO, A. V., and NILAN, J. G. 'Stored Energy Release below 80° K in Deuteron-irradiated Copper.' *Phys. Rev. Lett.* **6,** 171 (1961)

GREENLAND, K. M. 'Some Aspects of Research on Thin Solid Films.' *J. sci. Instrum.* **38,** 1 (1961)

GRINBERG, A. A., NOVIKOV, S. R., and RYVKIN, S. M. 'A New Negative Photoconduction Effect in the Magnetic Field.' *C. R. Acad. Sci. U.R.S.S.* **136,** 329 (1961)

GSCHWENDTNER, K., and WOLF, H. C. 'Das Einfrieren der Energieübertragung in organischen Mischkristallen.' *Naturwiss.* **48,** 42 (1961)

GUPTA, K. K., and MATHUR, V. S. 'Magnetic Field Dependence of Energy Gap in Superconductors.' *Phys. Rev.* **121,** 107 (1961)

HÄNNY, J. 'Eine Tieftemperaturanlage zur Gewinnung von schwerem Wasser.' *Die Kälte* **13,** 541 (1960)

HAYNES, M. K. 'Transient Analysis of Cryotron Networks by Computer Simulation.' *Proc. Inst. Radio Engrs, N.Y.* **49,** 245 (1961)

HEINZINGER, K. 'Die Wärmeleitfahigkeit von Normal- und Para-Wasserstoff bei 20° K.' *Z. Naturf.* **15a,** 1022 (1960)

HERVÉ, J., and VEILLET, P. 'Résonance Nucléaire Magnétique de ^{159}Tb dans le Terbium Métallique en Poudre à l'État Ferromagnétique.' *C. R. Acad. Sci., Paris* **252,** 99 (1961)

HONE, D. 'Self-Diffusion in Liquid He^3.' *Phys. Rev.* **121,** 669 (1961)

HORTON, G. K. 'On the Thermal Expansion of Metals at Low Temperatures.' *Canad. J. Phys.* **39,** 263 (1961)

HUGUENIN, R., and RIVIER, D. 'Effet Hall du Ni Très Pur à Basse Température.' *Helv. phys. acta* **33,** 973 (1960)

ITSKEVICH, E. S. 'The Heat Capacity of Bismuth Telluride at Low Temperatures.' *J. exp. theor. Phys.* **38,** 351 (1960), *Soviet Phys. JETP* **11,** 255 (1960)

JENNINGS, L. D. 'Design of Mutual Inductance Bridges for Cryogenic Measurements.' *Rev. sci. Instrum.* **31,** 1269 (1960)

JENNINGS, L. D., MILLER, R. E., and SPEDDING, F. H. 'Lattice Heat Capacity of the Rare Earths. Heat Capacities of Yttrium and Lutetium from 15–350° K.' *J. chem. Phys.* **33,** 1849 (1960)

JOSHI, S. K. 'Debye Temperature of Orthorhombic Crystals at 0° K.' *Phys. Rev.* **121,** 40 (1961)

JOSHI, S. K., and MITRA, S. S. 'Debye Θ of Some Crystals.' *Indian J. Phys.* **34,** 532 (1960)

KALASHNIKOV, S. G., and KUROVA, I. A. 'The Electrical Conductivity of Germanium at Low Temperatures.' *Soviet Phys. Solid State* **2,** 1756 (1961)

KLIPPING, G., and FOCK, H. W. 'Eine Nachfüllvorrichtung für tiefsiedende Flüssigkeiten.' *Kältetech.* **12,** 377 (1960)

KNIPPER, A. 'Contribution à l'Étude Expérimentale de Niveau Excités de Quelques Noyaux Radioactifs.' *Ann. Phys. Paris* **6,** 211 (1961)

KOCHELAEV, B. I. 'Longitudinal Relaxation of Nuclear Spins in a Paramagnetic Crystal at Very Low Temperatures.' *J. exp. theor. Phys.* **38,** 999 (1960), *Soviet Phys. JETP* **11,** 719 (1960)

KOENIG, S. H., and HALL, J. J. 'Low-temperature Transport in "Split *p*-germanium".' *Phys. Rev. Lett.* **5,** 550 (1960)

KOEPPE, W. 'Bemerkung zur Inversionskurve von Wasserstoff.' *Kältetech.* **12,** 376 (1960)

KONDORSKII, E. I., GALKINA, O. S., and CHERNIKOVA, L. A. 'Electrical Resistance Maximum for Ferromagnets at Their Curie Points at Low Temperatures.' *J. exp. theor. Phys.* **38,** 646 (1960), *Soviet Phys. JETP* **11,** 464 (1960)

KUNZLER, J. E., BUEHLER, E., HSU, F. S. L., and WERNICK, J. H. 'Superconductivity in Nb_3Sn at High Current Density in a Magnetic Field of 88 kgauss.' *Phys. Rev. Lett.* **6,** 89 (1961)

LEEFE, S., and LIEBSON, M. 'Leveling System for Liquid Nitrogen.' *Rev. sci. Instrum.* **31,** 1353 (1960)

LIKHTER, A. I. 'Plant for Electrical Measurements at Low Temperatures and Pressures up to 10,000 atm.' *Prib. i Tekh. Éksper.* No. 2, p. 127 (1960), *Instrum. Exper. Tech.* No. 2, p. 310 (1960)

LINDENFELD, P. 'Comparisons of Carbon and Germanium Thermometers.' *Rev. sci. Instrum.* **32,** 9 (1961)

LITVIN, F. F., and PERSONOV, R. I. 'The Fine Structure of Absorption and Fluorescence Spectra of Certain Pigments at 77° K.' *C. R. Acad. Sci. U.R.S.S.* **136,** 798 (1961)

LONGIN, P. 'Luminescence, en Phase Vapeur et en Solution Étendue, Crystallisée, à 77° K de Quelques Aldéhydes et Cétones Aliphatique.' *C. R. Acad. Sci., Paris* **251,** 2499 (1960)

LOW, F. J., and RORSCHACH, H. E. 'Nuclear Spin Relaxation in Liquid Helium 3.' *Phys. Rev.* **120,** 1111 (1960)

MARSHALL, B. J. 'Elastic Constants of CsBr from 4·2° K to 300° K.' *Phys. Rev.* **121,** 72 (1961)

MELNGAILIS, I. 'The Cryosister—A New Low-Temperature Three-Terminal Switch.' *Proc. Inst. Radio Engrs, N.Y.* **49,** 352 (1961)

MILLS, R. L., GRILLY, E. R., and SYDORIAK, S. G. 'Anomalous Melting Properties of He^3.' *Ann. Phys.* **12,** 41 (1961)

MUTO, Y. 'On the Resistance Anomaly of Dilute Zinc Alloys at Low Temperatures.' *J. phys. Soc. Japan* **15,** 2119 (1960)

NOSANOW, L. H., and VASUDEVAN, R. 'Nuclear Paramagnetic Susceptibility of the Possible Low-Temperature Phase of Liquid He^3.' *Phys. Rev. Lett.* **6,** 1 (1961)

NOVIKOVA, S. I. 'Thermal Expansion of Some Technical Materials at Lower Temperatures.' *Prib. i Tekh. Éksper.* No. 3, p. 147 (1960), *Instrum. Exper. Tech.* No. 3, p. 507 (1960)

OLSEN, J. L., and ROHRER, H. 'The Volume Dependence of the Electron Level Density and the Critical Temperature on Superconductors.' *Helv. phys. acta* **33,** 872 (1960)

ORBACH, R. 'On the Scattering of Phonons by Spins at Low Temperatures: Theoretical.' *Phil. Mag.* **5,** 1303 (1960)

PAO-HSIEN FANG, ROBBINS, C., and FORRAT, F. 'Propriétés ferroélectrique des Titanates Mixtes du Système $Bi_4Ti_3O_{12}$, *n*-$BaTiO_3$.' *C. R. Acad. Sci., Paris* **252,** 683 (1961)

PEARSON, F. J. 'Some Notes on Theories of Helium.' *Proc. phys. Soc. Lond.* **77,** 531 (1961)

PESHKOV, V. P. 'Second Sound in Helium II.' *J. exp. theor. Phys.* **38,** 799 (1960), *Soviet Phys. JETP* **11,** 580 (1960)

PHILLIPS, N. E., and MATTHIAS, B. T. 'Heat Capacity of Ferromagnetic Superconductors.' *Phys. Rev.* **121,** 105 (1961)

RAYNE, J. A. 'Band Structure of Noble Metal Alloys: Optical Absorption in Cu–Ge Alloys at 4·2° K.' *Phys. Rev.* **121,** 456 (1961)

RAYNE, J. A., and CHANDRASEKHAR, B. S. 'Elastic Constants of β Tin from 4·2° K to 300° K.' *Phys. Rev.* **120,** 1658 (1960)

REINOV, N. M., and SMIRNOV, A. P. 'Determination of the Elastic Limit of Metals at Very Low Temperatures.' *Prib. i Tekh. Éksper.* No. 1, p. 128 (1960), *Instrum. Exper. Tech.* No. 1, p. 143 (1960)

ROCKMORE, R. M. 'Nuclear Paramagnetic Susceptibility of Low-temperature He^3 and the Flow Properties of Superfluid Systems of Fermions.' *Phys. Rev. Lett.* **6,** 166 (1961)

ROSENBERG, H. M., and SUJAK, B. 'On the Scattering of Phonons by Spins at Low Temperatures.' *Phil. Mag.* **5,** 1299 (1960)

SCHRÖDER, K., and CHENG, C. H. 'Correlation of Low-Temperature Caloric and Magnetic Effects in TiFe.' *J. appl. Phys.* **31,** 2154 (1960)

SEIDEN, J. 'Theorie de Ferromagnetisme des Alliages Nickel–Cuivre.' *C. R. Acad. Sci., Paris* **252,** 249 (1961)

SELEKTOR, Y. M., AINUTDINOV, M. S., and ZOMBKOVSKII, S. M. 'Pressure and Hydrogen-level Meter for Liquid-hydrogen Bubble Chambers.' *Prib. i Tekh. Éksper.* No. 3, p. 29 (1960), *Instrum. Exper. Tech.* No. 3, p. 385 (1960)

SHARVIN, Y. V. 'A Measurement of the Surface Tension at the Boundary between the Superconducting and Normal Phases of Indium.' *J. exp. theor. Phys.* **38,** 298 (1960), *Soviet Phys. JETP* **11,** 216 (1960)

SHARVIN, Y. V., and GANTMAKHER, V. F. 'Anisotropy of Surface Tension at the Boundary between the Superconducting and Normal Phases of Tin.' *J. exp. theor. Phys.* **38,** 1456 (1960), *Soviet Phys. JETP* **11,** 1052 (1960)

SHAW, R. W., MAPOTHER, D. E., and HOPKINS, D. C. 'Isotope Effect in Superconducting Lead.' *Phys. Rev.* **121,** 86 (1961)

SHULMAN, R. G. 'Nuclear Magnetic Resonance and Magnetic Ordering in NiF_2.' *Phys. Rev.* **121,** 125 (1961)

THORSEN, A. C. 'Magnetic Studies on Single-Crystal Chrome Potassium Alum below 1° Kelvin.' *Phys. Rev.* **121,** 66 (1961)

TSUNETO, T. 'Ultrasonic Attenuation in Superconductors.' *Phys. Rev.* **121,** 402 (1961)

VAN ITTERBEEK, A., PEELAERS, W., and STEFFENS, F. 'The Magnetic Susceptibility of Ag-Mn and Cu-Mn Solid Solutions between 1·2° K and 368° K.' *Appl. Sci. Res. Hague* **8B,** 337 (1960)

VERMA, G. S., and JOSHI, S. K. 'Origin of Hypersonic Attenuation in Germanium at Low Temperatures.' *Phys. Rev.* **121,** 396 (1961)

VINEN, W. F. 'The Detection of Single Quanta of Circulation in Liquid Helium-II.' *Proc. roy. Soc.* **A260,** 218 (1961)

VUL, B. M. 'p–n Junctions at Low Temperatures.' *C. R. Acad. Sci. U.R.S.S.* **129,** 61 (1959), *Soviet Phys. Doklady* **4,** 1246 (1960)

VUL, B. M., and ZAVARITSKAYA, E. I. 'The Capacitance of *p–n* Junctions at Low Temperatures.' *J. exp. theor. Phys.* **38,** 10 (1960), *Soviet Phys. JETP* **11,** 6 (1960)

VUL, B. M., ZAVARITSKAYA, E. I., and KELDYSH, L. V. 'Impurity Conductivity of Germanium at Low Temperatures.' *C. R. Acad. Sci. U.R.S.S.* **135,** 1361 (1960)

WEITZEL, D. M., ROBBINS, R. F., BOPP, G. R., and BJORKLUND, W. R. 'Low Temperature Static Seals Using Elastomers and Plastics.' *Rev. sci. Instrum.* **31,** 1350 (1960)

WHITE, D., RUBIN, T., CAMKY, P., and JOHNSTON, H. L. 'The Virial Coefficients of Helium from 20 to 300° K.' *J. phys. Chem.* **64,** 1607 (1960)

WOLF, H. C. 'Die Eigenfluoreszenz des Naphthalin-kristalls bei 4·2° K.' *Naturwiss.* **48,** 43 (1961)

ZAVARITSKII, N. V. 'The Thermal Conductivity of Superconductors in the Intermediate State.' *J. exp. theor. Phys.* **38,** 1673 (1960), *Soviet Phys. JETP* **11,** 1207 (1960)

ZUBAREV, D. N. 'The Theory of Superconductivity.' *C. R. Acad. Sci. U.R.S.S.* **132,** 1055 (1960), *Soviet Phys. Doklady* **5,** 570 (1960)